ISSN: 2663-8770, E-ISSN: 2733-2055, DOI: 10.36962/ETM

EQUİPMENT TECHNOLOGİES MATERİALS

AVADANLIQLAR, TEXNOLOGİYALAR, MATERİALLAR

ОБОРУДОВАНИЕ, ТЕХНОЛОГИИ, МАТЕРИАЛЫ

VOLUME 05 ISSUE 01 2021

CİLD 05 BURAXILIŞ 01 2021

http://emtasoiu.com/index.php/en/

http://sc-media.org/etm/

ISSN: 2663-8770, E-ISSN: 2733-2055, DOI: 10.36962/ETM

EQUİPMENT TECHNOLOGİES MATERİALS

AVADANLIQLAR, TEXNOLOGİYALAR, MATERİALLAR

ОБОРУДОВАНИЕ, ТЕХНОЛОГИИ, МАТЕРИАЛЫ

VOLUME 05 ISSUE 01 2021 CİLD 05 BURAXILIŞ 01 2021

JOURNAL INDEXING
CROSSREF

AZERBAIJAN BAKU 2021

ISSN: 2663-8770, E-ISSN: 2733-2055
ETM
EQUİPMENT, TECHNOLOGİES, MATERİALS

ISSN: 2663-8770, E-ISSN: 2733-2055, DOI: 10.36962/ETM
EQUİPMENT TECHNOLOGİES MATERİALS
AVADANLIQLAR TEXNOLOGİYALAR MATERİALLAR

©Publisher: Azerbaijan State Oil and Industry University LLC. İ/C 1400196861 (Azerbaijan).
©Nəşriyyat: Azərbaycan Dövlət Neft və Sənaye Universiteti. MMC. VÖEN 1400196861 (Azərbaycan).
Rector: Mustafa Babanli. Doctor of Technical Sciences. Professor.
Rektor: Mustafa Babanlı. Texnika Elmləri Doktoru. Professor.
Registered address: 20, Azadlig pr., Baku, Azerbaijan, AZ1010.
Qeydiyyat ünvanı: Azadliq prospekti, 20. Bakı Azərbaycan, AZ1010.
©Editorial office: 20, Azadlig pr., Baku, Azerbaijan, AZ1010.
©Redaksiya: Azadliq prospekti, 20. Bakı Azərbaycan, AZ1010.
©Typography: Azerbaijan State Oil and Industry University İ/C 1400196861 (Azerbaijan).
©Mətbəə: Azərbaycan Dövlət Neft və Sənaye Universiteti VÖEN 1400196861 (Azərbaycan).
Registered address: 20, Azadlig pr., Baku, Azerbaijan, AZ 1010.
Qeydiyyat Ünvanı: Azadliq prospekti, 20. Bakı Azərbaycan, AZ1010.

Publisher: International Center for Research, Education & Training. MTÜ (Estonia, Tallinn), R/C 80550594
©Nəşriyyat: MTÜ Beynəlxalq Tədqiqat, Təhsil & Təlim Mərkəzi. Q/N 80550594.
Director and Founder: Seyfulla İsayev. (Azerbaijan)
Direktor və Təsisçi: Seyfulla İsayev. (Azərbaycan)
Deputy and Founder: Namig Isazade. PhD in Business Administration. (Azerbaijan).
Direktorun müavini və Təsisçi: Namiq Isazadə. PhD Biznesin İdarə Olunması. (Azərbaycan).
©Editorial office / Redaksiya: Harju maakond, Tallinn, Kesklinna linnaosa, Narva mnt 5, 10117
Telephones / Telefonlar: +994 55 241 70 12; +994 51 864 88 94
Website / Veb səhifə: http://sc-media.org/
E-mail: sc.mediagroup2020@gmail.com, sc.mediagroup2017@gmail.com

ISSN: 2663-8770, E-ISSN: 2733-2055
ETM
EQUİPMENT, TECHNOLOGİES, MATERİALS

TABLE OF CONTENTS / MÜNDƏRİCAT

ISSN: 2663-8770, E-ISSN: 2733-2055
ETM
EQUİPMENT, TECHNOLOGİES, MATERİALS

EQUİPMENT, TECHNOLOGİES, MATERİALS

VOLUME 05 ISSUE 01 2021

EVOLUTION OF THE QUALITY OF HIGH-PRESSURE VALVES DURING THE PERIOD OF THEIR INTENSIVE DEVELOPMENT

[1]Sabir Babaev, [2]Ibrahim Habibov, [3]Zohra Abiyeva

[1]SRI "Geotechnological problems of oil, gas and chemistry", Doctor of Technical Sciences. Professor. (Azerbaijan)

[2]Azerbaijan State Oil and Industry University, Doctor of Technical Sciences, Professor. (Azerbaijan).

[3]Azerbaijan State Oil and Industry University, Assistent “Engineer and Computer Graphics.

E-mail: [2]h.ibo@mail.ru ; [3]zohra.abiyeva@asoiu.edu.az

ABSTRACT

Prospects for the further development of the oil and gas industry are mainly associated with the development and commissioning of high-rate fields. In this regard, the production of more economical and durable equipment by machine-building enterprises, an increase in the level of its reliability and competitiveness, as well as further improvement of technological production processes, is of paramount importance.
The evolution of technology in a broad sense is a representation of changes in designs, manufacturing technology, their direction and patterns. In this case, a certain state of any class of TC is considered as a result of long-term changes in its previous state; transition from existing and applied in practice vehicles to new models that differ from previous designs. These transitions, as a rule, are associated with the improvement of any performance criteria or quality indicators of the vehicle and are progressive in nature.
The work is devoted to the study of the evolution of the quality of high-pressure valves during the period of their intensive development.
Keywords: technical system, evolution of technology, high-pressure valves, shut-off devices, gate.

INTRODUCTION

It is known [1, 2, etc.] that the development of technical systems is subject to the law of progressive evolution, which reflects the changes made in them, aimed at eliminating the shortcomings identified during operation. It has been established that, despite the individual characteristics inherent in various technical systems (TS), the law of progressive evolution, as a rule, is linked to the analysis of the "life cycle" of the TS, according to which, ultimately, a period of slowing down of the TS development comes, leading most often to the need to replace this TS with a more perfect system [3].
Such patterns are of great importance for clarifying the possibilities of further development of the TS and determining the feasibility of improving the applied system or creating a fundamentally new system. Therefore, the further development of any vehicle is based on the entire history of its design and technological evolution.
In addition, the study of the evolution of the TS makes it possible to identify the main stable factors influencing its development, as well as the possibility of moving to the next stage.
The law of progressive evolution, as a rule, is linked to the analysis of the TS "life cycle" [2] and represents a sequence of the following periods of its development: relatively slow development of the created TS, due to its development; intensive development of the vehicle at high growth rates of the efficiency criterion by eliminating the shortcomings identified in the process of its operation and using new progressive design and technological solutions; slow development of TC due to the approach of the efficiency criterion to its limiting value.
It was found [3] that further this TS either degrades, being replaced by a modernized or fundamentally new system, or its operation continues while maintaining the value of the efficiency criterion achieved by the system.
Often TS - parts, assembly units and assemblies connected by a certain commonality (first of all, which have the same functions with the given TS), in the process of evolution go through similar stages of development. These cases are referred to as "parallel lines of evolution" [4], since knowing at the moment the stage of development of one, as a rule, the most progressive of the systems, it is possible to predict with sufficient confidence the evolution of the second system.
In addition, possessing the listed generalizing features inherent in certain types of oilfield equipment, such representative objects make it possible to extend the findings to other similar vehicles.
In this regard, the performed studies are typical, the objects of which are high-pressure drilling and oilfield pumps, mobile lifting units, as well as equipment for pumping wellheads [5, 6].

ISSN: 2663-8770, E-ISSN: 2733-2055
ETM
EQUİPMENT, TECHNOLOGİES, MATERİALS

Objective. Considering that the production of a significant amount of oil and all natural gas is carried out by the flowing method, it is of considerable interest to study the evolution of wellhead equipment used in the gas-lift and flowing methods of operation.

With these methods of oil and gas production, wellhead surface equipment designed to seal the wellhead, regulate and control the operating mode, suspend pumping and compressor pipes and direct the produced product into the manifold is a Christmas tree. Fountain fittings consist of a pipe head and a Christmas tree, representing the articulation of valves, tees, crosses and other parts according to the required scheme, for pressure up to 100 MPa and above [5].

X-mas tree parts, especially valves, operate at high pressures, are exposed to corrosive, often highly corrosive environment, with a content of hydrogen sulfide (H2S) and carbon dioxide, (CO2) up to 6% by volume of each and mechanical impurities up to 25 mg / l. According to the requirements, the gate valves must remain operational until failure at 120 ÷ 125 conditional opening-closing cycles.

The main working body of the gate valves is the gate assembly, which ensures reliable blocking of the passage opening.

Depending on the design of the gate assembly, the gate valves are divided into wedge and straight-through. In wedge gate valves, the shut-off element is a wedge, and the seal occurs at a certain angle to the axial movement of the wedge.

Such valves in Christmas trees were used to equip wells in the initial period of their development [7]. The main disadvantages of wedge gates are: the susceptibility of the wedge gate in the open state to intense hydro-erosion, hydro- or gas-abrasive wear, as well as wear when the surfaces of the gate parts jam when it is closed.

The indicated drawbacks of wedge valves, when used in Christmas tree valves, were the reasons for reaching their "life cycle" of the limiting value, degradation as a result of this and, as a consequence, replacement for direct-flow valves.

In turn, the development of fundamentally new TS - once-through valves, led to their intensive progress at high rates of development. At the same time, in a fairly short period of time, a transition of this TS from the period of initial, slow development to the period of its intensive development is noted.

Direct-flow valves, in comparison with other designs of locking devices, have a number of undoubted advantages. This is the simplicity of design, manufacturability, relatively low torque on the flywheel.

Straight-through gate valves differ in both design and sealing principle. In fig. 1 shows a conditional classification of straight-flow valves with a plane-parallel valve, covering their main design features [8].

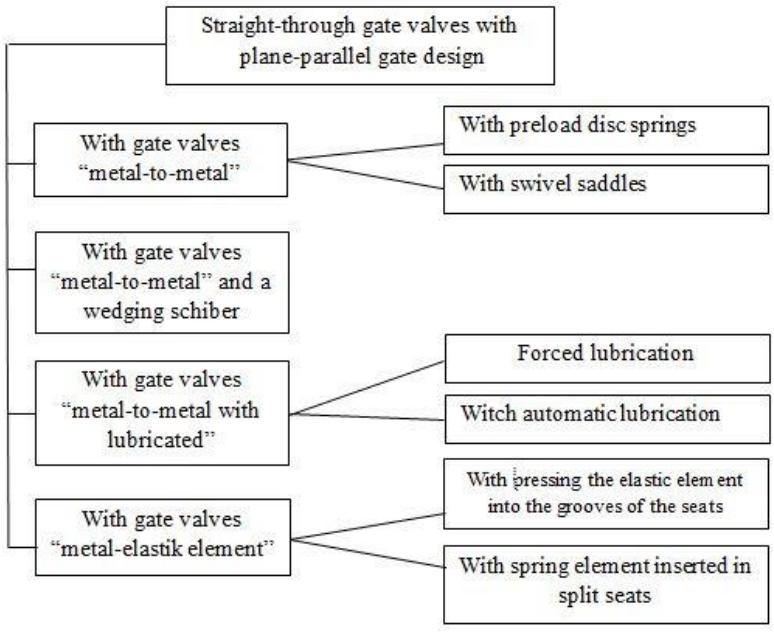

Figure 1.Classification of straight-flow valves with a plane-parallel design of the gate assembly

For the types of direct-flow valves listed in Fig. 1 with a plane-parallel design of the valve assembly, the following should be noted. The metal-to-metal pair is one of the most common types of sealing, in which a high

ISSN: 2663-8770, E-ISSN: 2733-2055
ETM
EQUİPMENT, TECHNOLOGİES, MATERİALS
EQUİPMENT, TECHNOLOGİES, MATERİALS
VOLUME 05 ISSUE 01 2021

degree of tightness of such a valve is achieved due to the treatment of the sealing surfaces. When a pair of "metal-metal with grease" is combined, an additional increase in the tightness of the valve is achieved by injecting grease into the area of the sealing surface of the seats. With the type of seal "metal - elastic element" the seal is due to the elasticity of the elastic element

A significant number of works [9, 10, etc.] have been devoted to improving the performance, reliability and efficiency of wellhead shut-off equipment, including the development of new designs of valves that meet modern requirements [5, 8]; ensuring reliable operation of wellhead equipment at abnormally high pressures, as well as with the content of hydrogen sulfide and carbon dioxide [12, 13, 14].

At the same time, it is required to ensure a further increase in the reliability of the applied Christmas tree.

Most of the enterprises produce direct-flow gate valves with gates of the "metal-to-metal", "metal-to-metal with lubrication" and "metal-elastic element" types for operating pressures of 21, 35 and 70 MPa.

The most practical application has been received by the Christmas tree with direct-flow valves with a metal-to-metal seal. In fig. 2 shows a direct-flow gate valve ZM-65 × 21 with a nominal bore of 65 mm, for a working pressure of 21 MPa.

The body 1 of the ZM-65 × 21 gate valve is filled with grease through the ball valve 9. Gate 12 is connected to the spindle 7 by means of a "T" -shaped groove. In the bores of the body, seats 13 are inserted, sealed with rubber elements, which are pressed against the gate surface by disc springs 11. A sliding spindle 7 with sealing collars is inserted into the body cover 2. and tightened with cap 8.

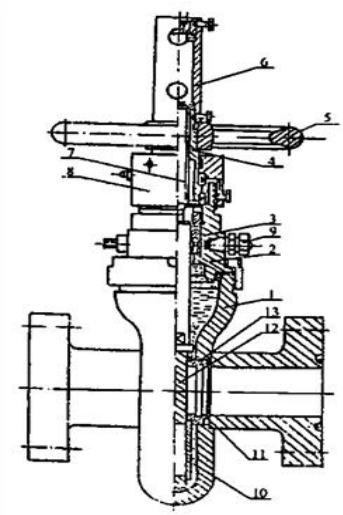

Figure 2. Direct-flow gate valve ZM-65 × 21 with a metal-to-metal gate: 1-body; 2-case cover; 3-sealing cuffs; 4-way nut; 5-flywheel; 6-casing; 7-spindle; 8-bearing cover; 9-ball valve; 10 shits; 11-disc spring; 12-gate; 13-saddle.

Shields 10 serve as guides for the gate in order to ensure the coincidence of its through hole with the holes of the seats when the valve is open, as well as to prevent the settling of abrasive particles and other inclusions carried by the medium into the housing on the sealing surfaces of the gate. The casing 6 is provided to protect the spindle threads in the open state, as well as for the intended adjustment of the alignment of the bores.

Gate valves of foreign companies are of certain interest in terms of the evolution of the design.

The original design of the gate assembly is provided by Cameron gate valves [8]. On the lateral surface of the valve saddles that rotate relative to the axis, there are teeth that mesh with the crackers on the gate. Each time, when the gate moves, the saddles are turned by crackers at a certain angle. This ensures uniform wear of the seats, reduces the likelihood of medium leakage and, accordingly, prolongs the service life of the valve as a whole.

In accordance with the classification shown in Fig. 1, gate valves (of the ZFP-65 × 21 type) are also used, in which the seal of the metal-to-metal gate is carried out by a wedging gate.

Gate valves with a similar design of the gate assembly [8] are manufactured by many foreign firms. For example, BREDA produces gate valves of this type with nominal bore from 2 "to 6" and working pressure up to 14 MPa (see Figure 3).

ISSN: 2663-8770, E-ISSN: 2733-2055
ETM
EQUİPMENT, TECHNOLOGİES, MATERİALS

The gate valve of this type consists of two dies 2 and 3, assembled and pressed against each other with the help of two special arcuate springs 2. Dice 3 is the leading, and the ram 2 is driven. When moving the gate, between its sealing surfaces and the sealing surfaces of the seats 4, a gap of 0.5 ... 1.0 mm is provided. When the driven ram 2 abuts against the end of the cover of the valve body 1, the leading ram of the valve 3 continues to move upward until the rams wedge between the seats and the through hole of the valve is closed.

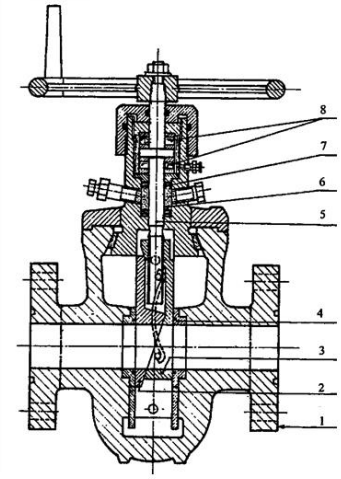

Figure 3. Straight-through gate valve with a wedging gate from BREDA.

Direct-flow gate valves with lubricant supply to the sealing surfaces of the gate-valve saddle pair have been widely used [9]. So, the gate valve assembly ZFP-50 × 32 and ZMAD-50 × 700 is made with automatic supply of sealing grease from the reservoirs to the annular grooves on the sealing surfaces of the seats, in the places of contact with the gate, and into the annular grooves of the seats provided for sealing with the body. When fluid leaks from the inlet side, in the closed state of the valve, the pressure inside the valve body increases, which leads to the squeezing of the sealing grease into the annular grooves of the seats.The presence of sealing grease between the sealing surfaces of the gate and the seats also further reduces the torque on the flywheel when controlling the valve.

Of considerable interest, in terms of the evolution of the design features of the gate assembly, is a direct-flow gate valve from "Gray" for a pressure of 210 MPa [15]. The plane-parallel gate in it consists of two halves, between which there is a wedge-shaped segment. When the gate moves along the segment, its halves are wedged and pressed against the seats. To ensure constant contact of the gate with the seats during the entire period of opening (or closing) the gate valve, springs are provided between the gate halves. The valve spindle is non-rising. A special anti-friction coating of the sealing surfaces of the valve parts greatly facilitates the valve control.

Gate valves model "C" from "McEvoy" company have a similar design [8]. The gate valve "Super Madwonder" by "McEvoy" is made according to the type of seal "metal-elastic element". On the sealing surfaces of the seats, there are annular grooves into which O-rings made of elastic synthetic rubber "Viton" or "Buna-N" are pressed (Fig. 4).

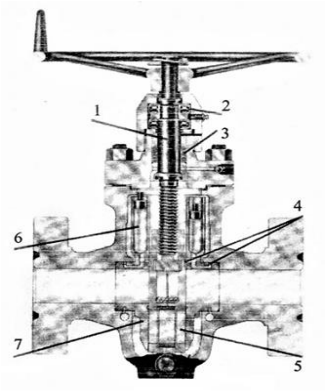

ISSN: 2663-8770, E-ISSN: 2733-2055
ETM
EQUİPMENT, TECHNOLOGİES, MATERİALS
EQUİPMENT, TECHNOLOGİES, MATERİALS
VOLUME 05 ISSUE 01 2021

Figure 4. Gate valve model "C" with automatic supply of sealing grease from "McEvoy": 1 - spindle; 2 - thrust bearings; 3 - spindle seal; 4 - system of channels for supplying lubricant; 5 - gate; 6 - reservoir for lubrication; 7 - cheek-saddle.

Figure 5 shows an MS-65 × 35-2f straight-through valve with forced lubrication supply, for an operating pressure of 35 MPa, developed by the AzINMASH Institute and manufactured by the oilfield machine-building plants of the Azneftkhimmash concern.

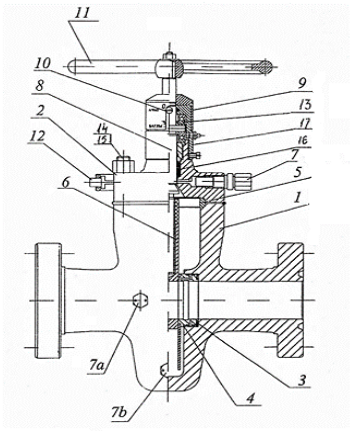

Figure 5. Winding gate MS-65 × 35-2f with forced lubrication

The gate valve consists of: cast or forged steel body 1; housing cover 2; Belleville springs 3; saddles 4; sealing strip 5; gate 6; check valve 7; two fittings for forced lubrication of the sealing surfaces of the valve parts 7a; housing flush fitting 7b; spindle 8; position indicator 9; pointer stopper 10; flywheel 11; discharge plugs 12; thrust bearings 13; studs with nuts 14, 15; spindle seals 16; bearing caps 17.

The firm "FMC" also produces direct-flow gate valves with forced lubrication for operating pressures of 14, 21 and 35 MPa with a gate, which uses composite seats [8]. Saddles consist of two steel rings, one of which is a support and is inserted into the housing seat. The support ring has a groove into which an elastoplastic O-ring is inserted. The outlet seat is designed so that between its support ring and the ring that locks the seal, there is a gap for a forced lubrication supply. In case of natural wear of the plastic sealing ring, the ground metal surface of the seats is tightly coupled with the valve sealing surface, thus forming a metal-to-metal seal.

The tightness of the seal can be increased by injecting a plastic grease through the fitting provided on the valve body. When pumped, the plastic grease fills the gaps, ensuring that the seat fits snugly against the gate sealing surfaces.

A review and analysis of the literature shows that foreign firms use various steel grades and methods of strengthening the sealing surfaces to manufacture parts of the gate valve assembly [8, 16]. So, by the firm "McEvoy", for the manufacture of gate valves, depending on the operating conditions, alloy steel with nickel plating or stainless steel is used. FMC uses 4130 low-alloy steel (30XM steel) with nitriding of the sealing surface, as well as 410SS alloy steel (12X13 steel) with case-hardening and surface hardening. For the manufacture of gate valves, 4130 steel with nitriding or 410SS with surface hardening is used. Firm "IKS" in the manufacture of parts of the valve assembly uses steel grade ASTMA-331 (steel 40XHM) chrome plated or coated with HF-7 (molybdenum disulfide).

Domestic machine-building enterprises use mainly steel 38X2MYUA with nitrogen, with volumetric quenching and tempering, steel 40X with chemical nickel plating, as well as steel 20X13 and 30X13 with surface hardening by high-frequency current. A disulfide-molybdenum coating is also used to reduce the coefficient of friction by up to 1.5 times [5].

A noticeable increase in the resource of the shut-off unit of the X-mas valves was achieved by the development and implementation of the process of cladding the sealing surfaces of the shutter elements, wear-resistant high-alloy coatings [9]. The developed technological processes of cladding with SNGN-50 powder and subsequent machining allow both the manufacture and restoration of locking elements of direct-flow valves with a plane-parallel gate assembly of all standard sizes. The high content of nickel, chromium and boron, as well as the carbon content of up to 0.5 ... 0.7%, provides high corrosion resistance and extreme pressure properties of the clad layer. During the tests of the gate and seats, with a wear-resistant coating applied to the working surfaces by the cladding method, the high sealing ability of the clad layer was confirmed. A rather high wear resistance of

ISSN: 2663-8770, E-ISSN: 2733-2055
ETM
EQUİPMENT, TECHNOLOGİES, MATERİALS

the clad layer was also noted under the conditions of vibrations of the gate valve assembly caused by pressure pulsations [9].
When seals of a gate of the "metal-elastic element" type, a hydron, fluoroplastic, composite materials based on fluoroplastic with graphite, Teflon (polytetrafluoroethylene) and others are used for the manufacture of sealing rings. Teflon-based pastes are used as plastic lubricants for metal-to-metal lubricated seals.
To limit the possible relative oscillatory movements of the sealing surfaces of the gate and seats due to the pulsations of the medium pressure, and, therefore, to exclude the main reason: fretting corrosion of the parts of the gate valve assembly, appropriate design solutions have been proposed [6, eight].
The first of the developed designs of high-pressure direct-flow valves is distinguished by the novelty of the saddles with collars and an increased contact area of interface with the gate valve (Fig. 6) [18].

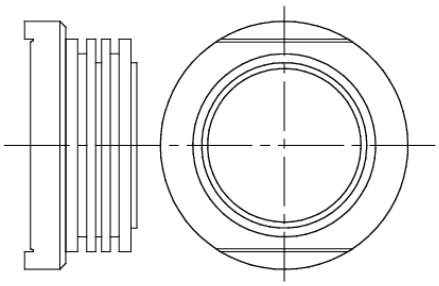

Figure 6. Newly designed saddle

At the same time, an increase in the interface area reduces the relative vibrations and displacements of the gate in the transverse direction, and the presence of collars eliminates the need to use guide shields.
Field tests of this direct-flow valve showed an increase in its service life by more than 1.2 times.
In the second developed design, the seat and gate valve were made with elliptical mating surfaces (see Figure 7). This made it possible, with unchanged dimensions of the gate in the transverse direction, to increase the area of the gate elements; thus, the emergence and development of fretting corrosion processes is excluded [19]. Also, the new design of the valve assembly limits the lateral displacement of the gate, which eliminates the need for guide shields.

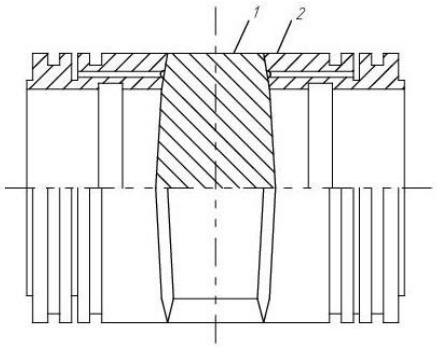

Figure 7. Cross-section of a gate valve with elliptical seals of gate (1) and seat (2).

The evolution process has also affected other elements of the Christmas tree. So, in the presence of sand in the produced product, due to significant wear, the chokes installed on the flow line of the valves are often replaced to maintain the required flow rate of the well. The problem was solved by replacing the fittings with adjustable chokes. At the same time, the necessary increase in the wear resistance of the throttle parts is provided by the use of hard alloys and ceramics.
Conclusions. Thus, on the basis of the research carried out, as well as using the provisions of the law of progressive evolution of technical systems (TS), the analysis of the "life cycle" of TS - high-pressure valves, used mainly in oil and gas production, has been made. It is shown that the period of relatively slow development of the TS (wedge valves) ended with significant changes in the design of the TS (gate valves) and the transition to the period of its intensive development.

Due to the use of new design and technological solutions, a significant improvement of the vehicle is noted with the elimination of deficiencies identified during operation, as well as with the creation of fundamentally new vehicles. A slowdown in the development of TS, and even more so their degradation, is not observed at the moment.

REFERENCES

1. Саламатов Ю.П. Система законов развития техники (основы теории развития технических систем). Красноярск РФ: Institute of Innovative Design, 1996.-136 с.
2. Курги Э.Э. Закономерности развития технических систем ЗРТС-96. ТРИЗ. Саммит – Спб.: 2006. htt://www.metodolog.ru/0081300813.html
3. Фейгенсон Н.Б. S-кривая – некоторые особенности третьего этапа развития систем //Журнал ТРИЗ, 2005, №1 (14) – С. 55-59.
4. S.Litvin, M.Gersman. Parallel Evolutionary Lines Application for Technology Forecast //Методы прогнозирования на основе ТРИЗ. Сб. науч. тр. «Библиотека Саммита разработчиков ТРИЗ». Вып.3. Спб.: 2010. – 280 с.
5. Бабаев С.Г., Кершенбаум В.Я., Габибов И.А. Эволюция качества трибосопряжений нефтегазовой техники. – Москва-Баку: НИНГ, 2018. – 526 с.
6. Бабаев С.Г., Кершенбаум В.Я., Габибов И.А. Эволюция надежности в комплексах «качество-конкурентоспособность» нефтепромыслового оборудования. Москва-Баку: НИНГ, 2020 – 416 с.
7. Бабаев С.Г., Зильберман Л.И. Повышение долговечности фонтанной арматуры. Тематический научно-технический обзор. М.: ВНИИОЭНГ, 1970. – 72 с.
8. Бабаев С.Г., Керимов В.И. Износостойкость затвора задвижек с уплотнением типа «металл-металл». Saarbrücken, Deutschland, LAP LAMBERT Academic Pablisching, 2015. – 101 с.
9. Бабаев С.Г., Абасов В.А., Гафаров В.В. и др. Исследование стойкости уплотнительных поверхностей узлов затвора задвижек фонтанных арматур в условиях пульсаций давлений. Ученые записки НИИ «Геотехнологические проблемы нефти, газа и химия». Том V. Баку: Элм, 2004. – с. 194 – 202.
10. Кахраманов Х.Т.,Подшибякина А.Л. Коррозионная стойкость сталей нефтепромысловой арматуры. М.: Химическое и нефтяное машиностроение, 1982, №2. – с. 23-24.
11. Бабаев С.Г., Керимов В.И. Новые конструкции узла затвора прямоточных задвижек высокого давления. Сборник статей научно – практической конференции «ХАЗАРНЕФТГАЗЯТАГ - 2012». Баку: 2013. – С. 127-130.
12. Мамедов Ф.Г., Этин З.М., Агавердиева Э.Р. Химическое никелирование деталей задвижек фонтанной арматуры, работающей в агрессивной сероводородосодержащей среде. М.: Химическое и нефтяное машиностроение, 1980, №2. С. 27-28.
13. Фаталиев Н.С., Сафаров Р.С., Алиева А.И. Применение дисульфидмолибденового покрытия деталей затвора задвижек устьевого оборудования. Экспресс-информация. Серия ХМ-3. М.: ЦИНТИхимнефтемаш, 1981, №4. – 3 с.
14. Владимиров А.И., Кершенбаум В.Я. Конкурентоспособность на фоне кризиса. Нефтегазовая техника. М.: «Национальный институт нефти и газа», 2009. – 696 с.
15. Отчет НИР по теме №3758-76-117 «Исследование по созданию устьевого эксплуатационного оборудования на Рр 100-150 МПа (1000-1500 кг/см2)». Фонд АзИНМАШа, 1977. – 48 с.
16. Кахраманов Х.Т. Выбор материалов для устьевого НПО, предназначенного для работы под высоким давлением в средах, содержащих сероводород. Материалы конференции, посвященной 75-летию АзИНМАШа. Баку: «Nurlan», 2005. – С. 183-189.
17. Бабаев С.Г., Керимов В.И. Результаты повышения надежности прямоточных задвижек высокого давления, применяемых в фонтанной и трубопроводных арматурах. М.: «Машиностроитель», 2012, №4. – С. 20-24.
18. Патент Азерб. Респ. İ 2008 0079. Прямоточная задвижка высокого давления. /Бабаев С.Г., Керимова Л.С., Керимов В.И. //Гос. регистрация: 30.04.2008.
19. Патент Азерб. Респ. İ 2008 0080. Прямоточная задвижка высокого давления. /Бабаев С.Г., Керимова Л.С., Керимов В.И. //Гос. регистрация: 30.04.2008.

ISSN: 2663-8770, E-ISSN: 2733-2055
ETM
EQUİPMENT, TECHNOLOGİES, MATERİALS

RESEARCH OF Al AND Mg MATRİX HYBRİD LAMİNATED COMPOSİTE MATERİALS

[1]Mustafa Babanli, [2]Yusif Tanriverdiyev

[1]Azerbaijan State Oil and Industry University, Doctor of Technical Sciences, Professor. (Azerbaijan)

[2]Azerbaijan State Oil and Industry University, "Intelligent Control and Decision Making Systems in Industry and Economics Research Laboratory", Engineer.

E-mail: yusif.tanriverdiyev@asoiu.edu.az

ABSTRACT

The main purpose of this research is to select suitable matrices and fillers for the preparation of composites that meet modern requirements to meet the needs of a rapidly growing industry. Studies in various databases have shown that metal-matrix hybrid laminated composite materials, mainly aluminum and magnesium alloy plates, are used as matrix materials, while carbon-based nanomaterials are used as fillers.
Keywords: composition, matrix, aluminum, magnesium.

The rapid development of science and technology, as well as improving the quality and reliability of manufactured products, required the creation of new modern construction materials that meet the needs of industry. In order to meet these needs, modern composite materials were laid in the 1930s with the discovery of fiberglass in the United States. Composite materials are used in all areas of industry today. [1] Although composite materials are considered relatively new and high-tech materials, their history is so ancient that archeological excavations have uncovered remains of composite materials used in ancient Rome, China, and Egypt.

Composite materials are new materials that are created by combining materials with two or more different properties at the macro level. The most important feature of the composite material is that these materials are not homogeneous at the micro level. Composition materials consist of 2 parts, a matrix and a filler [2,3]. The compositional materials are schematically shown in Figure 1.

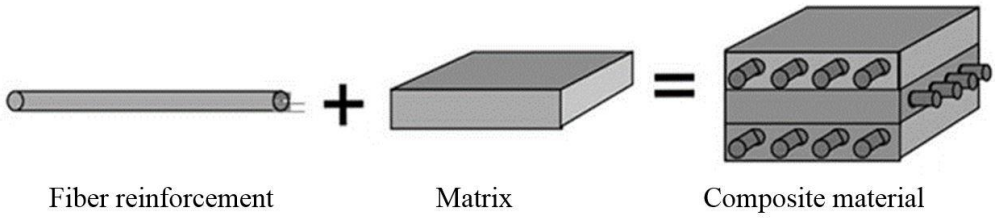

Figure 1. Schematic description of the composite material [2]

Matrix: Combines fibers in composite materials to protect them from external influences. Provides rigidity and durability in composite materials [2]. The filler evenly distributes the load on the composite materials in all directions and increases the resistance and durability of the material. According to the matrix material, the composition materials are conventionally divided into 3 groups [4]:

- Polymer matrix composite materials
- Ceramic matrix composite materials
- Metal matrix composite materials

Polymer matrix composite materials: Polymer matrix composite materials were developed in the 1940s for use in the aerospace industry. The main goal in improving these materials was to obtain a material that was lighter in weight but more durable, with higher hardness values and corrosion resistance. Polymer matrix composite materials are divided into thermoset and thermoplastic matrix. For the reinforcement of polymer matrix composite materials, aramide, basalt, jute, carbon, coconate, glass, etc. fibers are used as fillers.

Ceramic matrix composite materials: Ceramic matrix composite materials are widely used in industry due to their high heat resistance and light weight. These composite materials are mainly used in areas with high temperatures. Ceramic materials are very hard and brittle materials. As a matrix material, SiC, Cr2O3, TiN,

Si3N4, TiB, B4C and TiC are the most widely used materials in ceramic matrix composite materials. Metal and ceramic nanopowders are also used as fillers.
It should be noted that metal matrix composite materials have a higher ability to work in high temperature areas than polymer and ceramic matrix composite materials, the probability of combustion at high temperatures is very low and their service life is longer.
Metal matrix composite materials: Metal matrix composite materials are light metals with low density and good mechanical properties and their alloys are widely used in the industry as matrix materials. Metal matrix composite materials were developed in the early 1960s because of the need for materials with higher specific strength properties that could be used at temperatures higher than the current temperature of existing materials. Metal matrix composite materials are composite materials produced by combining two or more different materials, at least one of which is metal, at the macro level to provide the desired and required properties. Polymer, ceramic and nano materials are mostly used as filler materials in metal matrix composites.
The advantages of metal matrix composite materials are as follows: [6,7]

- Strength limit / density ratio (Specific strength)
- Elasticity modulus / density ratio (Special elasticity)
- Low density
- Impact resistance
- Surface hardness and crack resistance
- Resistance to thermal shocks
- Abrasion resistance
- Corrosion resistance

Disadvantages of metal matrix composite materials:

- Difficult and complex production processes of laminated composite material
- High cost of production costs and production equipment

Fillers. Depending on the place of use, the main features expected from the reinforcing element in metal matrix composite materials are mainly high modulus and resistance, low density, chemical compatibility with the matrix, ease of production, high temperature resistance, etc. The effect of the intermediate layer between the filler and the matrix on the mechanical properties of the material is great. As external forces are transferred and distributed by the matrix to the filler phase, the intermediate layer must meet high mechanical properties. In the intermediate layer, there must be a very weak chemical bond between the matrix and the filler, the filler must be evenly distributed in the matrix and, in particular, the composition of the filler must not change. Metal matrix composite materials use more ceramic compounds, non-metallic elements and nano fillers as fillers. [5,12]
Metal matrix composite materials have a reinforcing phase added to the metal matrix to provide properties that cannot be achieved with one-component alloys. Fillers are added to the material to create a reinforcing phase. [5,6,7]
These fillers are divided into 3 main classes (Figure 2) [5]:

- Particle filler metal matrix composite materials have low cost, hard and isotropic properties.

However, the deformation properties are low and the values of fracture stiffness during fracture are low.

- Fiber filler metal matrix composite materials are considered more expensive but more durable.
- Continious fiber or laminated metal matrix composite materials have the highest resistance and modulus of elasticity, but these materials show anisotropic properties and production costs are very high.

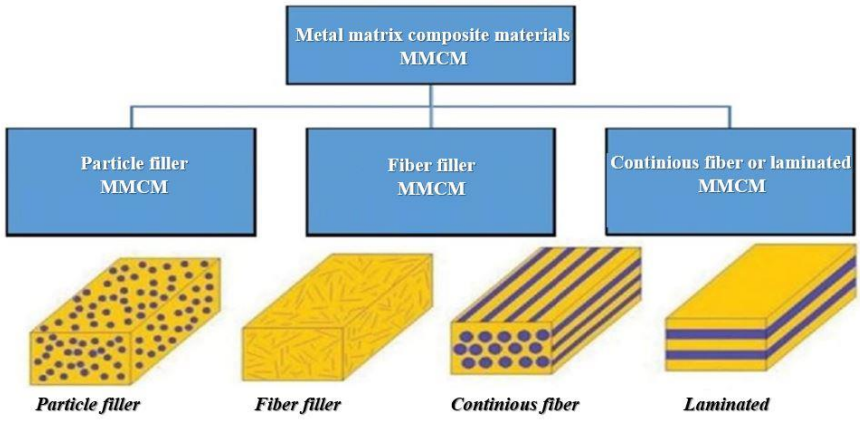

ISSN: 2663-8770, E-ISSN: 2733-2055
ETM
EQUİPMENT, TECHNOLOGİES, MATERİALS

Figure 2. Use of fillers in composite materials [5]

Fiber metal laminated composite materials are hybrid composite materials produced by combining fiber-reinforced polymeric materials into thin metal sheets. Hybrid composite materials have better properties than single-fiber reinforced composite materials. The most widely used system in hybrid composite materials, where matrix and fiber combinations can be used in different ways, is a system consisting of polymer matrix glass and carbon fibers. Hybrid composite materials have high resistance, fatigue and non-corrosion properties. A schematic description of hybrid laminated composite materials is given in Figure 3.

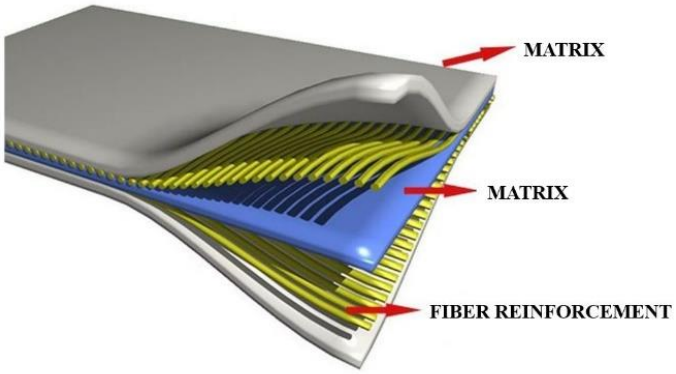

Figure 3. Schematic view of the fiber filler hybrid laminated composite material

Al and Mg matrix hybrid laminated composite materials

Aluminum and its alloys are widely used in the production of metal matrix composite materials due to their superior properties. In addition to aluminum, another non-ferrous metal, magnesium and its alloys, is widely used in the production of composite materials with a metal matrix. Our research on the characteristics of hybrid composite materials with matrix of aluminum and magnesium in the literature is reflected in this article [8-9].

The reasons for the most widespread use of Al and Mg metal as metal matrix in composite materials are as follows: [10]

- Being light
- Corrosion resistance
- High specific strength
- Ability to deform
- Conducts heat and electricity well
- Being economically efficient

Al alloys are divided into groups according to their mechanical, physical, chemical properties and microstructure: 1XXX, 2XXX, 3XXX, 4XXX, 5XXX, 6XXX, 7 XXX and 8XXX. The most heat-treated 2XXX, 3XXX and 7XXX series aluminum alloys are used in the production of composite materials. As a matrix material, 1mm thick 2XXX (2024-Al) aluminum plates and AZ-61 magnesium alloy plates are widely used in the production of composite materials. The chemical composition of these alloys is given in Tables l and 2. [10-11]

Chemical composition of 1 mm thick Al-2024 aluminum plate.

Table 1.

Composition	Al	Cr	Cu	Fe	Mg	Mn	Ti	Si	Zn
Wt.%	90.7-94.7	Max 0.1	3.8-4.9	Max 0.5	1.2-1.8	0.3-0.9	Max 0.15	Max 0.5	Max 0.25

Chemical composition of 1 mm thick AZ-61 magnesium plate.

Table 2.

Composition	Mg	Al	Zn	Mn	Si	Cu	Ni	Fe
Wt.%	92	5.80-7-20	0.40-1.50	0.15	0.10	0.050	0.0050	0.0050

Al-2024 and AZ-61 alloys were selected as the matrix material in our study due to the fact that they combine the necessary mechanical and physical properties and are particularly suitable for use in the aircraft and defense industries.

After the use of carbon nanotubes discovered by Iijima in 1991 as fillers in composite materials, a high increase in the mechanical and physical properties of composite materials was observed. As a result of the addition of graphite as a nano-filler to the composition materials, increased abrasion resistance, corrosion resistance and improved thermal properties were achieved. Short-fiber composites are used in areas where high resistance is required. The best combination of hardness and resistance is reflected in infinite fibrous or laminated composite materials with anisotropic properties and high production value. [12,13,14]

Due to the suitability of the properties of boards made of Al and Mg alloys in metal matrix composite materials, the use of graphite as a nano filler, the best combination of hardness and strength values is present in laminated composite materials. The production and application of composite materials in many industries is a topical issue. [10,15,16]

These composite materials are the basis of the fuselage of aircraft and helicopters in the defense industry due to their special strength, corrosion resistance and light weight. Because in the aviation industry, the most ideal option for reducing the weight of air transport, saving fuel, increasing durability and strength, ensuring longer life, minimizing crack layers are hybrid composite materials with a metal matrix. As an example, Figure 4 shows the use and application positions of hybrid composite materials with a metal matrix of 50% of the fuselage of a Boeing 787 passenger aircraft. [17,18,19]

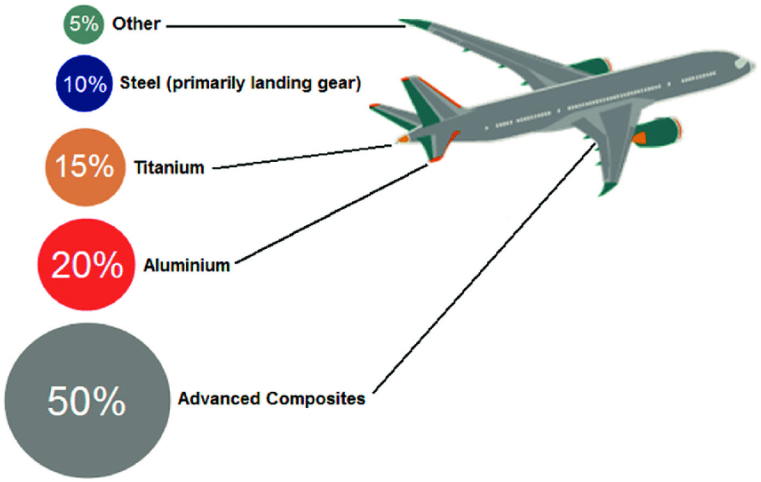

Figure 4. Material use in Boeing 787 passenger aircraft [18]

CONCLUSION

As a result of our literature research, it has been determined that the optimum properties of the new laminated hybrid composite material produced using boards made of Al or Mg alloys and graphite nanostructures impregnated with carbon fabrics as a matrix material allow its use in many industries. The high performance of metal matrix hybrid composite material in the defense and aviation industries of developed countries shows that the production and application of nano-graphite-filled aluminum or magnesium matrix hybrid composite materials in the defense and aviation industry is very relevant in our country.

REFERENCES

1. L.Ogin., P.Brondsted., J.Zangenber Composite materials: constituents, architecture, and generic damage, 3-23 (2016)

ISSN: 2663-8770, E-ISSN: 2733-2055
ETM
EQUİPMENT, TECHNOLOGİES, MATERİALS

2. https://en.wikipedia.org/wiki/Composite_material
3. https://www.twi-global.com/technical-knowledge/faqs/what-is-a-composite-material
4. P.S. Bains, S.S. Sidhu, H.S. Payal, Fabrication and machining of metal matrix composites: a review, Mater. Manuf. Processes 31 553–573 (2015)
5. https://prezi.com/ngtodkk9s-il/suryya-huseyn-metal-sasl-kompozisiya-materiallar-2018/
6. https://www.slideshare.net/SazzadHossain105/metal-matrix-composite-mmc
7. https://www.slideshare.net/HiepTran51/metal-matrix-composites-68130090
8. M. Shunmugasundaram, A. Praveen Kumar, L. Ponraj Sankar, S. Sivasankar Experimental investigation and process parameters optimization of stir cast aluminium metal matrix composites to improve material removal rate (2020)
9. R.Balokhonov., V.Romanova., A.Kulkov Microstructure-based analysis of deformation and fracture in metal-matrix composite materials (2020)
10. Navin Kumar , Shatrughan Soren Selection of reinforcement for Al/Mg alloy metal matrix composites Materials Today: Proceedings (2019)
11. Hui W., et al., "Warm forming behavior of high strength aluminum alloy AA7075", Transactions of Nonferrous Metals Society of China, 22 (1): 1-7, (2012)
12. S.Venkatesan , M. Anthony Xaviorb Characterization on Aluminum Alloy 7050 Metal Matrix Composite Reinforced with Graphene Nanoparticles (2018)
13. Jingyue Wang, Zhiqiang Li, Genlian Fan, Huanhuan Pan, Zhixin Chen, Di Zhang, Reinforcement with graphene nanosheets in aluminum matrix composites, Scripta Materialia 66 594-597 (2012)
14. Perez-Bustamante R, Bolanos-Morales D, Bonilla-Martinez J, Estrada-Guel I, Microstructural and hardness behaviour of graphene-nanoplatelets/aluminum composites synthesized by mechanical alloying, Journal of alloys and compounds 615 5578-5582 (2014)
15. Wang,J., Li, Z., Fan, G., Pan, H., Chen, Z and Zhang, D, Reinforcement with graphene nanosheets in aluminum matrix composites, Scripta Materialia 66(8) 594-597,(2012)
16. Kamyar Shirvanimoghaddam, Salah U. Hamim, Mohammad Karbalaei Akbari , Seyed Mousa Fakhrhoseini Carbon fiber reinforced metal matrix composites: Fabrication processes and properties Composites: Part A (2016)
17. Zimmermann, N., Hao Wang, P., A Review of Failure Modes and Fracture Analysis of Aircraft Composite Materials, Engineering Failure Analysis (2020)
18. Kadir Bilisik, Gaye Kaya, Huseyin Ozdemir, Mahmut Korkmaz and Gulhan Erdogan Applications of Glass Fibers in 3D Preform Composites (2018)
19. Edson Cocchieri Botelho, Rogério Almeida Silva, Luiz Cláudio Pardini, Mirabel Cerqueira Rezende A Review on the Development and Properties of Continuous Fiber/epoxy/aluminum Hybrid Compositesfor Aircraft

ISSN: 2663-8770, E-ISSN: 2733-2055
ETM
EQUİPMENT, TECHNOLOGİES, MATERİALS

EQUİPMENT, TECHNOLOGİES, MATERİALS

VOLUME 05 ISSUE 01 2021

NATIONAL ECONOMIC SIGNIFICANCE UNDER THE CONDITIONS OF THE ECONOMY OF KNOWLEDGE OF CASTING PRODUCTION AND THE KEY DIRECTIONS OF ITS DEVELOPMENT

Elman Aliyev

Azerbaijan State Oil and Industry University, R. L. "Nanomaterials and Nanotechnology" Deputy director

PhD in Economic (Baku, Azerbaijan).

E-mail: elmancam@gmail.com

ABSTRACT

The modern economy is increasingly based on knowledge and, more broadly, on intangible assets that ensure sustainable innovation growth. The formation of an innovative type of knowledge economy can be considered one of the fundamental development trends at the global level.
The modernization of the economy in the lifetime period means the introduction of modern technologies, increasing energy efficiency and labor productivity, producing high-quality products according to the most advanced standards. Ultimately, this is the creation of a competitive economy.
Keywords: Casting, billet, castings, method of making castings, injection molding, centrifugal casting, investment casting, shell casting, chill casting.

Relevance of a problem. In structure of domestic engineering industry, the essential part is assigned to castingproduction which serves as the keybillet base of this economic complex. As it is known, consumers of castings are all branches of mechanical engineering and therefore possibilities of their development largely depend on a condition of casting production. This defines the great economic importance of casting production and its role in providing branches of mechanical engineering with billets. It is specified in special literature that advantages of producing billets by methods of casting is the possibility of producing various sizes and weights and the most complex geometrical forms, a short cycle of production, rather low production cost, high mechanical and operational properties of cast alloys, possibility of producing products from the materials unmachinable under pressure[1].
Cast billets are most close to finished partsin size and configuration, and their mechanical processing capacity is less than the billets produced by other technological methods. Thus, one of the main requirements for castings is to increase their geometric accuracy and purity of the treated surface, as well as to reduce the weight and maximum approximation of the shape and size of castings to the finished products. This ensures metal savings both in the production and consumption of castings.
It is important to highlight that throughout the entire existence of casting production, the demand for maximum approximation of the configuration of castings to the shape of the finished product was the key trend in the development of casting production. However, the state of works in casting production cannot be considered satisfactory, which reflects, moreover, the data on utilization factor of metal. Our analysis on the indicators of various branches of mechanical engineering shows that the processing of castings into chips on average takes from 20 to 30% of castings weight, which is about half as when making parts from forgings.
Accuracy of geometrical forms of castings and purity of their surface in essential depends on how they are made. The most progressive, in this regard,ways of producing castings are exact methods of casting: injection molding, centrifugal casting, investment casting, shell casting,chill casting, etc. Their key advantage in comparison with production of castings in sand-earth forms is to provide high-quality surface of billets, lack of spatial deviations and high accuracy configuration.
A significant increase in the efficiency of casting production is achieved with the use of chill casting. Calculations oncasting materials show that this type of casting provides a metal saving of 2- 10% by reducing the weight of the billets; 11-23% decrease in machining labour intensity by increasing the accuracy of casting sizes and reducingsurface roughness; 8-63% decrease in the cost of billets of parts; improving the quality of produced parts. The latter is achieved due to the fact that chill castingincreases the density of castings and improves its structure, as a result of which mechanical properties increase by 15-30%.An efficient method of producing castings is also centrifugal casting, at which high quality cast parts and metal savingsare achieved due to increased yield of sound casting and reduction of allowance for mechanical processing. By changing the design of pattern and using a replacement insert, this method is also used under small-scale production conditions,

ISSN: 2663-8770, E-ISSN: 2733-2055
ETM
EQUİPMENT, TECHNOLOGİES, MATERİALS

which, according to the approximate calculations of individual authors, allows reducing the labor input of 1 ton of castings from 67 to 35.7 rate - hour, or by 46.7%.

Injection molding is a very economical and productive method of producing castings. The advantage of this method is that it enables to producethin-walled parts of complex configuration; complete elimination or minimization of subsequent mechanical processing; saving of expensive non-ferrous metal by 13-67% is achieved; significant decrease in losses from rejects, which are 1.6-3.0times less than with sand casting method.

With a number of economic advantages over other methods of producing billets, according to implemented models casting has been widely used in domestic engineering. This method allows producing castings with a high accuracy and surface purity. Metal saving reaches 40-60%, and further mechanical processing is sharply reduced or eliminated.

One of the progressive and relatively young technological processes in casting is shell casting. This method can provide metal saving due to reduction of cast weight by 15-20%, reduction of manufacturing labour intensity by 30-50%.

In most cases, the use of accurate casting methods allows producing castings with less material and labor costs, while reducing the technological cycle, the volume of suitable casting with area of 1 m² is increased and, accordingly, a lower cost is achieved.

Despite progressive and effective casting methods, the method of producing castings using sand molds (80.2% of the total casting output) prevailed in cast steel production. Meanwhile, it is generally known that the method of producing castings is the least productive compared to other more progressive methods-it does not provide sufficiently high accuracy and surface purity of the cast products, requires high metal consumption and the use of mechanical processing, etc., which ultimately leads to a significant increase in the cost of castings and products made from them. The form made of the ground cannot be reused, a lot of dust, dirt, etc. is released from the ground when making the forms, which negatively affects human health, safety, industrial injuries and occupational diseases.

Currently, one of the predominant method of casting in the republic is the production of castings using sand molds, which accounts for more than 82.2 of the total output, including 87.16 for cast iron and 82.5% for the rest.

The global economic crisis of the beginning of the 21st century, which hit Azerbaijan industry, was reflected in a significant drop in production, an increase in unemployment and sharp decline in economic indicators, especially in engineering. Problems in casting of the machine-building complex have accumulated for decades due to the lack of investment in the reconstruction and construction of workshops, low degree of implementation of scientific and technical developments and daily use of outdated technologies and materials.

In the republic, as a result of the liquidation of advanced castings or the privatization by non-competent people, the drop in production level amounted to more than 75%. Raiding, forced bankruptcy of casting shops and organizations, unemployment among high-quality specialists and workers have reached mass levels.

Enhancing the application of liquid self-solidifying mixtures in manufacture of molds and rods is the reserve for improving quality, reducing labor intensity and on this basis the cost of manufacturing castings. High strength and gas permeability of molds and rods made of liquid self-solidifying mixtures improves the quality of casting, and significantly reduces rejects.

Labour intensity of rod production is reduced by half, which provides an increase in labor productivity, in addition, a decrease in fuel consumption for rod drying and savings in wages are achieved.

With regard to casting, the implementation of these tasks determines two main technical directions for the development of the industry.

The first direction is to implement technological processes, materials and casting equipment, which ensure the production of accurate castings with maximum approximation in size and weight to finished part, and therefore with minimal allowance for mechanical processing.

The second direction is the comprehensive mechanization and automation of all processes of casting production, providing an increase in productivity and a radical improvement in the working conditions of casters.

Implementation of these directions can be performed both by introduction of new, more advanced technological processes, materials, equipment, means of mechanization and automation of production, and by improvement of existing ones[2].

The high pace of development of mechanical engineering requires a significant increase in the volume of production of billets, an increase in their quality, and a change in the structure of production. The main tasks of casting development include:

- Acceleration of productivity growth through the creation and implementation of new high-performance equipment, machine systems, complex mechanization and automation of production processes and management systems:

- improvement of quality, reliability, accuracy and purity of casting surface with their optimal approximation to the sizes of finished parts:
- reduction of mechanical processing, reduction of billet and parts mass by 15-20% and introduction of progressive alloys and technological processes:
- further improvement of casting structure to increase the specific gravity of castings from high-quality cast iron and alloys with improved physical and mechanical properties;
- deepening of specialization and concentration of casting production

After the collapse of the Soviet Union, noany melting shop has been established in Azerbaijan. On the contrary, two mould casting plants Baku Steel Plant and “Sentrolit”have been completely destroyed and are out of service. The rest of the existing workshops operateusing outdated methods and this negatively affects the development of machine-building production. For example, in Russia, new workshops provide “Gusar”reinforcing plant with high-quality billets which comply with all the standards and requirements for the production of wedge and gate valves.

Casting production is equipped with the following equipment: smelting furnaces manufactured by Inductotherm (England), molding line manufactured by “FAT” (Germany) thermal furnaces Bosto (Slovenia), blasting equipment Wheelabrator (Germany). Manufactured mold patterns are performed on 3 and 5 CNC axial machines using CAD /CAM/ CAE – projection systems. The design of castings is developed using a specialized software complex for modeling the conditions of crystallization MagmaSoft [3].

Similar products are produced by OJSC Baku Machine-Building Plant

Advantages of foundry Gusar LLC

1. Own design-engineering department - development of structures in the SoliWorks using modeling programs for crystallization process MagmaSoft;
2. Manufacturing mold patterns on CNC machine - reduction of manufacturing time of patterns and increase in geometric accuracy;
3. Production for a chrome sand casting mixture - improves the quality of casting surface and increases the density and continuity of metal, eliminates shrinkage porosity:
4. Control of melting furnaces using software - provides improvement of metal quality:
5. Cast molding from joinery ladle– excludes "slag blow hole" type defects in castings:
6. Thermal furnaces with programmed control provide uniform temperature distribution in working space of the furnace, which improves the quality of heat treatment;
7. Control is performed for all technological processing of casting with recording the data in factory control journals and centralized electronic database.

Installed and operated main technological and laboratory equipment allows producing castings:

- from carbon (low-carbon and medium-carbon) non-alloyed ferrite and ferrite - pearlite steels;
- from carbon low- alloyed steels, including cold resistant, pearlitic classes;
- from middle-alloyed steels including heat-resistant, heat-resistant pearlite-ferrite and pearlite-martensitic classes;
- from high-alloyed non-corrosive, heat-resistant ferrite, martensitic, martensitic-ferrite, austinite-ferrite and austinite steels.

The level of production and equipment shows the quality of casting. Therefore, reducing the metal consumption of castings and their manufactured parts, as well as improving their operational properties, are the most important tasks of casting production and its solution should be comprehensively stimulated, including with the help of wholesale prices for castings. However, progressive changes in this direction occur at slower paces than required. The difficulties in solving these problems are caused primarily by the fact that additional costs are usually requiredto improve the quality of casting production. Therefore, when adequate compensations are not available for these costs, it becomes unprofitable for enterprises to introduce new equipment and technology. This obstacle becomes particularly difficult in casting production, where poor sanitary and hygienic working conditions cause a chronic shortage of labour, and therefore even a slight decrease in the profitability of production and, as a result, economic stimulus funds, due to the introduction of an economically disadvantageous innovation, can lead to personnel leakage and significantly hamper the implementation of production plans.

ISSN: 2663-8770, E-ISSN: 2733-2055
ETM
EQUİPMENT, TECHNOLOGİES, MATERİALS

However, despite the high growth rate in the production of castings, the demands for mechanical engineering are not fully satisfied by casting production. Some industries of mechanical engineering are constantly experiencing lack of small and complex castings. A significant part of the castings is made with excessive allowance for mechanical processing, which leads to additional loading of machines and an increase in the cost of machines. The metal utilization factor is 0.85 for casting iron and 0.75 for cast steel.

The main direction of technological progress of cast production is to improve the accuracy of castings of the operational reliability of cast parts. A significant reserve for improving efficiency is to develop the concentration and specialization in cast production.

Analyzing the formation and development of cast production in the republic, it should be stated that it has long developed as an auxiliary production within engineering enterprises, which were built based on the principle of a closed production cycle. Almost every machine-building enterprise had a small foundry or workshop and produced the necessary cast stamping, forging, etc. Thus, the small-batch manufacturing was dominant for a long period. Currently, many enterprises also continue to maintain small foundry plants. This negatively affects the quality and cost of castings, which is due to the technical backwardness of a significant part of the key production assets of cast production, as well as the shortcomings of the current pricing system and the evaluation of the operation of cast shops.

The radical improvement of the state in cast production, in our opinion, could be facilitated by the separation of this industry into an independent one with an appropriate central management scheme.

Considering the importance of cast products for the national economy, the separation of new industry management body can be carried out on the basis of enterprises that deal with the manufacture of machine-building casting. At present, many enterprises producing products of their own use have the potential to increase sharply the output and, accordingly, increase technical and economic indicators. However, the owner of these enterprises, as a rule, is not interested in capital investment and in further expansion of production volumes, and even more so in their reconstruction, since the available capacity mainly provides their needs, and the supply of casting to the side does not improve the performance of their production and economic activities.

The subordination of such enterprises to one center opens up opportunities for the development of specialization and concentration of production, the widespread use of advanced methods and technology, mechanization and automation of production processes. The tasks of liquidation of non-promising enterprises, workshops and areas are being solved, which will ensure the increase in the production efficiency in the relevant branches of mechanical engineering [4].

The implementation of this proposal on castingwill significantly facilitate the solution of complex tasks on planning, management and pricing due to the specifics of the industry. So, for example, in the USSR, the Ministry of machine tool and tool building industry created a special association, including more than ten casting plants. This significantly increased the production in the industry using special casting methods.

As a result, the highest increase is achieved in the manufacture of chill castings and by centrifugal method, injection molding, according to melted models, by continuous method [5].

Currently, most of these plants have successfully introduced expensive equipment and as a result provide machine builders with high-quality casting.

One of the key indicators of the development of cast production is a casting yield from a metal charge. At a high casting yield the costs of sound casting and the consumption of charge materials are reduced.

Analysis of technical and economic performance indicators of casting enterprise in the republic shows that in the overwhelming majority of cast plants the volume of casting yield is lower than the optimum size (according to foreign and domestic researchers, the minimum allowable capacity of iron foundry is currently 10 thousand tons of cast per year). According to our calculations, the implementation of the proposal on specialization and concentration of foundry will reduce the number of foundry shops and sites; iron foundry from 87 to 49 units and increase the average capacity of foundry from 8,300 tons to 14,500 tons of steel casting - from 53 to 36 units, and increase the average capacity of the workshop from 4600 to 6800 tons and finally non-ferrous foundry - from 88 to 49 units and increase the average capacity of the workshop from 680 to 1000 tons of cast per year [6].

As the analysis of the experience of foreign foundries and sites shows, due to the use of more advanced equipment and high level of mechanization and automation, as well as effective methods of organizing

production, we may significantly increase the technical and economic performance. Estimated calculations show that an increase in the average capacity of iron foundries from 8,300 to 14,500 tons of cast per year allows increasing labor productivity averagely for 60-70%, or from 34.5 to 55-59 tons per year, while reducing the average cost of 1 ton of annual cast. Technical level of casting production is determined by the volumes of casting yield by progressive methods, using the machine method of making molds and rods, mechanized casting of liquid metal on casting conveyers, as well as by complex-mechanized and automatic flow lines in general.

The characteristic of foundry is uneven level of mechanization and automation in various areas of the main production. As a result, there is an imbalance in the productivity of the interconnected production departments of foundries, which hampers the complex mechanization and automation of the foundry as a whole and improvement of its effectiveness. At the same time, the level of mechanization and automation of the most labor-intensive processes is very low.

Herewith, the level of mechanization and automation of the most labor-intensive processes is very low.

CONCLUSION

The efficiency of improving the technical capabilities of cast production is achieved not only by quantitative growth or qualitative replacement of foundry equipment, but also by wide use of progressive technological processes and special casting methods, which make it possible to mechanize and automate production as much as possible and sharply reduce the labor intensity of casting and increase labor productivity. There are currently about 50 different methods of making casting in the foundry. These methods can be divided into two large groups by types of moulds used; casting into one-time green sand casting and permanent metal castings.

REFERENCES

1. Мирский Э.М. и др. Научная политика XXI века: тенденции, ориентиры и механизмы. Науковедение. 2003. jsfo 1 (www.courier.com.ru).
2. А. А. Минаев, «современные представления о закономерностях развития технологии литейного производства».литье и металургия. 3(38).2000г.с.40-49
3. и. А. Дибров, « состояние и основные направления развития литейного производства россии». Литье и металургия. 4..2000г. С.91-93.
4. Литье по выплавляемым моделям :моногр. / с. А. Казеннов [и др.] ; под ред. Я. И. Шкленника, в. А. Озерова. – 2-е изд., перераб. И доп. – м. : машиностроение, 1971. – 436 с.
5. Алиев э.а. «цена и качество в литейном производсте» ж. «литейное производства» г.москва 1990г. № 12. . С. 17.
6. Голеусова г. З. Совершенствование ценообразования на литейную продукцию // там же. 1989. № 9. С. 24.

ISSN: 2663-8770, E-ISSN: 2733-2055
ETM
EQUİPMENT, TECHNOLOGİES, MATERİALS

CYCLIC TORSION WITH INTERNAL PRESSURE OF PRE-STRETCHED THIN-WALLED CYLINDERS

[1]Alasgar Gulgazli, [2]Ali Hikmat Ahmadov

[1]Azerbaijan State Oil and Industry University, Doctor of Technical Sciences, Professor (Azerbaijan)

[2]Azerbaijan State Oil and Industry University, PhD in Technical Sciences.Associate professor.

E-mail: [1]alesker.gulgezli@mail.ru; [2]alihikmat.ahmedov@asoiu.edu.az

ABSTRACT

The article considers the following two tasks. 1) Strength calculations are carried out for a long thin-walled cylinder, the ends of which are not closed during reloading. At the first loading, the thin-walled cylinder is stretched by a longitudinal force leading to longitudinal plastic deformations. When reloaded, the cylinder twists and at the same time uniform pressure acts from the inside. It is noted that, in particular, the shaft of wind generators is subjected to such loading. It is proved that the equation of the yield curve in the plane of the normal and tangential stresses of the stress space is an ellipse, whose semi axes are a function of the mechanical characteristics of the material and the residual stresses after the first loading. 2) We consider cyclic twisting with internal pressure of pre-stretched thin-walled cylinders. The yield surface equation is obtained for a thin-walled cylinder under repeated loading τ + p. which stretched upon first loading.
It is proved that the yield surface equations also yield the fatigue surface equations if the yield stress $\sigma_{T.}$ is replaced by the fatigue stress $\sigma_{0.}$
Expressions are found for the number of cycles required for fatigue failure under an asymmetric loading cycle under repeated loading.
It is proved that in order to increase the number of cycles required for fatigue fracture, during the first loading, when the material is strengthened due to plastic deformation, and with repeated cyclic loading, the same stress components must take place. It is proved that if during repeated loading the end of the loading path is inside the endurance surface, then the number of cycles required for fatigue failure in an asymmetric loading cycle tends to infinity.
Keywords: Initial loading, reloading, cyclic loading, strength, fatigue failure, plastic deformation, residual stress, yield surface.

INTRODUCTION

This cyclic loading occurs, for example, on the shaft of wind turbines. Wind turbines have three blades. The fewer blades a turbine has, the higher its rotation speed and the lower the torque generated on the shaft. The more blades in size, the higher the torque and the lower the rotational speed due to the increase in drag. The lower the speed, the more complex the system of gearboxes transmitting rotation to the generator shaft. Therefore, the three-blade design is recognized as optimal, at least for mega-watt installations.
Formulation of the problem. The stresses arising in the cylinder will be denoted using the local Cartesian coordinate system by x, y, z (see Fig. 1): the x-axis is parallel to the generatrix of the cylinder, the z-axis is directed tangentially to the midline of the cross-section, the y-axis is the continuation of the radius R.

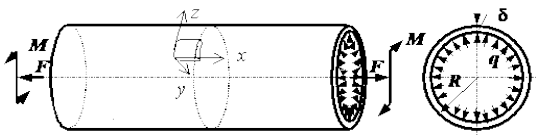

Fig. 1. General view of a loaded thin-walled cylinder and its cross-section.

Suppose, during the first loading, a thin-walled cylinder is stretched by a longitudinal force. Because of the thinness, it is assumed that the stress state in the cylinder will be uniformly, i.e., it does not change from point to point of the cylinder and changes only when the tensile force changes. The stress components at the first loading will be:

$$\sigma_{xx} = \sigma_0; \qquad \sigma_{xy} = \sigma_{xz} = \sigma_{yy} = \sigma_{yz} = \sigma_{zz} = 0 \tag{1}$$

ISSN: 2663-8770, E-ISSN: 2733-2055
ETM
EQUİPMENT, TECHNOLOGİES, MATERİALS
EQUİPMENT, TECHNOLOGİES, MATERİALS
VOLUME 05 ISSUE 01 2021

Upon repeated loading, the cylinder is twisted and at the same time a uniform pressure acts from the inside, i.e. the repeated loading is M + P (the ends of the cylinder are not closed). In this case, the components of the stress tensor $\sigma_{zz} = \sigma_z$ and $\sigma_{yz} = \tau$ are nonzero.
In [1], an equation obtained for the loading surface was in the following form:

$$\mathcal{I}_1^2 + 2(1+\nu)\mathcal{I}_2 = \frac{k_0+1}{2}\left[\mathcal{I}_1^{0^2} + 2(1+\nu)\mathcal{I}_2^0\right] \quad (2)$$

Where $\mathcal{I}_1$ and $\mathcal{I}_2$ are, respectively, the first and second invariants of the stress tensor under repeated loading, and $\mathcal{I}_1^0$ and $\mathcal{I}_2^0$ are under the first loading, ν is Poisson's ratio,

$$k_0 = \sqrt{\frac{2k^2}{\mathcal{I}_1^{0^2} + 2(1+\nu)\mathcal{I}_2^0} - 1} \quad (3)$$

$2k^2 = \sigma_{1T}^2 + \sigma_{2T}^2$; σ_{1T}, σ_{2T} – yield strength in tension and compression, respectively. We will assume that $\sigma_{1T} = \sigma_{2T} = \sigma_T$. Then the first and second invariants of stresses under the first loading, respectively, will be:

$$\mathcal{I}_1^0 = \sigma_0\,; \quad \mathcal{I}_2^0 = 0 \quad (4)$$

and upon repeated loading

$$\mathcal{I}_1 = \sigma_z\,; \quad \mathcal{I}_1 = \tau^2 \quad (5)$$

Substituting (4) into (3), we obtain:

$$k_0 = \frac{\sqrt{2\sigma_T^2 - \sigma_0^2}}{\sigma_0} \quad (6)$$

Moreover, it is assumed that $\sqrt{2}\sigma_T > \sigma_0 > \sigma_T$. Substituting (4), (5), (6) in (2), we get

$$\sigma_z^2 + (1+\nu)\tau^2 = (\sqrt{2\sigma_T^2 - \sigma_0^2} + \sigma_0)\sigma_0 \quad (7)$$

Divide both parts (7) into

$$k_1 = (\sqrt{2\sigma_T^2 - \sigma_0^2} + \sigma_0)\sigma_0$$

Then

$$\frac{\sigma_z^2}{k_1^2} + \frac{\tau^2}{k_2^2} = 1 \quad (8)$$

where

$$k_2^2 = \frac{k_1^2}{2(1+\nu)}$$

Equation (8) is the equation of an ellipse with semiaxes k_1 and k_2.
In [5],was obtained the following expression for the number of cycles required for fatigue failure under an asymmetric loading cycle.

$$N = \frac{2\sigma_T^2}{\left[\left(\mathcal{I}_1^2 + 2(1+\nu)\mathcal{I}_2 - (1+\nu)\sigma_{ij}\sigma'_{ij} + \nu\mathcal{I}'_1\mathcal{I}_1\right)\right](1-k_B)} \quad (10)$$

Where

$$\mathcal{I}_1 = \sigma_{ij}g_{ij};\ \mathcal{I}'_1 = \sigma'_{ij}g_{ij} \quad (11)$$

σ'_{ij} end σ_{ij}- respectively, the stress values at the beginning and at the end of the cycle. In (10) and (11), the summation from 1 to 3 is performed over the repeated indices i, j.

$$k_B = \sqrt{\frac{2\sigma_B^2}{\mathcal{I}_1^2 + 2(1+\nu)\mathcal{I}_2} - 1} \quad (12)$$

σ_B - endurance limit.
In [2], was obtained an equation for the yield surface for the initial loading in the following form:

ISSN: 2663-8770, E-ISSN: 2733-2055
ETM
EQUİPMENT, TECHNOLOGİES, MATERİALS

$$\mathcal{J}_1^2 + 2(1+\nu)\mathcal{J}_2 = \sigma_T^2$$

and the equation of the endurance surface in the form:

$$\mathcal{J}_1^2 + 2(1+\nu)\mathcal{J}_2 = \sigma_в^2$$

As can be seen from the last two equations, in order to obtain the fatigue surface equation in the first equation, the yield stress σ_T should be replaced with the fatigue limit $\sigma_в$. If we take into account the second equation in (12), we obtain $k_в = 1$, then the denominator of the right-hand side of (10) turns to zero and the number of cycles required for fatigue failure under an asymmetric loading cycle tends to infinity.

It was obtained in [5] that

$$\sigma_{ij}^* = \frac{1-k_0}{2}\sigma_{ij}^0 \tag{13}$$

Expressions (13) determine the residual stresses after loading with stresses $\sigma_{ij}^* = 0$, where $k_0 = 1$ is determined by formula (3).

It is known that when there are no plastic deformations [3] and as seen from (13). Thus, residual stresses arise only in the presence of plastic deformation. Based on (13) for this problem we have:

$$\sigma_x^* = \frac{\sigma_0 - \sqrt{2k^2 - \sigma_0^2}}{2} \tag{14}$$

Based on (13), we find that all other components of the tensor $\sigma_{ij}^{'}$ are equal to zero. From (11) and (14)

$$\mathcal{J}_1' = \sigma_x^* = \frac{\sigma_0 - \sqrt{2k^2 - \sigma_0^2}}{2} \tag{15}$$

J1, J2 are determined from (5).

Now let us determine the components included in the denominator of equality (10). For this problem, taking into account (5)

$$\mathcal{J}_1^2 + 2(1+\nu)\mathcal{J}_2 = \sigma_z^2 + 2(1+\nu)\tau^2 \tag{16}$$

The tensor σ_{ij}' differs from zero only $\sigma_{xx}^{'} = \sigma_x^{'}$, all other components are equal to zero, because at the beginning of repeated loading there are only initial stresses, therefore, from (14)

$$\sigma_{xx}^{'} = \sigma_x^{'} = \sigma_x^* = \frac{\sigma_0 - \sqrt{2k^2 - \sigma_0^2}}{2} \tag{17}$$

$$\mathcal{J}_1' = \sigma_x^* = \frac{\sigma_0 - \sqrt{2k^2 - \sigma_0^2}}{2} \tag{18}$$

The tensor σ_{ij} is nonzero $\sigma_{xx} = \sigma_x$ and $\sigma_{xz} = \tau$, all other components are zero. Then from (17)

$$\sigma_{ij}\sigma_{ij}' = \sigma_z \frac{\sigma_0 - \sqrt{2k^2 - \sigma_0^2}}{2} \tag{19}$$

Substituting (16) into (12) we have:

$$k_в = \sqrt{\frac{2\sigma_B^2}{\sigma_z^2 + 2(1+\nu)\tau^2} - 1} \tag{20}$$

Substituting (16) - (20) into (10) for the denominator of the right-hand side, we obtain:

$$\mathcal{J}_1^2 + 2(1+\nu)\mathcal{J}_2 - (1+\nu)\sigma_{ij}\sigma_{ij}' + \nu\mathcal{J}_1'\mathcal{J}_1 =$$

$$= [\sigma_z^2 + 2(1+\nu)\tau^2 + \nu\frac{\sigma_0 - \sqrt{2k^2 - \sigma_0^2}}{2}(\tau + \sigma_z)](1 - \sqrt{\frac{2\sigma_B^2}{\sigma_z^2 + 2(1+\nu)\tau^2} - 1}) \tag{21}$$

As can be seen from this expression, with an increase in σ_0, the denominator increases, hence the number of cycles required for fatigue failure decreases. The denominator decreases due to the component $(1+\nu)\sigma_{ij}\sigma_{ij}'$. This

means that in order to increase the number of cycles required for fatigue failure during the first loading, when the material is hardened due to plastic deformation, and during repeated cyclic loading, the same stress components must occur, and the larger the number of the same stress components, the stronger the increase the number of cycles required for fatigue failure. It should be noted that for fatigue failure of structural parts, the end of the path during repeated loading must be located between the loading and endurance surfaces.
At the end, we note the main conclusions of this section.

Conclusion

1.An equation for the yield surface is obtained for a thin-walled cylinder under repeated loading τ + p. which was stretched at the first loading.
2. It is proved that the equations of the yield surface also give the equations of the fatigue surface, if the yield stress σ_T is replaced by the fatigue limit $\sigma_{в.}$
3. Expressions are found for the number of cycles required for fatigue failure under an asymmetric loading cycle under repeated loading.
4. It has been proved that in order to increase the number of cycles required for fatigue failure during the first loading, when the material is hardened due to plastic deformation, and during repeated cyclic loading, the stress components of the same name must occur.
5. It has been proved that if during repeated loading the end of the loading path is inside the fatigue surface, then the number of cycles required for fatigue failure under an asymmetric loading cycle tends to infinity.

REFERENCES

1. A.S., Gulgazli Energy condition of plasticity ISSN 0021-8944, Journal of Applied Mechanics and Technical Physics, 2018, Vol. 59, No. 2, pp. 310–315.
2. А. С. Гулгазли Пластичность и длительная проч2ость при повторном нагружении. LAPLAMBERT Acad.Publishing., Saarbrücken, Germany 2017; с. 307
3. Ю.Я.Логинов, В.А.Шерстнев. Об одной особенности сопротивления меди циклическому нагружению. Деп. В ВИНИТИ, №2242 - В 86, 1986
4. Структурные уровни пластической деформации и разрушения. Панин В.Е., Гриняев Ю.В., Данилов В.И. и др. - Новосибирск: Наука. Сиб. отделение, 1990, стр.8-9
5. Gulgazli A.S., Abbasov S.H. Babayev A.M. New energy theory for endurance when loading is asymmetric. The USA Journal of Applied Sciences. USA www.cibunet.com №3,2016,p.31-35

ISSN: 2663-8770, E-ISSN: 2733-2055
ETM
EQUİPMENT, TECHNOLOGİES, MATERİALS

DETERMINATION OF THE RELATIONSHIP BETWEEN THE WEAR RATE OF GRINDING BALLS IN THE SAG MILL MILL AND THE PARAMETERS THAT CONTROL THE PROCESS

Famil Hamidov

"Azerbaijan International Mining Company", Grinding manager.

E-mail: famil-433@mail.ru

ABSTRACT

Since the end of the 20th century and the beginning of the 21st century, as a result of the large-scale implementation of the industrialization policy in Azerbaijan, a large number of industrial enterprises with powerful potential have been created. Based on this, the volume of industrial production over the past 10-15 years has increased 2.7-3.0 times. The current state of the country's economy has created ample opportunities for the development of the non-oil sectors along with the oil sector. At the same time, attention is drawn to the variety and speed of work on the extraction of precious metals.

Azerbaijan International Mining Company (AIMC) is one such company and is currently engaged in exploration, production and processing at the Gadabay deposit.

The high technology used here and the associated equipment and tools emphasize the need to apply and update recovery technologies, as well as various improvements over time. One of the main directions of scientific and practical work carried out here is to increase the resistance of grinding balls to corrosion.

The article is devoted to determining the relationship between the wear rate of grinding balls of a semi-autogenous grinding mill and the parameters that control the process.

Keywords: industrialization, industrial production, non-oil sector, mining company, drum mill, grinding balls, wear, the relationship between process controllers.

INTRODUCTION

Azerbaijan International Mining Company, operating in Azerbaijan since 2009 (51% - Azerbaijan, 49% Anglo Asian Mining PLC), began to extract gold (2009), silver and copper (2010) at the Kedabek mine, and since 2013 - at the site Double. provides gold mining. Precious metals at the Gadir site will be available from the summer of 2015, and at the Ugur mine - from the fall of 2017. Besides, AIMKL was instructed to continue geological exploration work and carry out the processing process [1]. As a whole, AIMKL was instructed to conduct exploration, mining and processing at 6 locations (-1 in Nakhchivan, -2 in Kedabek, -3 in Kelbajar and Zangilan).

The production capacity of the enterprise was 2,200 tons / day until 2013, but in 2013, as a result of modernization, the company increased it to 4,000 tons / day, and in 2020 to 6,000 tons/day.

The efficiency of the processing process at the enterprise is related to the energy consumption of the mills used here, as well as the intensive consumption of linings and balls. For this reason, all research work to reduce them is relevant.

The purpose of the work. Determination of the relationship between the wear rate of grinding balls in the SAG Mill mill and the parameters that control the process

Materials and research methods. As a result of our research, it was determined that the average daily ball consumption in mills is 2.2-2.5 tons for d = 40 mm; 1.0-1.1 tons for d = 100 mm. This is 90-120 tons / month for balls with an average monthly ball consumption d = 40 mm; For spheres with d = 100 mm, it is equal to 31-33 tons / month. In addition, balls with diameter d = 125 mm were used in the tests.

The test balls were manufactured in Baku Oil Drilling Equipment CJSC and Baku Steel Casting OJSC based on the technology produced in Turkey and Ukraine, as well as the technology offered by us.

From the methodological point of view, each time the mill was stopped for a short time after 100 hours of operation, 10 balls d = 100 and d = 125 mm were taken from them and subjected to measurements.

Results and their discussions. In order to assess the effectiveness of the balls against corrosion and spillage in the experimental tests, 100 balls with a diameter of 70 mm and a weight of 6 tons, a diameter of 100 and a weight of 12 tons, as well as 100 balls with a diameter of 125 mm were made according to the proposed technology [2].

The use of a diameter of 125 mm was adopted in order to distinguish them from the wear and tear that occurs in them. Table 1 shows a comparison of the amount of food consumed in the spheres prepared and operated on the basis of existing and proposed technology.

ISSN: 2663-8770, E-ISSN: 2733-2055
ETM
EQUİPMENT, TECHNOLOGİES, MATERİALS
EQUİPMENT, TECHNOLOGİES, MATERİALS
VOLUME 05 ISSUE 01 2021

Table 1

Comparison of the amount of food consumed on the basis of existing and proposed technology

№	Name of ore deposit and diameter of spheres used	Erosion by diameter of spheres,%				
		Service life, days				
		3	5	10	15	20
1	Gadir, d = 100 mm d=125 mm	3,8	9,4	26,8	51,5	-
		2,3	5,7	14,8	28,7	40,5
2	Gadabay d = 100 mm d=125 mm	3,2	7,8	21,6	44,4	56,4
		1,8	4,1	12,8	23,8	37,4
3	Uqur, d = 100 mm d=125 mm	2,6	6,2	14,4	34,6	48,5
		1,5	3,2	8,1	16,2	23,8

As can be seen from the analysis of the Y change in the spheres with diameter d = 100 mm, the value of this change in the Ugur, Gadabay and Gadir fields after the first 3 days is (2.6 - 3.8) / (1.5-2.3), respectively. , After 5 days (6,2-9,4) / (3,2-5,7), after 10 days (14,4 - 26,8) / (8,1-14,8), after 15 days (34.6 - 51.5) / (16.2-25.7).
The comparative analysis shows that although the ore from the Qadir field loses more than 50% of its size on the 15th day of operation when processed using existing balls, the proposed balls are able to maintain their capacity and only 32.5% of their resources are available on the 20th day of operation. % used. This indicator was more effective in ores with low hardness.
In general, the resources of the spheres made on the basis of the proposed technology are on average 13.6-18.1% more than the existing ones.
Experiments have shown that the hardness of the processed ores and the speed of rotation of the mill have a significant impact on the rate of change (wear) of the balls in diameter compared to other factors.
In addition, based on numerous experiments in research and the results of repeated studies (Y = f (t), Y = f (H) and Y = f (V)) in the MILLTRAJ simulation program, The existence of the following empirical relationship between:

$$Y=k\cdot(H+4)\cdot Va\cdot Tc=(0{,}012\cdot H+0{,}048)\cdot V0{,}2\cdot T2 \qquad (1)$$

Here, the wear rate of Y spheres,%
V- speed of the mill, period / min;
T - service life of the mill, days.
H - hardness of the processed ore, on the Mohs scale;
k - correction factor, k = 0.012;
The results of using the empirical expression are given below.
Example 1: In a mill with a rotational speed of 13.1 rpm, let's determine the lost resource of the balls in the process of processing ore with a hardness of H = 5 on the Mohs scale (T = 12 days):

$$Y= k\cdot(H+4)\cdot Va\cdot Tc =0.012\cdot(5+4)\cdot V0{,}2\cdot T2 =$$

$$0{,}108\cdot 13{,}10.2\cdot 122 = 26{,}02\ \%.$$

Example 2: In a mill with a rotational speed of 13.8 revolutions / min, determine the lost resource of the spheres in the process of processing ore with a hardness of H = 3 on the Mohs scale (T = 18 days):

$$Y= k\cdot(H+4)\cdot Va\cdot Tc =0.012\cdot(3+4)\cdot V0{,}2\cdot T2 =$$

$$0{,}084\cdot 13{,}80.2\cdot 182 = 46\ \%.$$

Example 3: In a mill with a rotational speed of 14 revolutions / min, determine the lost resource of the balls in the process of processing ore with a hardness of H = 7 on the Mohs scale (T = 10 days):

$$Y= k\cdot(H+4)\cdot Va\cdot Tc =0.012\cdot(7+4)\cdot V0{,}2\cdot T2 =$$

$$0{,}132\cdot 140.2\cdot 102 = 22{,}38\ \%$$

As can be seen from the above reports, in Example 1 (T = 12 days), the spheres lost only 26.02% of their resources and can be exploited successfully. In Example 2 (T = 18 days), the spheres lost only 46% of their

ISSN: 2663-8770, E-ISSN: 2733-2055
ETM
EQUİPMENT, TECHNOLOGİES, MATERİALS

resources and their use was inefficient. In Example 3 (T = 10 days), the spheres lost only 22.38% of their resources and can be exploited successfully.
Results. Thus, based on the results of experimental work to determine the relationship between the wear rate of grinding balls and the parameters that control the process at the SAG Mill mill, an empirical expression was proposed for the purpose of operational control of the processing process.

REFERENCES

1. Габибов И.А.,Гамидов Ф.М., Чакраборти П.П. Результаты усовершенствований мельниц типа SAG, используемых в Азербайджанской международной горнодобывающей компании.// Известия уральского государственного горного университета, 2018. Вып. 2(50). С. 102-106.
2. Hamidov F.M., Habibov I.A. Establishment Of The Relationship Between Productivity And Technological Parameters Of The Process Of Grinding Ore In Ball Mills //International Journal of Innovative Technology and Exploring Engineering (IJITEE), VOLUME-9 ISSUE-1, NOVEMBER 2019

ISSN: 2663-8770, E-ISSN: 2733-2055
ETM
EQUİPMENT, TECHNOLOGİES, MATERİALS

EQUİPMENT, TECHNOLOGİES, MATERİALS

VOLUME 05 ISSUE 01 2021

MODELING THE HARDNESS AND POROSITY OF BRAKE PAD MATERIALS

Fikret Yusubov

"Azerbaijan State Oil and Industry University", junior researcher.

E-mail: fikratyusub@gmail.com

ABSTRACT

In this study, experiment were conducted to determine influental process parameters to the hardness and porosity properties of newly developed brake pad composites. Brake pad composites were preperad by traditional powder metallurgy methods. The development of friction brake pad specimens used in this work were based on a non-asbestos organic type formulation. The plan of experiments conducted to by 2-level design model using 5 factor on base L8 array. Results of analysis of variance showed that "plasticizer" was most important factor to influence both properties.
Keywords: friction composites, hardness, porosity, powder metallurgy, Taguchi's technique

Relevance of the issue: The safety is one of the key factors for achieving effiency of the brake system [1]. Brake couples are constantly subjected high thermomechanical loading during braking process. High thermal stresses are ultimately leads to increase wear and decrease friction properties. Non-stable friction characteristics affect the safety and overall performance of braking system [2]. For such reasons, new materials are constantly needed to meet modern requirments of industry. Nowadays, non-asbestos organic friction composites are most researched and demanded materials in various type of tribotechnical units [3]. These polymer composites not only used in consturction, textile, sporting good and etc. but are widely used in tribological areas as well, due to their excellent properties such as lightness, high strengh, cost-effetivness and simple processing features [4]. However, there is a still great demand for increasing the quality and further improving the properties of friction polymer composites [5]. Current trend in machine and application safety impose the development of new eco-friendly, low-cost and high thermally stable materials [6,7].
The purpose of the study: The purpose of this paper is to develop new sustainable friction material for medium or heavly loaded braking systems. The present work aim to establish correlation between design parameters and physical properties of new organic polymer composites.
Materials and equipment: The main constituents of brake pad materials are usually consist of these main components: space filler, binder, fibers abrasive and solid lubricants [8]. In this study phenolic resin was used as binder material. Barite was used as space filler. Eleven ingredients were selected as raw materials to prepare composite materials. The composite formulation was used by following weight proportions: 25% barite, 25% phenolic resin, 7% aluminum dioxide, 10% lead, 10% tin, 7% copper-graphite (80% Cu 20% C), 5% silicon dioxide and 5% wollastonite. The samples were fabricated in rectangular form (in size of 22.9 x 15.7 x 7.8 mm) by conventional powder metallurgy methods including ball-milling, dry mixing (for 16 hours with speed of 60 cycles/min on a horizontal drum mixer), following mixing with glcyerin (plasticizer), pressing (pre-forming and hot pressing) and sintering in muffle furnace (for 5 hours in 140°C).
The plan of experiments was conducted considering five parameters and two level design based on the Taguchi L8. Following parameters determined to produce specimens: heating tempearture (X1) and time (X3), plasticizer (X4), hot pressure (X2) and pressing time (X5). Levels of choosen variables are given in Tab.1.

Table 1.

Design factors and levels

Code	Design factors	Units	Levels	
			1	2
X1	Heating temperature	°C	160	120
X2	Hot pressure	MPa	25.5	10
X3	Heating time	min	155	20
X4	Plasticizer	wt.%	10	5
X5	Pressing time	min	40	5

The experimental results and analysis of variance (ANOVA) were processed by Minitab 19 software. Hardness of signal-to-noise ratios (S/N ratio) was calculated with setting goal of the experiment to "larger-the-better" and

ISSN: 2663-8770, E-ISSN: 2733-2055
ETM
EQUİPMENT, TECHNOLOGİES, MATERİALS

porosity S/N ratio was calculated using “smaller-is-better” criteria. S/N ratios were calculated using logarithmic loss function (1) and (2) [9].

$$\frac{S}{N}\,(\text{Hardness}) = -10\log\left[\frac{1}{n}\sum_{i=1}^{n}\frac{1}{y_i^2}\right] \quad (1)$$

$$\frac{S}{N}\,(\text{Porosity}) = -10\log\left[\frac{1}{n}\sum_{i=1}^{n}y_i^2\right] \quad (2)$$

Where, y - response for the given factor level, n - number of experiments
The hardness test was carried out using Brinell hardness testing method with a load of 62.5 kg·f and a steel ball with a diameter of 2.5 mm in accordance with with GOST 9012-59.
In order to calculate the porosity, the JIS D 4418: 1996 standard (Japan) was applied [10]. Samples were initially stored in a desiccator at room temperature for 24 hours. Before immersing the samples in oil, their mass was weighed on an electronic balance. The samples were then placed in an oil-filled container and stored in an furnace at 90°C ± 1°C for 8 hours. The tests used crude oil with a density of 0.850 g/cm3. Then the container with the specimen removed from the furnace was left at room temperature for 12 hours to cool the oil. Finally, the samples were rolled on a dry cloth several times for remove oil and weighed again. The percentage of porosity is calculated using the formula:

$$\text{Porosity}\,(\%) = \frac{m_2 - m_1}{\rho}\ \text{x}\ \frac{1}{V}\ \text{x}\ 100$$

where, m1 is the mass of the sample before immersion in oil (g), m2 is the mass of the sample after immersion in oil (g), ρ is the density of oil (g/cm3) and V is the volume of the sample (cm3).

Results and discussion: Tab.2 shows the response of hardness (Y1, HB), porosity (Y2, %) and corresponding S/N ratio (dB) values for each combination of the levels of the five factors. Obtained experimental data are converted to S/N ratio to estimate the quality characteristics of process.

Table 2.

Design of experiments and results

Run	Design matrix					Response		S/N ratio	
	X1	X2	X3	X4	X5	Y1	Y2	Y1	Y2
1	1	1	1	1	1	42.1	0.00012	32.4856	78.4164
2	1	1	1	2	2	34.5	0.00065	30.7564	63.7417
3	1	2	2	1	1	41.2	0.00024	32.2979	72.3958
4	1	2	2	2	2	40.5	0.00017	32.1491	75.3910
5	2	1	2	1	2	41.0	0.00020	32.2557	73.9794
6	2	1	2	2	1	33.6	0.00078	30.5268	62.1581
7	2	2	1	1	2	41.2	0.00023	32.2979	72.7654
8	2	2	1	2	1	33.7	0.00071	30.5526	62.9748

Brake friction materials must have efficient hardness and low porosity to ensure reliable friction by developing a improved contact surface [11, 12]. Based on the S/N ratio result, it is possible to determine which is the most influential factor in increasing the hardness and decrasing porosity. The ranking of input parameters using obtained result S/N ratios (Fig.1) are given in Fig.2.

ISSN: 2663-8770, E-ISSN: 2733-2055
ETM
EQUİPMENT, TECHNOLOGİES, MATERİALS
EQUİPMENT, TECHNOLOGİES, MATERİALS
VOLUME 05 ISSUE 01 2021

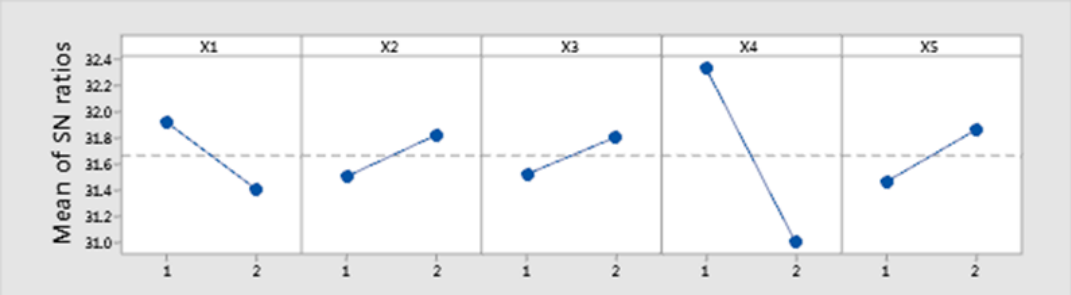

Figure 1. Main effect plots (data means) for the hardness

S/N ratio results for both parameter are almost the same, only hardness (Y1) are shown in Fig.1.It is clear from S/N ratio plots (Fig. 1) and ranking graphs that plasticizer (X4) (Fig. 2) is most significant parameter which is influences both response parameters. By performing ANOVA it can be determined the percentage contribution of each factor and interactions on output parameters.

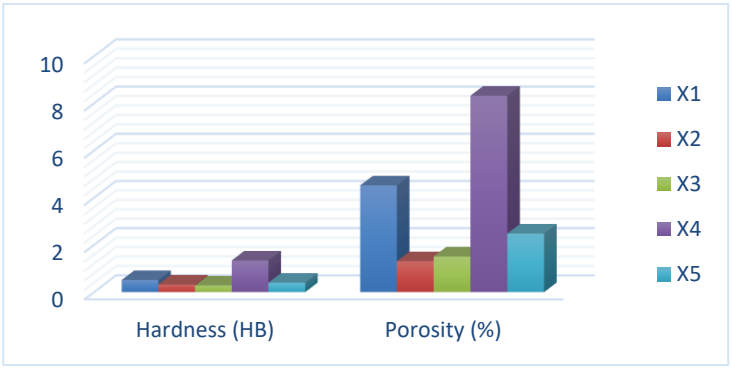

Figure 2. The ranking of design parameters

In order to understand the effect of chosen design parameters and their interactions ANOVA is studied at 95% level ($p \leq 0.05$) of confidence. The results of ANOVA for hardness and porosity are presented in Tab. 3 and 4, respectively. Obtained informations about significty of the factors and conditions were then used for final regression model.

Table 3.

ANOVA table for hardness

Source	DF	Seq SS	Contribution	Adj SS	Adj MS	F-Value	P-Value
X1	1	9.680	9.60%	9.680	9.680	1.63	0.330
X2	1	3.645	3.61%	3.645	3.645	0.61	0.516
X3	1	2.880	2.86%	2.880	2.880	0.48	0.559
X4	1	67.280	66.72%	67.280	67.280	11.30	0.078
X5	1	5.445	5.40%	5.445	5.445	0.91	0.440
Error	2	11.905	11.81%	11.905	5.952		
Total	7	100.835	100.00%				

Table 4.

ANOVA table for porosity

Source	DF	Seq SS	Contribution	Adj SS	Adj MS	F-Value	P-Value
X1	1	-	12.98%	-	-	1.48	0.348
X2	1	-	3.79%	-	-	0.43	0.578
X3	1	-	2.43%	-	-	0.28	0.651
X4	1	-	54.74%	-	-	6.24	0.130
X5	1	-	8.53%	-	-	0.97	0.428
Error	2	-	17.53%	-	-		
Total	7	0.000001	100.00%				

ISSN: 2663-8770, E-ISSN: 2733-2055
ETM
EQUİPMENT, TECHNOLOGİES, MATERİALS

Where, DF is degrees of freedom, Seq SS is sequential sum of squares, Adj SS is adjusted sum of squares, contribution is percentage of contribution. P-values of selected design factors from Tab.3 and 4 was higher than 0.05, which is proves that their significanty on hardness and porosity properties. ANOVA results confirmed that plasticizer is the most dominant control factor for hardness with 66.72% and porosity with 54.74%. After plasticizer (X4) following percentage of contribution were determined: X1-9.60%, X5-5.40%, X2-3.61% and X3-2.86% for hardness. Besides X1-12.98%, X5-8.53%, X2-3.79% and X3-2.43% for porosity. The results show that the effect of the factors for both parameters is very close to each other. This effect can be better observed in comparison of output parameters (Fig.3).

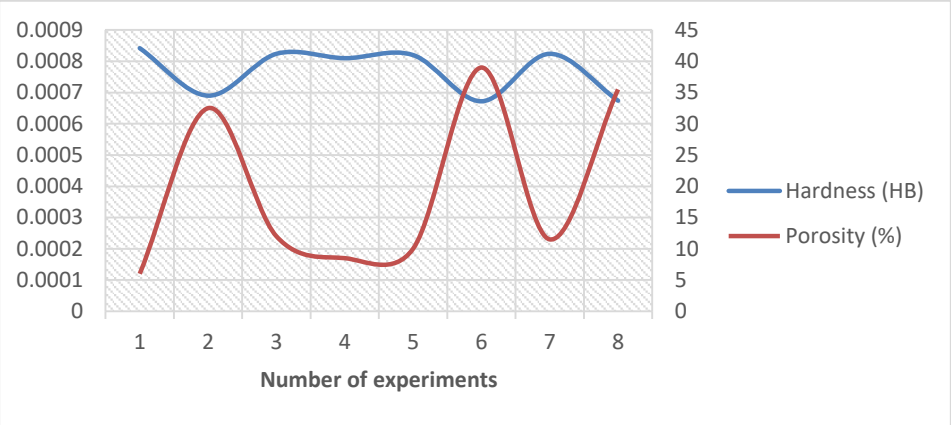

Figure 3. Comparison of the relationship between hardness and porosity

Fig. 4 shows that decrease of hardness leads to accordingly an increase in porosity percentage. It is known that lower porosity will result in higher friction coefficient and lower wear resistance due to higher contact areas between brake couples surfaces [12]. Plasticizer (X4) (Fig.4 a) and pressing time (X5) (Fig.4 b) with dependence of heating temperature (X1) are great influence on porosity. By changing the levels of these parameters, output value can be affected.

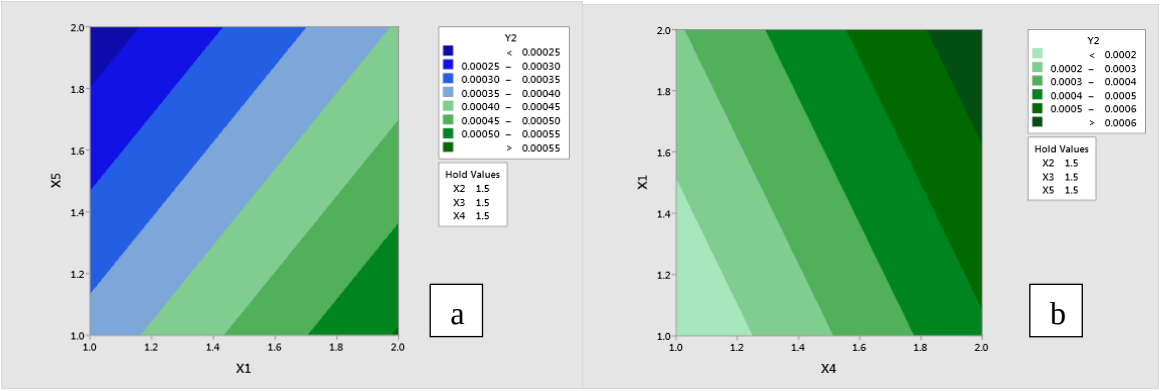

Figure 4. Contour plot dependece between porosity and input parameters: a) X5-X1 b) X1-X4

From the porosity results it can be seen that for all specimens porosity were very low (0.0008 >) (Tab.2). The fact that the porosity in the investigated specimens is almost non-existent should be taken as very high achievement for friction materials. Mentioned result can be explained by role of glycerin which is used as a plasticizer. Glycerin had a very great impact on the formation process by affecting contact between the particles. Even though in general, glycerin in sharply reduces the porosity in all samples, the use of 10 wt.% plasticizer is more purposeful. This also applies to the hardness property. If we look at the values of hardness, it can be seen that this claim is justified. Another important benefit of glycerin was preventing sticking of specimen mold on the press-die walls. As a result of all the above mentioned features of plasticizer led to improved hardness and porosity properties.

In Fig.5 plot dependence between hardness and design factors are given. Fig.5 a demonstrates that best performance be achieved only second levels of heating temperature (X1) and pressing time (X5). Similar effect

ISSN: 2663-8770, E-ISSN: 2733-2055
ETM
EQUİPMENT, TECHNOLOGİES, MATERİALS
EQUİPMENT, TECHNOLOGİES, MATERİALS
VOLUME 05 ISSUE 01 2021

can be observed for heating temperature (X1) and heating time (X3) and parameters (Fig.5 b). For these parameters only first level values are effective.

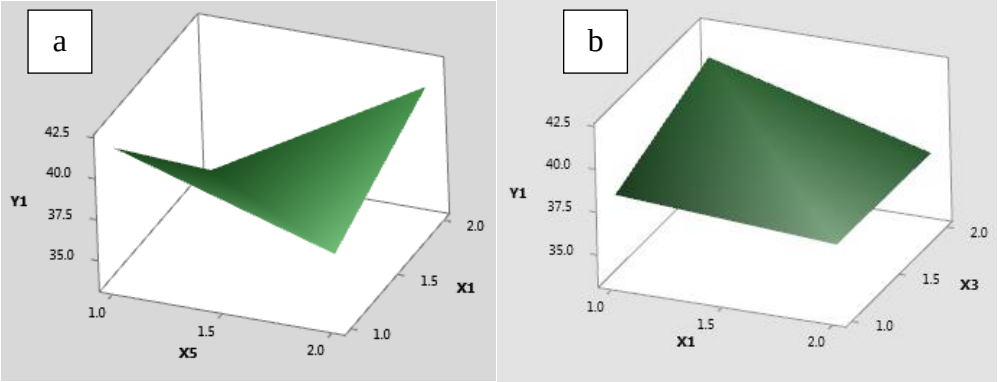

Figure 5. Surface plot dependece between hardness and input parameters: a) X5-X1 b) X1-X3

The linear regression equation, showing the coded relationship between the predicted and predictor variables for hardness concluded as follows:

Y1 = 52.05 - 2.20 X1 - 3.90 X2 + 1.20 X3 - 5.80 X4 - 3.60 X5 + 3.50 X2*X5

The information about model summary and coefficients can be found in Tab.5 and 6, respectively. For hardness and porosity R-sq are 94.27% and 94.08%, respectively. Regression model showing that most important interaction factor which is affecting in increase of hardness is X2*X5. The positive values of X3, and X4*X5 terms is indicate that increase in heating time and hot pressure and pressure-plasticizer increases the hardness.

Table 5.

Model Summary

Model	S	R-sq	R-sq (adj)
Hardness (Y1)	2.40416	94.27%	59.88%
Porosity (Y2)	0.0001768	94.08%	58.53%

Where, R-sq is coefficient of determination and S is standard error of the regression. Smaller values of S indicates that the observations are closer to the fitted line [13].

Table 6.

Regression coefficients for hardness

Term	Coef	SE Coef	T-Value	P-Value
Constant	52.05	9.58	5.43	0.116
X1	-2.20	1.70	-1.29	0.419
X2	-3.90	5.38	-0.73	0.600
X3	1.20	1.70	0.71	0.609
X4	-5.80	1.70	-3.41	0.182
X5	-3.60	5.38	-0.67	0.624
X2*X5	3.50	3.40	1.03	0.491

The linear regression model for porosity was concluded as follows:

Y2 = -0.000752 + 0.000185 X1 + 0.000425 X2 - 0.000080 X3 + 0.000905 X4 - 0.000150 X5 - 0.000350 X2*X4

The information about model summary and coefficients can be found in Tab.5 and 7, respectively. Regression model showing that most important interaction factor which is affecting in increase of porosity is X2*X4. The negative values of X3 and X2*X4 terms is indicate that decrease in heating time and hot pressure*plasticizer combination decreases the porosity.

Table 7.

Regression coefficients for porosity

ISSN: 2663-8770, E-ISSN: 2733-2055
ETM
EQUİPMENT, TECHNOLOGİES, MATERİALS

Term	Coef	SE Coef	T-Value	P-Value
Constant	-0.000752	0.000704	-1.07	0.479
X1	0.000185	0.000125	1.48	0.378
X2	0.000425	0.000395	1.08	0.477
X3	-0.000080	0.000125	-0.64	0.638
X4	0.000905	0.000395	2.29	0.262
X5	-0.000150	0.000125	-1.20	0.442
X2*X4	-0.000350	0.000250	-1.40	0.395

Results of optimization tests are given Tab.7. As mentioned above, the results of the optimization were the same for both output parameter because the relationship between the two properties was similar.

Table 8.

Results of optimization tests

Parameters					Solution						
Response	Goal	Lower	Target	Upper	X1	X2	X3	X4	X5	Y1 Fit	Y2 Fit
Y1	Max.	33.6	42.1000	-	1	1	2	1	2	44.075	-0.0000475
Y2	Min.	-	0.0001	0.00078							

Because the models are compatible, their probability test has yielded very similar results, and therefore only hardness results have been given (Fig.6).

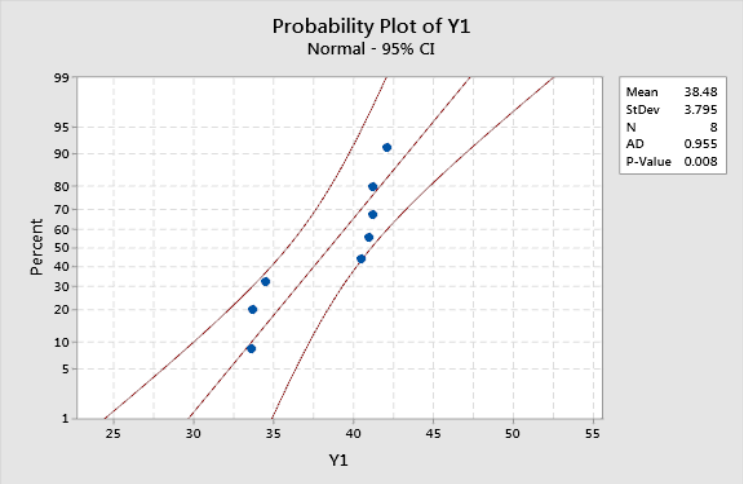

Figure 6. Predicted values of hardness

The probability plots proves appropriateness of the obtained results to the model. Taguchi's method is used to find optimum combinations to achieve better physical and mechanical properties for organic friction brake pad composites. The obtained results can be used in the preparation of new composite materials.

Results: The ANOVA results showed that plasticizer is the most significant parameter affecting on hardness (66.72%) and porosity (54.74%).
Hot pressure*plasticizer and hot pressure*pressing time combinations were most significant interaction factor which is affecting process.
The obtained regression model show that heating time and hot pressure and pressure*plasticizer has positively related for hardness. Also regression model for porosity show that heating time and hot pressure and hot pressure-plasticizer combination has negatively related for porosity.
Optimal combination for hardnes and porosity was determined to be heating temperature (160°C), hot pressure (25.5MPa), heating time (20 min), plasticizer (10 wt.%) and pressing time (5 min).
P-values of selected design factors was higher than 0.05, which is proves that their significanty on hardness and porosity properties.

REFERENCES

1. Asif, M., Chandra, K., Misra, P.S. Characterization of iron based hot powder brake pads for heavy duty applications, International Journal of Mechanical and Materials Engineering, 2012. Vol.8 (2), p. 94–104.
2. Abhay, T., Bhatia, O.S. Tribological performance of inorganic-metallic fiber reinforced automotive brake friction materials, International Research Journal of Engineering and Technology, 2016, Vol. 3(2), p.443-448.
3. Singh, T., Tiwari, A., Patnaik, A. [et al.]. Influence of wollastonite shape and amount on tribo-performance of non-asbestos organic brake friction composites, Wear, 2017, № 386–387, p.157-164.
4. Jakob, M., Florian, G.,Florian, S. [et al.]. Application of high performance composite polymers with steel counterparts in dry rolling/sliding contacts, Polymer Testing, - 2018. №.66, - p.371-382.
5. Friedrich, K. Polymer composites for tribological applications, Advanced Industrial and Engineering Polymer Research, 2018, Vol.1 (1), p.3-39.
6. Haruna, V.N., Abdulrahman, A.S., Zubairu, P.T. [et al.], Prospects and challenges of composites in a developing country, ARPN Journal of Engineering and Applied Sciences, 2014. Vol.9(7), p.1069-1075.
7. Ayman, A. A., El-Shafei B. Z., Abdallah A. A. [et.al]. Friction and wear of polymer composites filled by nano-particles: A Review, World Journal of Nano Science and Engineering, Vol. 2 (1), SCIRP. 2012, p.32-39.
8. Öztürk, B., Arslan, F., Öztürk, S. Effects of different kinds of fibers on mechanical and tribological properties of brake friction materials, Tribology Transactions, Taylor & Francis, 2013, 56 (4), p.536–545.
9. Dhanalakshmi, S., Mohanasundararaju,N, Venkatakrishnan, P.G. [et.al]. Optimization of friction and wear behaviour of Al7075-Al2O3-B4C metal matrix composites using Taguchi method. IOP Conference Series: Materials Science and Engineering, 2018, Vol.314 (1). 012025-8.
10. Maleque, M.A., Atiqah, A., Talib, R.J., Zahurin, H. New natural fibre reinforced aluminium composite for automotive brake pad, International Journal of Mechanical and Materials Engineering (IJMME), 2012, Vol.7. (2), p. 166-170.
11. Xingming, X.,Yan, Y., Jiusheng, B. [et.al], Review on the friction and wear of brake materials, Adv. Mech. Eng. (2016) 8(5) 1-10.
12. Andrei, C., Camelia, P. Advanced Materials with Natural Fibred Reinforced Aluminiu Composite for Automotive Brake Disc, Solid State Phenomena, 2016, Vol.254, p. 91-96.
13. Ranjit, K. R. A Primer on the Taguchi Method, (2nd Edition), Society of Manufacturing Engineers, 2010, 329 p.

ISSN: 2663-8770, E-ISSN: 2733-2055
ETM
EQUİPMENT, TECHNOLOGİES, MATERİALS

CİLD 05 BURAXILIŞ 01 2021

COMPARATIVE EVALUATION OF RESISTANCE OF HEATING EXCHANGE APPARATUS FOR NEW CONSTRUCTIONS FOR GAS COMPRESSOR STATIONS

Rabia Najafkulieva

Azerbaijan State Oil and Industry University, Senior Lecturer “Engineer and Computer Graphics”

E-mail: rabiya.nadjafkuliyeva@gmail.com

ABSTRACT

The main volume of gas produced in the Republic of Azerbaijan is formed in offshore fields. Some of this gas is transported to the shore, and the other part is used in gas-operated wells. In both cases, multi-stage compressors on SOCAR's balance sheet are used. In the process of compressing gas in compressor stations, its temperature rises (T = 115 ÷ 118 ℃) and it is important to cool it to T = 35 ÷ 38 ℃ before sending it to the outlet.
The heat exchanger proposed by the authors differs in this respect by its simplicity and functional advantages. The article provides a comparative analysis of the durability of existing and newly constructed heat exchangers used in compressor stations.
Keywords: heat exchanger, selection, flicker noise spectroscopy, multitaper spectral evaluation.

The actuality of the subject. As important as it is to determine the design parameters of heat exchangers, it is equally important to assess the vibrations that may occur during the operation of the device and their impact on the work process.
It is known that vibrations are classified into two groups according to their nature: mechanical and aerohydro. In the first case, they are based on vibrations caused by the kinematic effect of the equipment entering the system (compressor, pot, etc.), and in the second case, they are vibrations caused by aerohydrodynamic effects caused by air or liquid flows. In this case, the effect of the latter is more important than the former, so that the mechanical effects in the system can be regulated and regulated by packaging measures. On the basis of the second effects, there are cases of abrupt disturbances inside the heat exchanger, the formation of turbulent pulsations in the liquid or stream, and the violation of the structural stability under the influence of hydro and aero.
The purpose of the work. The article is devoted to a comparative assessment of the reliability effect of vibrations caused by hydrodynamic effects in a newly constructed heat exchanger.
Methodical base of research work and materials used. Figures 1 and 2 show the schematic diagrams of the newly constructed heat exchangers (IMEs) currently used in existing compressor stations, respectively. The proposed IME consists of cylindrical hollow metal tubes in operation and is based on the principle of a hydriaeroelastic system as a result of the action of two agents moving along the inner surface.

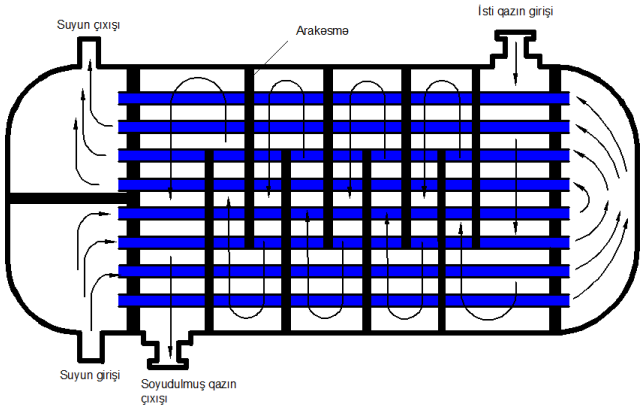

Figure 1. Kinematic scheme of existing heat exchanger used in compressor stations

ISSN: 2663-8770, E-ISSN: 2733-2055
ETM
EQUİPMENT, TECHNOLOGİES, MATERİALS
EQUİPMENT, TECHNOLOGİES, MATERİALS
VOLUME 05 ISSUE 01 2021

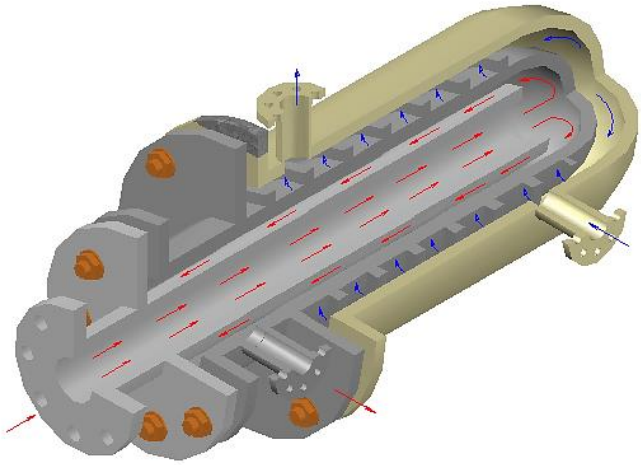

Figure 2. The scheme of movement of coolant and cooled gas in the newly built heat exchanger
The hydrodynamic force created here will cause certain elastic deformations
in the structure and, as a result, vibrations.

In the newly constructed IME, the flow rate of the coolant is ϑ = 1.0 - 1.5 m / s, passing through the first pipe with an inner diameter of d1 = 200 mm, moving in a straight flow, touching the second pipe (d2 = 500 mm) to the spherical surface and backwards fills the gap between pipes I and II. The heated gas moving on the outer surface of pipe II and collected between pipes II and III cools in this temperature exchange.

3. Results of experiments and their discussion. We will show the results of the study using the example of calculating vibration in a cooling heat exchanger used at a gas-lift compressor station and compare them with the traditional method of calculation. The figure shows a graphical representation of the measurement results with a step Δt = 0.2 sec. stress σ (t) in the annular space obtained using a tensometer.

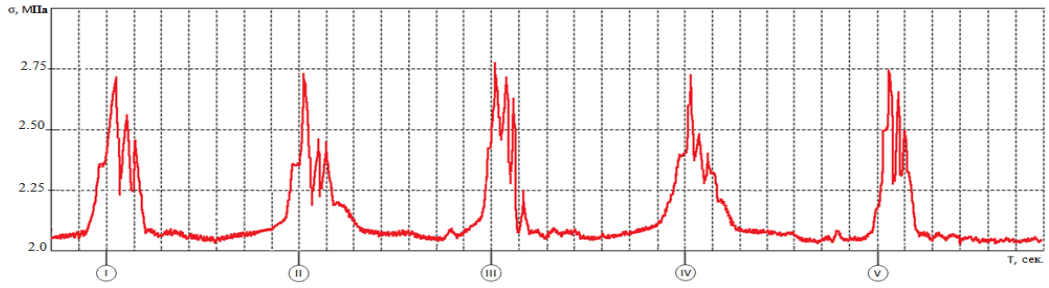

Figure 3. The nature of the voltage change in the shell side of the heat exchanger

The well-known method for calculating the vibration of a pipe in heat exchangers is described in detail in scientific papers [1, 2]. The calculation is based on determining the vibration amplitude of the pipe and establishing the value of the ultimate stress in this case. By calculation, it was found that the maximum values of the amplitude of the oscillations and stresses in this case, respectively, are $y_{max}^{турб}$ = 3,24 mm and σ = 2,24 MPa.

A comparative calculation based on the principles of multitaper estimation of pipe vibration power, according to the recommendations [4-8], showed that they are $P_d \leq 0{,}99$ x_{max} $x_{max} \leq 2{,}71$ with a confidence level.

As expected, the value $x_{max} \leq 2.71$, obtained by the multitaper method, was estimated to be slightly higher compared to the value x_{max} = 2.24, obtained from the linear differential equation.

4. Conclusion. Thus, the following conclusions can be drawn:

-use of the multitaper method, the assessment of the power spectrum of free oscillations of the heat exchanger, gives a more accurate estimate of the maximum voltage value;

- the resulting value of $\sigma_{max} \leq 2.71$, greater than σ_{max} = 2.4 MPa, established using a linear differential equation.

ISSN: 2663-8770, E-ISSN: 2733-2055
ETM
EQUİPMENT, TECHNOLOGİES, MATERİALS

REFERENCES

1. Шишкин Б.В. Прочность и вибрация кожухотрубчатых теплообменных аппаратов. Комсомольск-на-Амуре [Электронный ресурс]: КнАГТУ, 2013, 142с.
2. Динамика конструкций гидроаэроупругих систем /Отв. ред. С.М. Каплунов, Л.В. Смирнов, Ин-т Машиноведения им. А.А. Благонравова – М.: Наука, 2002-397 с.
3. РД 24.271.01-88. Методы оценки вибрационных характеристик трубных систем регенеративных подогревателей низкого давления и подогревателей сетевой воды – М.: Минтяжмаш СССР, 1990-37 с.
4. Percival D.B., Walden A.T. Spectral analysis for physical applications. Multitaper and conventional univariate techniques. - Cambridge: Cambridge University Press, 1993
5. Slepian D. Prolate Spheroidal Ware/Functions, Fourier Analysis and Uncertainty – V: The Discrete Case// Bell System Technikal Journal, 57, 1371-1430 (1978)
6. Riedel K.S., Sidorenko A. Minimum bias multiple taper spectral estimation //IEEE Trans. Signal Processing, 1995, vol. 43, pp. 188-195
7. Тимашев С.Ф. Фликкер-шумовая спектроскопия: информация в хаотических сигналах – М: ФИЗМАТЛИТ, 2007 – 248с.
8. Тимашев С.Ф., Встовский Г.В. Фликкер-шумовая спектроскопия в анализе хаотических временных рядов динамических переменных и проблема отношения «сигнал-шум» //Электрохимия, 2003, т. 39, №2, с.156-169.

ISSN: 2663-8770, E-ISSN: 2733-2055
ETM
EQUİPMENT, TECHNOLOGİES, MATERİALS

EQUİPMENT, TECHNOLOGİES, MATERİALS

VOLUME 05 ISSUE 01 2021

DYNAMICS OF IMPACT OF ABRASIVES ON GEARS ON TEETH

Nazim Ibrahimov

Azerbaijan State Oil and Industry University, Doctor of Technical Sciences, Professor. (Azerbaijan).

E-mail: nazim.ibragimov.2015 @mail.ru

ABSTRACT

This article discusses the effect of abrasive between the leading and the driven gear teeth on the formation of a stress state. In this case, normal and tangential stresses are calculated under the action of normal and tangential forces

Keywords: gears, abrasives, normal and tangential stresses, segmented shapes, fracture limit, wear depth.

INTRODUCTION

In the dynamics of abrasive particles, the process of abrasive after deformation in the space between the teeth is considered. In this case, the movement of the abrasive on the surfaces of both the lead and the carried teeth is a complex process.

The abrasive between the two teeth, the lead and the extracted teeth, is deformed by various influences, often resulting in the disintegration of the particles into smaller particles by changing their geometric dimensions. These fissile particles continue their friction and wear processes by acting on the surfaces of the teeth.

The purpose of the work. It is a theoretical and practical solution to the dynamic processes of intensive abrasion caused by deformed abrasives on the surfaces of teeth.

To solve this problem, abrasive particles are considered as spherical elements, and research is carried out within the limits of elasticity, plasticity and micro-shear. It should be noted that the spherical particle is accepted in accordance with the standards, as in the known literature [1, 2, 3].

Problem statement .The gears move the abrasives at the moment of rotation during a certain rotation. In this case, as the abrasive moves back and forth and rotates according to the state of rotation of the gears, plane-parallel movements are considered. These movements create a friction process by repeating the movements of the abrasive tooth along the curved profile. The effect of internal and external forces created by this abrasive during its movement on the profile of the tooth surface creates tensions. It is known that abrasive particles remain deformed on the surface of the teeth for some time, so it is advisable to conduct research by classical methods.

Studies show that these tiny particles damage the profiles of the teeth during deformation, forming segmented slots at certain depths. In this process, scratches, abrasions, tears and hot spots appear on the segmental surfaces of the teeth. The main source of deformations depends on the design of the gears, manufacturing technology and operating conditions. Therefore, in such cases, there are cracks in the profiles of the teeth, partial collapse. During subsequent operation, the gears are damaged as a result of abrasive wear. Practical experience shows that gears operating in severe conditions break down in a short time [4,5].

To prevent this, it is important to ensure full strength and rigidity on the surfaces of the tooth profiles. It is possible to increase the strength and wear resistance of the tooth profile by various recycling methods and application of coatings. Again, stresses caused by heavy loading can lead to abrasive collapse, damage to tooth profiles and various forms of deformation.

Depending on the duration of exposure to these deformations, different geometric foci initially appear within the tooth profiles within the elastic limit. The most common is the segmental elastic deformation. These segments form spherical segments of various shapes and sizes on the teeth of the drive gears. These segments manage to destroy the profiles of the teeth by creating cracks in a short time. For this reason, they take various measures against the strength and wear of the teeth within the elastic deformation. The most important of these is to increase resilience, and it is advisable to make theoretical and practical calculations. Figure 1 shows a diagram of the segmental deformations caused by the teeth and the forces and stresses acting on them. This figure shows the direction of change of normal and tangential stresses under the influence of normal and shear forces. It is known that under the influence of these stresses, abrasive particles with a spherical shape are deformed.

Most of the most influential are normal voltages, which form segmental slots. Sliding and its tangential stresses occur under the influence of friction in the direction of contact. Therefore, the calculations mainly require the study of the characteristics of the effect of changes in normal stress on the profile of the tooth. Taking these into account, it is proposed to conduct theoretical research on the process of changing the effect of normal voltage and torque of gears.

ISSN: 2663-8770, E-ISSN: 2733-2055
ETM
EQUİPMENT, TECHNOLOGİES, MATERİALS

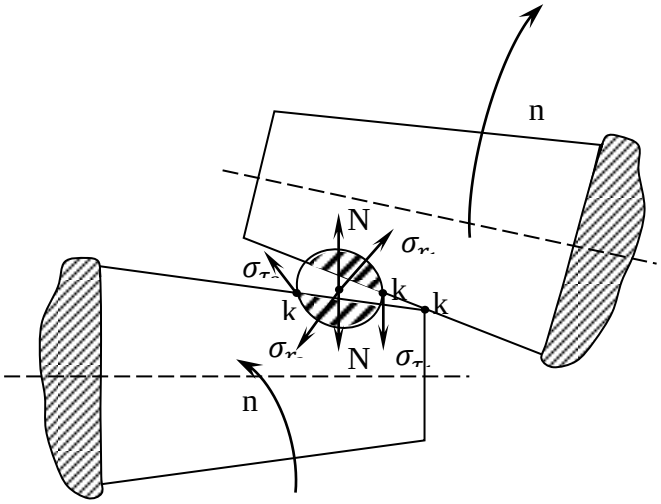

Figure 1. Scheme of forces and tensions caused by the abrasive in the interdental space

Thus, it is possible to obtain a mathematical dependence on the changes in the received deformations and stresses, the torque of the impact gears and the resulting normal force. Thus, knowing the operating conditions of the gears and the force factors that affect it, it is possible to determine their durability and wear intensity.
The most important thing is that different types of gears determine the strength and wear parameters depending on their geometric dimensions and mechanical characteristics. [5,6]
In view of this, it is expedient to first study their erosion process and calculate the strength limit at a later stage.
It is possible to give the characteristic of change of strength after long-term use. Strength limits can be determined based on the 3-rd and 4-th strength theories. Fig. Figure 2 shows the change characteristics of the stresses in the abrasive.
The process of abrasion on the profiles of the teeth goes from elastic deformation to gradual plastic deformation. In this case, different erosions occur in the profiles of the leading and extracted teeth. Their diversity depends on the physical and mechanical properties of the abrasive and teeth, as well as internal factors. These factors depend on the operating conditions of the gears and the trajectory of the abrasive. The main thing is that different types of gears, depending on their geometric dimensions and mechanical characteristics, determine the normal stresses as follows.Uzun müddətli istismardan sonra möhkəmliyin dəyişmə xarakteristikasını vermək olar.

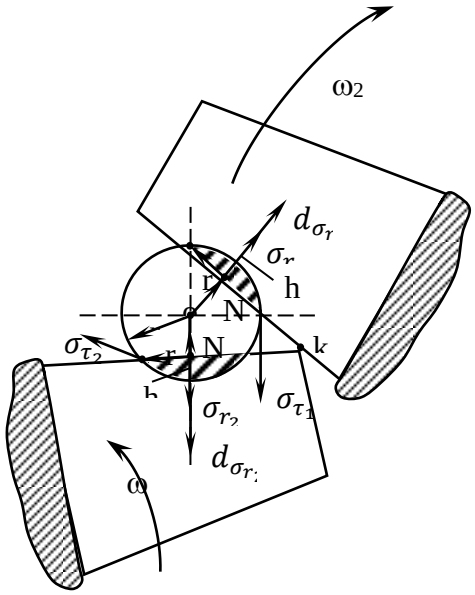

Figure 2. The location of the abrasive in the gap and on it the scheme of variation of the affected voltages

ISSN: 2663-8770, E-ISSN: 2733-2055
ETM
EQUİPMENT, TECHNOLOGİES, MATERİALS
EQUİPMENT, TECHNOLOGİES, MATERİALS
VOLUME 05 ISSUE 01 2021

$$\sigma_r = \frac{N}{\pi r_1^2}$$

$$\sigma_\tau = \frac{F_S}{2\pi r_1 h} = \frac{fN}{2\pi r_1 h} \quad (1)$$

Where r_1 - is the inner radius of the spherical segment;
h - is the height of the spherical segment;
f - coefficient of friction;
It is known that abrasive particles break down under the influence of external and internal factors and break down into small particles. In this case, additional expression is required to characterize the small particles. Thus, the process of disintegration of abrasive particles can be determined in the following mathematical sequence:
1. The breaking point of the abrasive is drawn:

$$PM = Pa \quad (2)$$

where PM = σT π r2 - is the maximum force exerted by the tooth on the abrasives;
σT - is the stress at the abrasive flow limit;
Pa - is the largest normal force of abrasive on the tooth surface:

$$Pa = Ar \cdot (HB) = 2\,\pi\, r\, hmax \cdot (HB) \quad (3)$$

Ar = 2 π r hmax - is the area of influence of the segment in the cavity formed in the tooth.
HB - is the hardness of the abrasive
2. The process of disintegration of abrasives on the profiles of teeth is determined:

$$\sigma T \pi\, r2 = 2\,\pi\, r\, hmax \cdot (HB)$$

Here

$$\left(\frac{h}{r}\right)_{max} = \frac{1}{2}\ \left(\frac{\sigma_T}{HB}\right)\ \text{alınır} \quad (4)$$

Table 1 below shows the main parameters of abrasive particles to calculate the degree of disintegration.

Table 1.

Parameters for calculating the scattering limit on

№	Tooth surface materials Dişlərin səthlərinin materialları	Flow limit, MPa Axma həddi, MPa	Surface hardness, HB Səthin bərkliyi,HB	Contact area, mm2	Touchi tension, MPa	Penetration layer, mm
1	Steel Steel-45	270	60	10 – 20	92	0,18
2	Poliamide P - 10	115	25	15 – 28	81	0,19
3	Textolite	172	32	12 – 15	77	0,12
4	Metal coating	220	65	20 – 30	89	0,25
5	Non-metallic coating	190	45	35 – 45	67	0,15

These stresses and deformations increase the effect of the abrasive on the tooth surfaces to the maximum extent within the micro-cutting limit, causing the teeth to break down. In this case, it breaks down into abrasive micro-particles and forms micro-macro crack layers by opening segmented slots in the profile boundaries of the teeth.
In subsequent use, these complications penetrate deeper and cause gradual tooth loss. In order to prevent these processes, it is especially expedient to carry out processes to increase the strength and wear resistance of the tooth surface. Studies and experiments show that it is important to choose technological methods to increase the durability of gears, depending on the operating conditions.
Thus, the study of abrasive wear on gears in the research work is to complete the selection and implementation of a technological method for the durability of their surfaces. The implementation of new methods and technologies in the chosen direction reflects the completion of scientific work.

ISSN: 2663-8770, E-ISSN: 2733-2055
ETM
EQUİPMENT, TECHNOLOGİES, MATERİALS

CONCLUSION

1. Intensive wear with elastic deformation occurs under the influence of abrasive on the profiles of the teeth of the gears. Dependence of normal and tangential stresses on external and internal forces on wear parameters is obtained. This dependence reflects the normal force, the coefficient of friction and the geometric dimensions of the resulting spherical segment.
2. Tension on the surfaces of the teeth in contact causes more intensive wear to the extent of plastic deformation. The rate of this erosion is characterized by physical-mechanical and geometric parameters.
3. At maximum stresses in the contact areas of the teeth, micro-cutting limits are formed under the influence of the abrasive. In this case, intensive erosion with the collapse of the abrasive results in the formation of cracks on the teeth.

REFERENCES

1. Крагельский И.В. и др. Основы реагентов на трения и износ. М.: Машиностроение, 2001 г.,-576 с.
2. Babayev C.H. Mustafayev S.M. Sürtünmə və yeyilmə nəzəriyyəsinin əsasları. Bakı, ADNA, 1998-ci il, 127 s.
3. Canəhmədov Ə.X., Əliyev Ə.M. Tribotexnika. Bakı, “Elm”, 2006-ci il.-137s
4. Елагина О.Ю. Технологические методы повышения износостойкости деталей машин. М.: «Логос», 2009 г., 486 с.
5. Гаркунов Д.Н. Триботехника. М.: Машиностроение, 2010 г., -442 с.
6. İbrahimov N.Y. Dişli çarxlarda abraziv yeyilmə prosesi.Bakı Neftin,qazın geotexnoloji problemləri və kimya elmi –tədqiqat institunun Elmi əsərləri-xy-cild,2014-ci il s.174-181

ISSN: 2663-8770, E-ISSN: 2733-2055
ETM
EQUİPMENT, TECHNOLOGİES, MATERİALS

EQUİPMENT, TECHNOLOGİES, MATERİALS

VOLUME 05 ISSUE 01 2021

INCREMENTEL OF RELIABILITY OF OIL PUMPS'S HYDRAULIC SECTIONS

[1]Ibrahim Habibov, [2]**Gulnaz Rzayeva**, [3]Javidan Veliev

[1]Azerbaijan State Oil and Industry University, [1]Doctor of Technical Sciences, Professor. (Azerbaijan)

[2]Azerbaijan State Oil and Industry University, PhD in Technical Sciences, Associate professor. (Azerbaijan)

[3]Azerbaijan State Oil and Industry University, Master. (Azerbaijan)

E-mail: [1]h.ibo@mail.ru; [2]gulnaz.rzayeva@bk.ru

ABSTRACT

Present days' high market competitiveness requires wide range of design and production solutions to ensure reliable and efficient usage of various types of machines and equipment. From the different perspective provision of equipment with effective preservation and maintenance characteristics is a critical factor to be taken into an account. Arising from these factors, systematic approach for solution is require together with identification failure related to maintenance and operability of the equipment.
Various pumps are used in oilfields and particularly their hydraulic parts are among the equipment sets, requires frequent execution of maintenance and modernization works.
The article discusses the issue of increasing the reliability of the hydraulic part of oil field pumps.
Keywords: oilfield pump, hydraulic part, reliability, modernization, parameters of statistical distribution.

INTRODUCTION

High Pressure pumps are the set of equipment, which are widely used in cementing of wells in oil and gas fields, as well as during repair and modernization work. The state of current of high-pressure oilfield pumps progress is discussed in detail [1]. As an outcome of this study initial pumping units used in industry mainly consisted of two pistons, which were are designed for a larger supply of working fluid than plunger pumps, however, the latter have a higher pressure range than piston pumps. The author of the research paper states that the "life cycle" of this technical system (TS), covers period between 1950-2010, including five generations of oilfield pumps. During this period, starting from the second generation, there has been a transition to the production of triple plunger pumps. Currently, equipment sets are used for well cementing are being produced by more than ten Russian enterprises covering almost the entire model range of Pumping equipment [2]. In Azerbaijan, the Sabunchi Scientific and Production Association DOJSC manufactures pumping units equipped with an upgraded three-plunger pump, H5-160 based on provided by the AzINMASH Institute [3].
The level of reliability and the main reasons for the failure of the hydraulic part of oil field pumps. The design and operability of the oilfield pumps predetermine the requirements to ensure their reliable, continuous operation. Main concern is wear parts and assembly units of the hydraulic part of high-pressure plunger pumps. Despite a significant number of works devoted to improving the performance of oil field pumps, their hydraulic parts still do not meet requirements of current industrty in terms of reliability.
Table 1 demonstrates the MTBF(Mean time between failures) of hydraulic parts and the plunger pump as a whole, obtained on the basis of statistical data. The obtained values of the coefficient of variation indicates a significant scatter in the data, which is generally typical for high pressure pumps.

Table 1

Results of statistical processing of data

Details	Distribution laws	Statistical parameters of distributions		
		Mean time to failure T1 , hour	Standard deviation σ, hour	Variation Coefficient V=σ /T1
Plunger	Normal	257,3	153,0	0,59
Seal	Weibull	45,5	25,6	0,56
Valve disc	Logarithmically Normal	305,0	107,6	0,35
Hydraulic part as a whole	Weibull	13,9	9,3	1,67

ISSN: 2663-8770, E-ISSN: 2733-2055
ETM
EQUİPMENT, TECHNOLOGİES, MATERİALS

Three-plunger pump H5-160 is designed for pumping service water, abrasive and corrosive compounds, flushing and squeezing of liquids into the well during treatment of the bottomhole formation zone with salt and carbon dioxide, flushing sand plugs and cementing wells during overhauling. Usage of steel 45 as a raw material for manufacturing of H5-160 (Fig. 1) fosters further interest in design of the equipment.
Operating surface of equipment is hardened by high-frequency currents (HFC) to a depth of 1.2-1.5 mm to ensure the hardness HRC 51-57, then polished to ensure the roughness R α = 0.2 μm. The plunger seal is a multi-piece design with rubber seals.

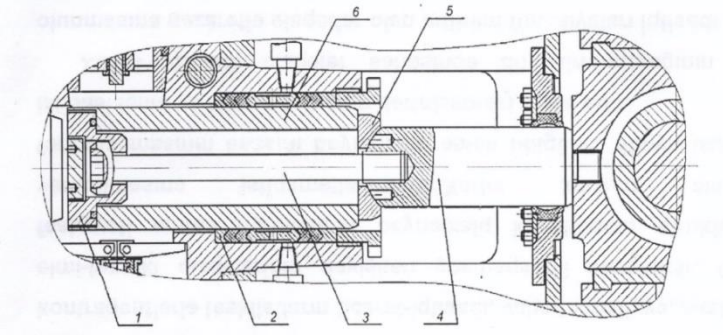

Figure 1. The main parts of the oil field pump plunger unit 1-plunger; 2-crosshead; 3-stock; 4-washer; 5-thrust; 6-plug; 7-crosshead pad; 8-clamping nut.

Characteristics of the plunger seal enables fluid pressure to be directed against the collars opposite to the friction force. This reduces the risk of pushing the rear of the collar into the gap between the plunger and the packing follower. The disadvantage of the plunger seal is the tightening of abrasive particles under the cuffs at each suction stroke, which leads to an increase in the plunger wear rate [4]. Another feature of the pump plunger assembly H5-160 is the docking of the plunger with the stem (see Fig. 1) with the possibility of sole compensation lateral displacements. As a result of dimensional calculations for chains of the hydraulic parts' system, potential crosshead of the pump [5], angular displacements of the plunger have been identified that can lead to consequence of scratches on the metal surfaces of the plunger and packing follower. In combination with the effect of the abrasive layer, scratches on plunger, subsequently may leads to cracks and leaks.
Due to the initial pressure drop through the formed leaks, an abrasive jet starts cracking, which leads to hydroerosive-abrasive wear of the working surface of the parts. However, in single-acting plunger pumps it is often possible to prevent such destruction of the working surface of the plunger by timely adjustment via compensation of the plunger's lateral displacements.[5]. Due to difficulties to establish the degree of influence of each component link on the closing link when calculating dimensional chains, additional statistical studies have been performed. Investigation of two H5-160 triple-plunger pumps under well-flushing conditions made it possible to obtain independent data samples on failures of six plunger-seal pairs with various deviations of the closing links of their dimensional chains. A total of 56 failures of parts of this pair were noted. The total variation series showed the difference in the operating time of nodes to failure T1 from 362 to 556 h (Table 2), with the mean time to failure T1 = 455.8 h.

Table 2

General variation range of operating times to failure of pairs of plunger-seal

T_1,h	Rank	Row number	T_1,h	Rank	Row number	T_1,h	Rank	Row number
362	1	I	444	20	I	470	39,5	IV
386	2	IV	445	21	VI	470	39,5	V
395	3	II	447	22	IV	473	41	III
398	4	II	449	23	IV	477	41	III
403	5	III	450	24	I	479	42	VI
406	6	III	452	25	V	482	44	I
410	7	V	453	26	V	484	45	II
417	8	V	455	27	III	487	46	III
418	9	VI	457	28.5	II	489	47	IV
421	10	I	457	28,5	VI	490	48	I
423	11	VI	458	30,5	I	494	49	IV
424	12	IV	458	30,5	III	497	50	VI

427	13	II	459	32	V	507	51	II
430	14	II	461	33	V	509	52	V
434	15	I	462	34	II	518	53	I
436	16	III	463	35	VI	526	54	VI
438	17	VI	466	36	VI	535	55	V
439	18	IV	467	37	1	556	56	IV
442	19	V	469	38	T_1=455,8 ч			

The requirement was established to analyze combined six independent samples as a single general population of data. However, due to criteria as homogeneity of mean values or homogeneity of variances, it is necessary for investigated random characteristic in each of the variational series to be distributed according to the normal or logarithmically normal distribution law. Since these criteria is incorrect for other distribution laws, its usage can lead to inaccurate results (in this case, such information is not available). In addition, to test hypotheses about the form of the distribution function, the volumes of the obtained samples may also be insufficient to obtain desired results.

In case of the absence of data ton confirm the validity of the use of the normal distribution law, the null hypothesis that a number of independent samples belong to a single general population of data can be verified by nonparametric analysis of variance, including using the nonparametric Kruskal – Wallis rank test [6]. To perform this test the total number of test results belonging to m independent samples is placed in a single variation series, and each value of the series member is assigned ranks from 1 to n, indicating the plunger sample number. The members of the variation series, equal in value, but belong to different samples with the same (average) rank (see Table 1).

Kruskal Wallis Test

$$H = \frac{12}{n(n+1)}\left(\sum_{i=1}^{m}\frac{R_i^2}{n_i}\right) - 3(n+1) \quad (1)$$

Ri - the sum of the ranks of the i-th sample,

The correctness of the calculation of the rank sums Ri is verified by the formula

$$\sum_{i=1}^{m} R_i = \frac{1}{2}n(n+1) \quad (2)$$

It is proved that for · ni≥5 and mi≥4, the value of H is distributed according to the law χ^2 с к= т-1 degrees of freedom in the case of inequality

$$H \le \chi^2 \quad (3)$$

In such case, the hypothesis about the identity of the distributions from which the samples are taken is accepted. Otherwise, an alternative hypothesis about the heterogeneity of the populations is accepted.

Based on the variation series obtained from the observation results above, in Table 1, the results of ranking the operating time to failure of six plunger-seal pairs for two plunger pumps H5-160 are being demonstrated. Plungers I, II, III refer to pump 1. Plungers IV, V. VI - to pump 2. Let us check the null hypothesis that the six samples in Table 1 belong to a single general population of data with the significance level α = 0.05

In such case, the hypothesis about the identity of the distributions from which the samples are taken is accepted. Otherwise, an alternative hypothesis about the heterogeneity of the populations is accepted.

Based on the data in Table 1, we calculate the rank sums: $R_1 = 282{,}5$; $R_2 = 230{,}5$; $R_3 = 268{,}5$; $R_4 = 268{,}5$; $R_5 = 296{,}4$; $R_6 = 304{,}5$.

In conformance with the formula(2)

$$\sum_{i=1}^{6} R_i = 282{,}5 + 230{,}5 + 213{,}5 + 268{,}5 + 296{,}5\,4 - 304{,}5 = 1596;$$

$$\frac{1}{2}n(n+1) = 0{,}5 \cdot 56 \cdot 57 = 1596$$

With the use of formula (1), we obtain H = 0.632. From the tabulated values $\chi^2_\alpha 2$ of the significance level α = 0.05 and the number of degrees of freedom k = m-1 = 5 [7], we find the critical value $\chi^2_{0.05}$ = 11,1. As a condition (3) is satisfied, the null hypothesis is not rejected.

In addition to evaluating the MTBF of a pair of plunger - seal of pumps H5-160, the average values of diametric wear of plungers H in the zone of its greatest value were determined. The random variable H was 2.55-0.62 = 1.93 mm.

ISSN: 2663-8770, E-ISSN: 2733-2055
ETM
EQUİPMENT, TECHNOLOGİES, MATERİALS

The parameters of the empirical distribution: arithmetic mean $\overline{D}$, variance σ^2, standard deviation σ and coefficient of variation V-were calculated using the following formulas:

$$\overline{D} = \frac{\overline{D}_i \cdot \Delta n_i}{\sum \Delta n_i} = \frac{86{,}6}{56} = 1{,}55 \text{ мм}, \quad (4)$$

$$\sigma^2 = \frac{\sum \overline{D}_i^2 \cdot \Delta n_i}{\sum \Delta n_i} - \overline{D}^2 = \frac{148{,}2}{56} - 1{,}55^2 = 0{,}16 \text{ мм}^2, \quad (5)$$

$$\sigma = \sqrt{0{,}16} = 0{,}4 \text{ мм}, \quad (6)$$

$$V = \frac{\sigma}{\overline{D}} \cong 0{,}26 \text{ мм}. \quad (7)$$

Based on the analysis of the obtained results, a hypothesis was put forward about the correspondence of the empirical distribution function to the normal law. Since $\overline{D}>3\sigma$ the non-truncated normal law of probability distribution was used. When comparing and checking the convergence of the empirical distribution with the theoretical one, the following parameters were taken into account.
Probability of the each interval:

$$P(\overline{D}_i) = \left(\frac{\Delta D}{\sigma}\right) \varphi \frac{\overline{D}_i - \overline{D}}{\sigma} \quad \text{где } \Delta D=0{,}2,$$

Function values $\varphi(t) = \frac{1}{\sqrt{2\pi}} \exp(-t^2/2)$

Theoretical frequencies

$$\Delta n_i^{`} = P(\overline{D}_i) \cdot (\sum \Delta n_i) \quad (8)$$

The theoretical frequencies were used to construct the distribution function of the studied random variable. Substituting the values of $\overline{D}$ and σ in the formula for the density of the normal distribution. Obtained result:

$$f(D) = \frac{1}{\sigma\sqrt{2\pi}} exp\left[-\frac{(D-\overline{D})^2}{2\sigma^2}\right] = \frac{1}{0{,}4\sqrt{2\pi}} exp\left[-\frac{(D-1{,}55)^2}{0{,}32}\right] \quad (9)$$

The hypothesis of the normal distribution of a random variable was tested using the Kolmogorov test. For this, the modulus of the difference d between the empirical and theoretical distribution functions was determined. The calculation results are shown in Table 3.

Table 3

Determination of the maximum value of the modulus of the difference

Interval number	$\overline{D}_i$, Мм	Frequency		$\sum_{i=1}^{i} \Delta n_i$	$\sum_{i=1}^{i} \Delta n_i^{`}$	$d = \left\lvert \sum_{i=1}^{i} \Delta n_i - \sum_{i=1}^{i} \Delta n_i^{`} \right\rvert$
		Empirical Δn_i	teoretical $\Delta n_i^{`}$			
1	0,7	1	0,196	1	1,196	0,196
2	0,9	3	3,032	4	4,228	0,228
3	1,1	6	6,000	10	10,228	0,228
4	1,3	11	9.246	21	1 9.474	1,526
5	1,5	13	11.096	34	30,570	3.430
6	1.7	9	10.374	43	10,944	2,056
7	1.9	5	7,552	48	48,496	0,496
8	2,1	4	4,281	52	52,777	0,777
9	2,3	2	1,890	54	54,667	0,667
10	2,5	2	0,652	56	55,319	0,681

In order to determine the Kolmogorov coefficient, an auxiliary coefficient is required $\lambda_k = d\sqrt{N} = 0{,}46$
The maximum modulus of the difference between the empirical and theoretical accumulated frequencies

$d_{max} = 3{,}430$ (see table 2); $d_{max} = \frac{3{,}430}{56} = 0{,}06125$ и $\lambda_k = 3{,}340\sqrt{56} = 0{,}46$.

Using the tabulated values [7], obtained probability p (0.46) = 0.9827. Such probability is high, therefore, the accepted hypothesis about the normal distribution of diametrical wear of the plunger of the pump H5-160 is realistic.

In conclusion, on the basis of the studies performed, it can be declared that the change in the diametrical wear of the pump plungers according to the normal distribution law with obtained coefficient of variation V = 0.25 indicates a desirable manufacturing quality of the pump plungers H5-160. At the same time, the given data on the MTBF of the plunger-seal pair indicate the need to further increase the wear resistance of both the pump plunger and its sealing elements.

REFERENCES

1. Даутов Т.М., Газаров Р.Е. Новое поколение плунжерных насосов высокого давления производства ОАО «Ижнефтемаш». М.: «Нефтепромысловое оборудование», 2003, №3. – С.32-38.
2. Владимиров А.И., Кершенбаум В.Я. Конкурентоспособность на фоне кризиса. Нефтегазовая техника. М.: «Национальный институт нефти и газа», 2009. – 696 с.
3. 3.Отчет о НИР по теме № 3758-86-56, «Исследования с целью определения действительных показателей надежности быстроизнашивающихся деталей насоса Н5-160». Фонд АзИНМАШа. Баку: 1987. – 120 с.
4. Бабаев С.Г., Габибов И.А., Керимова Л.С. Обеспечение точности функционирования нефтепромыслового оборудования. Обзорная информация. Баку: изд. АГНА, 1994. – 113 с.
5. Бабаев С.Г., Мунзер А.А., Аббасов Г.Г. Анализ точности взаимодействия подвижных элементов системы «гидравлическая часть-крейцпкопф плунжерного насоса»: Обзорная информация «Передовой производственный (научный) опыт, рекомендуемый для внедрения, М.: ЦИНТИхимнефтемаш», 1991, №1. – С.8-10.
6. Кремер Н.Ш. Теория вероятности и математическая статистика. М.: ЮНИТИ-ДАНА, 2007. – 537 с.
7. Степнов М.Н. Статистические методы обработки результатов механических испытаний. /Справочник. М.: Машиностроение, 1985. – 232 с.

ISSN: 2663-8770, E-ISSN: 2733-2055
ETM
EQUİPMENT, TECHNOLOGİES, MATERİALS

INFLUENCE OF HOLDING TIME WITHOUT PRESSURE IN THE MANUFACTURE OF PLASTIC DETAILS OPERATING IN OIL FIELD EQUIPMENT

[1]Naila Gasanova, [2]Vafa Pashayeva

[1]Azerbaijan State Oil and Industry University, PhD in Technical Sciences, Associate professor. (Azerbaijan)

[2]Azerbaijan State Oil and Industry University, Assistant. (Azerbaijan)

E-mail: [1]haciyevanaila64@gmail.com

ABSTRACT

When manufacturing technologically complex details from polymer materials, it is possible to achieve the necessary quality with the control of production regimes depending on the grade of the materials and the design of the manufactured details. In this article, the influence of holding time without pressure in the manufacture of plastic details operating in oil field equipment was investigated.
Keywords: parts made of plastic materials, press molds, technological regimes, delay time without pressure, quality indicators.

INTRODUCTION

The study of the operating conditions of oil equipment made it possible to identify a set of indicators that most fully characterize the quality of plastic details. It is known that the quality of details of products made of various materials is a combination of mechanical, physical and operational indicators of any equipment. It partly formed during their manufacture, depending on their materials and manufacturing method. And plastic details, depending on the area of application, are very different from metals. This is due to the technologies for manufacturing structural products and individual parts from them [1].

The regime of production of plastic details during pressing and die-casting is determined by three components: temperature, residence time of the detail in the press-mold and pressure.

The purpose of the study. The holding time without pressure (t0) is necessary to prevent the detail from sticking to the mold, to ensure sufficient rigidity of the detail, determined by the presence of internal stresses that contribute to the swelling and warping of the detail, i.e., affects the quality of the details.

In the figure 1 shows the dependencies of the quality indicators of thermoplastic details on the time of holding without pressure. The holding time without pressure was varied by us in the following interval for ABS – (14–16) seconds, for polyamide – (9–41) seconds. Here are the curves of dependence of shrinkage (Sb), density (ρ) and surface roughness (Ra) of details made of ABS-plastic material depending on the holding time without pressure.

It can be seen from the curves that as the holding time without pressure increases, the shrinkage and roughness of the surface increases to their maximum values, that is, by the heights of the irregularities of the press mold walls and is achieved at t0=40÷50 seconds per mm of thickness.

ISSN: 2663-8770, E-ISSN: 2733-2055
ETM
EQUİPMENT, TECHNOLOGİES, MATERİALS
EQUİPMENT, TECHNOLOGİES, MATERİALS
VOLUME 05 ISSUE 01 2021

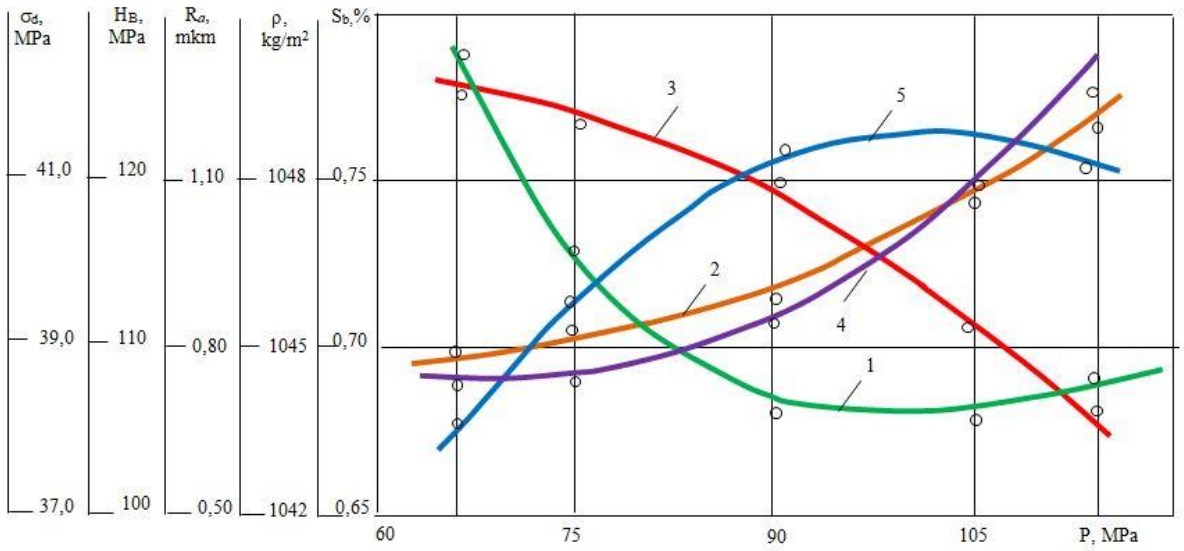

Figure 1. Dependence of shrinkage (1), density (2), surface roughness (3), hardness (4), disruptive voltage when stretching (5) of details made of the ABS plastic from pressure

And the density (ρ) of details, on the contrary, with an increase in t0 first increases and then decreases, and the intensity begins with slow speeds.

Methodological base of the research. This pattern is a consequence of the fact that with a long cooling time without pressure does not contribute to the compaction of the material in the mold, which leads to a deterioration in shrinkage and roughness of the surfaces. On the other hand, the melt in the mold without pressure is poorly oriented over the entire surface of the mold and the thickness of the manufactured part [2]. A slight decrease in density (ρ) over time is the consequence of slowing down the mechanism of temperature stress and breaking the bonds of structural elements as a whole.

In the figure 1 shows the relationships hardness (HB) and disruptive voltage (σd) when stretching ABS plastic details from holding time without pressure. Here, the hardness of the details increases with increasing holding time without pressure, and then begins to decrease after t0 =45 mm/s.

On the other hand, the relaxation process proceeds slowly with the restoration of the orientation of the material along the entire contour of the press mold, which is a normal-uniform redistribution of internal stresses and as a result of which the density and roughness of the surfaces of the details are improved when they are in the mold (under normal cooling).

As can be seen from the dependency curves, the density (ρ) and surface roughness (HB) increase with an increase in the holding time without pressure. Apparently, this is due to the fact that when the melt in the form of a material, for a long time, the compaction process is completely completed, as a result of which the material is released from internal stresses that reduce the orientation process, the melt when in the form.

On the other hand, the relaxation process proceeds slowly with the restoration of the orientation of the material along the entire contour of the press molds, which is a normal redistribution of internal stresses along the entire section and, as a result, an improvement in the density and roughness of the surfaces of the parts when they are in the mold.

And the shrinkage of details with an increase in the holding time without pressure decreases (t0 =10÷35 min/mm), and then increases, starting from t =10÷35 min/mm. This once again confirms the regularity that at t0 > 35 min/mm, the redistribution of temperature voltages is violated, contributing to the deterioration of the main quality indicators – strength and density of details.

In the figure 2 shows the dependencies of hardness (HB) and disruptive voltage when stretching (σs) on the holding time without pressure of details made of capron. As you can see, of the curves with an increase in holding time without pressure, it almost does not change.

ISSN: 2663-8770, E-ISSN: 2733-2055
ETM
EQUİPMENT, TECHNOLOGİES, MATERİALS

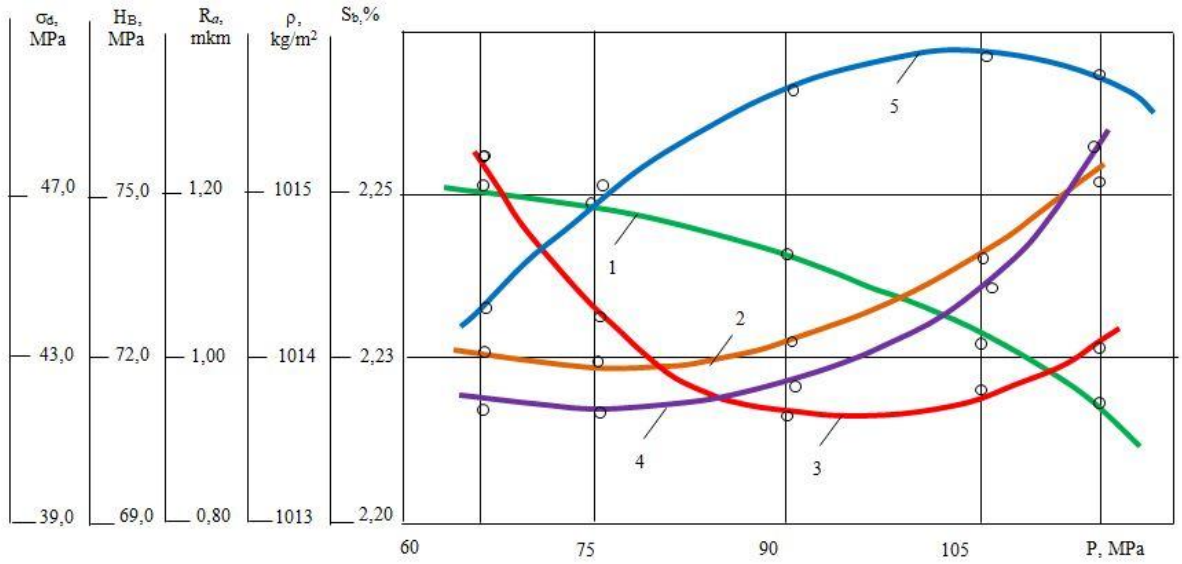

Figure 2. Dependence of shrinkage (1), density (2), surface roughness (3), hardness (4), disruptive voltage when stretching (5) of details made of the polyamide from pressure

Within the chosen limits of t0, we got into the region of the conditional optimum for the study of HB. And the disruptive voltage when stretching with an increase in t0, asymptomatically decreases and does not change at the end. This is due to the fact that at the indicated values of t0, the material is still in the form, the relaxation process ends completely, and the process of equilibrium is almost stabilized.

In the figure 3 shows the dependencies of the main shrinkage indices (Sb), density (ρ) and surface roughness (Ra) of the details on the holding time without pressure of details made from the polypropylene material. As can be seen, the shrinkage decreases as the holding time without pressure increases. So at t0 =30 mm/min shrinkage corresponds to 2,90%, at t0 =50 mm/min shrinkage is equal to 2,70%.

The influence of the holding time without pressure on the density and roughness of the surfaces is the same in nature, that is, with an increase in t0, both of these indices decrease and reach their minimum value and a further decrease of these criteria in the area of the received mode parameters is not observed, i.e. stabilization of the selected criteria occurs. Apparently, this is due to the fact that when compiling the technological modes of experiments, we accidentally – almost got to the conditional optimum of these mode parameters.

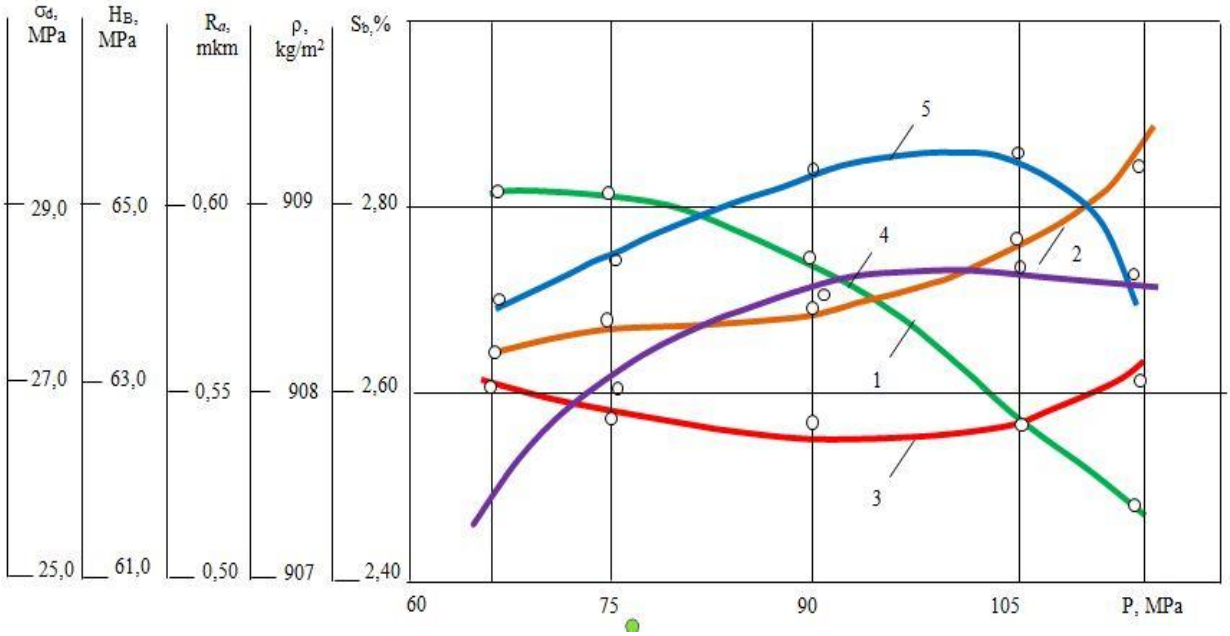

Figure 3. Dependence of shrinkage (1), density (2), surface roughness (3), hardness (4), disruptive voltage when stretching (5) of details made of the polypropylene from pressure

In the figure 3 shows the dependences the hardness (HB) and disruptive voltage when stretching of details on the holding time without pressure of details made of polypropylene. As can be seen from the hardness curves with an increase of t0, first increases (t0=30÷55 mm/min) and reaches its maximum in the studied areas of mode parameters, then decreases. And the hardness decreases and reaches its minimum. It should be noted that both quality indices achieve the best values at ((t0=45÷55 mm/min), which is very characteristic of this material when processing them in terms of ensuring the quality of details in oilfield conditions [3-5].

As shown in the figures, shrinkage of details from ABS-plastic increases with increasing holding time without pressure. The shrinkage of the amorphous thermoplastic is more determined by the degree of orientation of the polymer chains. With an increase in t0, the degree of orientation increases, and this increases shrinkage.

The shrinkage of details from polyamide with increasing t0 decreases to a certain value and then stabilizes. As the cooling time increases, the degree of crystallinity of the polyamide, which also decreases to a certain value, is then stabilized. The unpressurized holding time has little effect on the density of ABS plastic details.

The disruptive voltage when stretching (5) of details made of the ABS plastic increases with an increase in t0 due to an increase in the degree of orientation, which is confirmed by an increase in shrinkage.

In parts made of ABS-plastic and polyamide, surface roughness increases with increasing holding time without pressure. This is because an increase holding time details made of ABS-plastic and polyamide in the mold reduces the possibility of complete contact of the material with the mold surface.

Discussion of the results obtained. From the results of the experiment, it was found that the holding time without pressure has an insignificant effect on the mechanical characteristics the details made of polyamide.

In this article, by analyzing the results obtained, it can be concluded that when manufacturing technologically complex parts from polymer materials, the necessary quality can be achieved with the control of production modes depending on the grade of materials and the design of the manufactured details.

REFERENCES

1. Kerimov D.A. Study of the accuracy of making machine details from thermosetting plastics when pressing in vacuum. Dissertation of Candidate Technical Sciences., Baku, Azerbaijan Institute of Oil and Chemistry named after M.Azizbekov, 1971
2. Kerimov D.A., Kurbanova S.K. Bases of designing of plastic details and press-molds. Baku: “Elm” publishing house, 1997, 504 p.
3. Kerimov D.A., Gasanova N.A. Influence of processing regimes on accuracy and shrinkage of threaded plastic details of oilfield equipment. Topical problems of humanities and natural sciences/Journal of scientific publications, No. 08 August 2017, Part I, Moscow 2017, p. 38-44
4. Gasanova N.A. Determination of mechanical indexes of plastic details of oilfield equipment. Scientific and technical journal "Equipment and technologies for the oil and gas complex. No. 2, Moscow, 2014
5. Gasanova N.A. Definition of mechanical indicators of plastic details of the oil field equipment. International Journal of Innovative Research in Computer Science & Technology (IJIRCST), Innovative Research Publication, Lucknow (U.P.), India, July 2020, Volume-8, Issue-4, p.313-314

ISSN: 2663-8770, E-ISSN: 2733-2055
ETM
EQUİPMENT, TECHNOLOGİES, MATERİALS

RESEARCH OF THE TECHNOLOGY OF OPENING HOLES IN COMPACT AND POWDER MATERIALS

[1]Heybet Eldarzade, [2]Aghali Quliyev, [3]Aynur Sherifova, [4]Rafiqa Shahmarova, [5]Tamilla Xankishiyeva

[1,2]Azerbaijan State Oil and Industry University, [1,2]Candidate of Technical Sciences, Associate professor. (Azerbaijan).

[3,4,5]Azerbaijan State Oil and Industry University, Asistent. [3,5]PhD in Technical Sciences, (Azerbaijan)

E-mail: heldarov@rambler.ru

ABSTRACT

This article is devoted to one of the important problems of mechanical engineering, including processing by cutting and deploying in sintered antifriction powder material in optimal modes with maximum performance. The study was conducted for small diameter cylindrical bushings. Processing of bushings was carried out by reamers from high-speed and carbide tools on materials from porous powder and cast iron. It is established that the temperature of the tools should not exceed the permissible upper limits, for pressing the bushings, it is necessary to use planting with small strains in the cold state.
Keywords: engine valve, bushing, powder material, cast iron, reamer, cold pressing.

Relevance: One of the main problems of modern mechanical engineering is the determination of cutting conditions during processing, both known materials and new difficult-to-machine materials. To determine the optimal cutting modes and the conditions for the maximum performance of the tools, long-term expensive durable laboratory tests are required, which lead to certain financial costs, as well as to the loss of time [1].

The study of the processing of powder materials with various cutting tools to determine and improve the machinability of individual materials, their characteristics, is one of the main tasks of the science of metal cutting [2].

The reamer is used for finishing small diameter cylindrical holes. The accuracy and roughness of the reamer surface is higher than in the application of other blade tools, therefore reamers are used for final processing after drilling, reaming, countersinking and boring.

The working movements of reaming holes are similar to those using drills and countersinks. Even many types of reamers (other than adjustable ones) are similar to drills or countersinks, although they have shallow grooves and a shallow angle of the cutting edge. Their main functional difference is high precision and quality of processing up to 6 kvapitet and roughness Ra from 2 to 0.5 microns.

Such indicators are provided by small allowances (from 0.05 to 0.5 mm), which provides a small depth of cut, as well as structural rigidity. Reaming of cylindrical surfaces is carried out with low cutting speeds: with an all-metal tool 5 ÷ 15 m / min., adjustable with hard alloy, plates - up to 40 m / min. As a rule, reamers have straight cutting edges, but a special type with spiral teeth is used to deploy holes in viscous materials.

Recently, the world's leading manufacturers have been producing modular tooling systems for machining, in which different holders can be connected in different versions with both solid and adjustable cutting parts. The finished assembly can be classified according to how it is used.

In modern mechanical engineering, all types of assembly tools are widely used, including reamers, we have analyzed the design of branching lines of domestic and foreign firms and identified the main design changes. Based on the results of the study in [3] it has been determined that each reamer has its own instrumental intensity factor K1c, and there is a relationship between them, which is expressed in an inversely proportional relationship:

$$\frac{K_{i1}}{K_{i2}} = \frac{K_{1c1}}{K_{1c2}} \quad (1)$$

When processing porous materials, it is not recommended to use water-based cooling lubricant fluids, as well as those containing alkalis and acids, since the entering of such fluids into the pores of parts can cause corrosion, both during storage and subsequent operation.

The durability of cutting tools and cutting speed increase when processing oil-impregnated antifriction parts due to the fact that impregnation reduces the surface roughness by about one class, by 1.3-1.5 times the cutting force and most significantly affects the processing of powder materials without graphite.

When machining iron-graphite materials, materials with a ferritic structure are better machined. Then, in order of deterioration of machinability, materials with a ferrite-pearlite, pearlite and pearlite structure with cementite

ISSN: 2663-8770, E-ISSN: 2733-2055
ETM
EQUİPMENT, TECHNOLOGİES, MATERİALS
EQUİPMENT, TECHNOLOGİES, MATERİALS
VOLUME 05 ISSUE 01 2021

inclusions are arranged. The effect of different porous material structures on cutting speed is similar to the effect of compact material structures. An increase in the porosity of the material from 15 to 30% increases the roughness of the surfaces of the parts by about one class, however, the cutting force decreases by a factor of 1.6 - 1.7 times.

When processing iron-graphite powder compositions, the cutting forces are also reduced. In this case, graphite, having a complex atomic-crystalline structure, acts as a dry lubricant. Oil impregnation of such materials leads to an increase in cutting speed by only 30%, since the oil acts mainly as a coolant, lowering the temperature in the cutting zone. Oil impregnation of non-graphite materials increases cutting speed by 2.5 - 4 times.

When cutting powder materials, tools from high-speed steel, hard alloys, mineral ceramics, diamonds, etc are used. The choice of tool material is determined by the economic feasibility of its use, durability and productivity. For the processing of porous materials based on iron, bronze and some others, it is most rational to use hard alloys of the BK group, which, in order of increasing resistance, are arranged in the following row: BK8, BK3M, BK6M. With a decrease in porosity, mineral ceramics can be used. For the processing of powder materials of high hardness, superhard tool materials are recommended.

In [4], on the basis of research, it has been proved that each processed material has its own thermal structure of maximum machinability θ m.r., on the basis of which the temperature can be determined by changing the physical and mechanical characteristics of materials. And each instrumental material has its own temperature of maximum working capacity θ m.r. at which its ability to withstand loads increases, accordingly wear decreases and reliability raises. Based on this, we can conclude that when processing materials by cutting, the option of coincidence of these temperatures will be ideal. This can be achieved by choosing the appropriate tool material and maintaining the required temperature in the cutting zone (by assigning appropriate modes) [5].

For the correct choice of hard alloy when assessing the quality of assembled tools, on which the reliability indicators, durability (cutting path) and reliability depend significantly, it is proposed to introduce the coefficient of thermal compatibility Kt.c.. of the processed material and tool hard alloy. Thermal Compatibility Coefficient:

$$Kt.c. = \left(\frac{\theta_{m.p}}{\theta_{m.h}}\right)^{n} \qquad (2)$$

where, $\theta_{m.p}$ and $\theta_{m.h}$- the temperature of the maximum performance of the hard alloy and the machinability of the material; n = 3 at θm.p. < θm.h. ; n = 3 at θm.h. < θm.p.

Research technique: Low-alloy (XBG, 9XC) and high-speed (R18, R6M5) steel is used in the production of reamers. In the catalogs of tools of foreign companies, the material is designated HSS. Reamers are tools for finishing pre-drilled or countersunk holes. Figure 1 shows the design of an all-metal reamer. The operation allows to obtain high-class geometric parameters, dimensional accuracy and surface roughness. As it can be seen from Fig. 3, the operation of boring the guide bushing (Fig. 2) of the valve is better divided into several stages: roughing and finishing. The allowance for the rough cut is 0.1-0.15 mm and for the finishing pass 0.014-0.05 mm (Table 1).

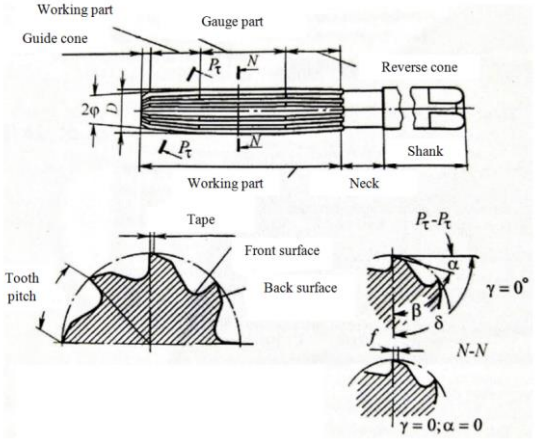

Figure 1. General view of the cross-sectional surface of the N-N gauge part and angles of the working part in the section Pτ - Pτ and N-N.

ISSN: 2663-8770, E-ISSN: 2733-2055
ETM
EQUİPMENT, TECHNOLOGİES, MATERİALS

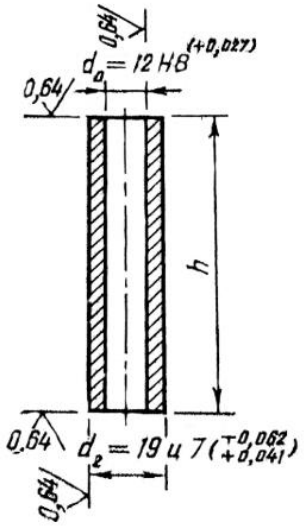

Figure 2. Valve guide

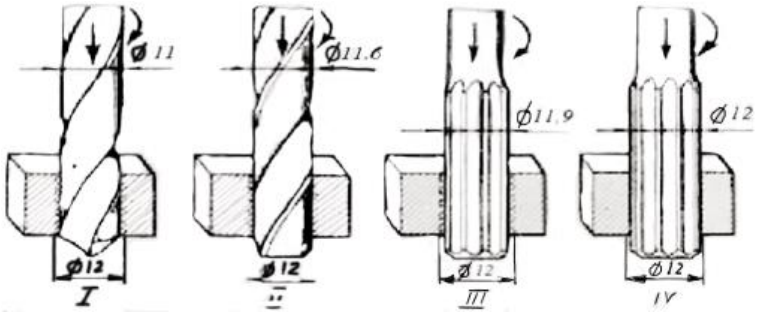

Figure 3. Hole machining sequence

Table 1

Allowances values in reaming

Allowance type	Allowances (mm) with hole diameter, mm.				
	12-18	18-30	30-50	50-75	100
General for finishing and rough reaming	0,15	0,20	0,25	0,30	0,40
For rough deployment	0,1-0,11	0,14	0,18	0,2-0,22	0,3
For finishing reaming	0,04-0,05	0,06	0,07	0,08-0,1	0,1

In order to understand in more detail how the deployment is carried out, the procedure for carrying out such a technological operation using a specific example can be considered. To get a hole with a diameter of 12H8+0.027, first a drill with a diameter of 11mm is used, then the resulting hole is countersunk to a diameter of 11.6mm, processing is carried out with a rough reamer with a diameter of 11.95mm, and then finishing is performed by using a tool with a diameter of 12H8 mm, with which the allowance 0.024 ... 0.027 mm is removed.

The sequence of machining a hole with a diameter of 12 mm in a steel part made of powder materials (ЖГр1.5Д2.5) according to 6-7 grades:

1 - drilling a hole with a diameter of 11 mm
2 - countersinking with 11.6 mm diameter countersink
3 - unfolding with 11.9 mm diameter rough
4 - reaming with 12 mm diameter finishing reaming

ISSN: 2663-8770, E-ISSN: 2733-2055
ETM
EQUİPMENT, TECHNOLOGİES, MATERİALS
EQUİPMENT, TECHNOLOGİES, MATERİALS
VOLUME 05 ISSUE 01 2021

How high the accuracy of the hole obtained during reaming will distinguish, as well as the degree of roughness of its surface is significantly influenced not only by the geometric parameters of the tool used, but also by the type of lubricating and cooling fluid used during processing. When reaming holes in steel parts, special emulsions mixed with mineral oil are used as such a liquid. When processing bronze and brass parts, mineral oils are not added to the lubricating coolant composition [6, 7].

From Table 2. the processed material ЖГр1.5D2.5 was selected. The original composition, in addition to iron powder ПЖ2М3 (GOST 9849-74), includes 2.5% copper powder (GOST 4950-78), 1.5% pencil graphite ГК-3 (GOST 4404-78), technical sulfur (GOST 126-76). The porosity of the material after sintering was 18.0% [8].

Reamers have an even (Z≥4) number of teeth located diametrically opposite each other. Each tooth cuts a thin layer, which makes it possible to obtain high accuracy.

Table 2

Processed material and microstructure

Processed material	Microstructure	HB, MPa
ЖГр1.5	Lamellar perlite, a small amount ferrite, places of inclusion of cementite	900
ЖГр1.5	Ferrite + perlite	700
Ж	Ferrite	500
ЖГр1.5Д 2.5К (sulfiding)	Ferrite + sulfides + lamellar perlite	700
ЖГр1.5Д 2.5К (sulfiding)	Ferrite + sulfides + granular perlite	700
ЖД3	Ferrite + solid solution of copper in iron	550
ЖГр1.5Д 2.5	Lamellar perlite, small amount of ferrite, places of inclusion of cementite	1000

Reaming allowance:

$$t = 0.5 (D-d) \quad (3)$$

where, D - tool diameter, mm; d is the diameter of the preliminary hole, mm.

When drilling holes, the recommended drilling feed is doubled. Recommended deployment feeds are given in Table 3.

Feed rate S mm/rev. in a rough reaming, the high-speed steel reamers is given in table. 3.

Table 3

Recommended deployment feeds

Processed material	Sweep diameter, D, mm							
	Up to 10	St. 10 until 15	St. 15 up to 20	St. 20 up to 25	St. 25 up to 30	St. 10 until 15	St. 30 up to 35	Over 40 up to 50
ЖГр1.5D 2.5	0,1	0,13	0,15	0,17	0,2	0,23	0,26	0,3
Cast iron, HB≤200 and copper alloys	2,2	2,4	2,6	2,7	3,1	3,2	3,4	3,8
Cast iron, HB> 200	1,7	1,9	2,0	2,2	2,4	2,6	2,7	3,1

Note:

1. When finishing reaming, with the feed should be reduced multiplying by the factor KOS= 0,75.
2. When using reamers with a carbide cutting part, the feed must be reduced by multiplying by the KUS= 0,7 factor.
3. When expanding blind holes, the feed should not exceed 0.2 ... 0.5 mm / rev.

The assigned feed must be adjusted according to the passport of the selected machine. In this case, it is necessary to meet the condition:

$$Sm \leq S \quad (4)$$

ISSN: 2663-8770, E-ISSN: 2733-2055
ETM
EQUİPMENT, TECHNOLOGİES, MATERİALS

where, Sm is the value of the feed finally established according to the passport.
Cutting speed (m / min) during reaming is determined by:

$$Vp = \frac{Cv \times Dq}{T^m \times t^x \times S^y} Kv \,, \quad (5)$$

where, D is the diameter of the reaming, mm;
Kv is the total correction factor.
The values of the Kv coefficient and exponent are shown for reaming in Table 4.

Table 4

Cv value and exponents for determining cutting speed during reaming

Processed material	Type of treatment	Tool material	Cv factor and values				
			Cv	q	x	y	m
ЖГр1.5D 2.5	Reaming	Highspeed steel	10,5	0,3	0,2	0,65	0,4
		Hard alloy	0,06	0,3	0,2	0,65	0,35
Gray cast	Reaming	Highspeed steel	15,6	0,2	0,1	0,5	0,3
		Hard alloy	109	0,2	0,0	0,5	0,45

The value of the period of durability T is given in table 5.

Table 5

Average value of the period of durability T min, drills, countersinks and reamers

Tool (operation)	Processed material	Tool material	T min, with tool diameter					
			Up to 5	6-10	11-20	21-30	31-40	41-50
Ream (reaming)	ЖГр1.5D 2.5	Highspeed steel	-	25	40	80	80	120
		Hard alloy	-	20	30	50	70	90
	Gray and Ductile Iron	Highspeed steel	-	-	60	120	120	180
		Hard alloy	-	-	45	75	105	135

The general correction factor for cutting speed (Table 6), taking into account the actual cutting conditions, is determined by the formula:

$$KV = KMV \cdot KiV \cdot K1V \cdot K2V \,, \quad (6)$$

where, KMV - coefficient for the processed material;
KiV - coefficient for tool material;
K1V - coefficient taking into account the depth of deployment;
K2V - coefficient of porosity of materials.

Table 6

Coefficient taking into account the effect of material porosity on cutting speed

Processed material	Porosity,%	For products, soaked in oil	For products not soaked in oil
Based on	15	0,85	0,8
Iron	20	1,0	1,1
ЖГр1.5D2.5	30	1,25	1,1

The KMV coefficient is calculated by the following formula:

ISSN: 2663-8770, E-ISSN: 2733-2055
ETM
EQUİPMENT, TECHNOLOGİES, MATERİALS
EQUİPMENT, TECHNOLOGİES, MATERİALS
VOLUME 05 ISSUE 01 2021

KMV = $\left(\frac{750}{\sigma_b}\right)^{nv}$ when processing ЖГр1.5D2.5.

The KMV coefficient is calculated by the following formula:

KMV = $\left(\frac{1900}{HB}\right)^{nv}$ when machining gray cast iron.

The KMV coefficient is calculated by the following formula:

KMV = $\left(\frac{150}{HB}\right)^{nv}$ when machining ductile iron.

where, σ_b is the ultimate strength of the workpiece material, MPa;
HB is the hardness of the workpiece material, MPa.
In this case, the tools are high-speed steel reamers and reamers equipped with plates of tungsten hard alloys (BK8, BK6M). Preference should be given to reamers with hard alloy. The use of high-speed steel reamers is limited by low durability, especially at speeds over 30-40 m / min.
When processing porous materials, the greatest wear is observed at the transition of the cutting part to the gauging part, as well as when processing compact materials. As a criterion for determining the amount of wear, the wear on the back surface is taken, which should not exceed 0.2 ... 0.3 mm.
The most significant influence of the considered features of mechanical processing of powder materials has on the value of the cutting speed (Table 7) [9, 10].

Table 7

Cutting speed when processing various materials, m / min.

Tool material	Durability, m / min.	Processed material		
		Steel 40KH (annealed)	Cast iron СЧ 15	ЖГр 1.5D 2.5
BK8	24	210	180	60-98

For materials on an iron base with a porosity of 18%, the following reaming mode is recommended, cutting speed 15-60 m / min, cutting allowance no more than 0.1-0.2 mm, feed no more than 0.2-0.3 mm / rev. Geometric parameters of reaming: φ=10o, γ = 0o, α = 6o. When reaming, it is necessary to use a cutting fluid such as spindle oil, which helps to improve the quality of the treated surface.
When drilling, countersinking and reaming, K1V=1,0.
After determining the cutting speed, the machine spindle speed nc (1 / min) is calculated:

$$nc = \frac{1000\, V_p}{\pi\, D}, \quad (7)$$

where, D - tool diameter, mm.
The resulting value nc is corrected according to the passport of the machine and the nearest smaller step nst is accepted, i.e. the condition must be met: nst ≤ nc. In further calculations, only nst is used.
The torque, Nm, and the axial force, N are calculated using the following formulas for reaming and countersinking:

$$Mt = 10 \cdot CM \cdot Dq \cdot tx \cdot Sy \cdot Kp \quad (8)$$

$$Po = 10 \cdot Cp \cdot tx \cdot Sy \cdot Kp \quad (9)$$

where, Cm and Cp are coefficients that take into account cutting conditions; the Kp coefficient in this case is depends only on the workpiece material.
To determine the reaming torque, each tooth of the tool can be viewed as a boring bit. Then, with a sweep diameter D, the torque is calculated:

$$Mt = \frac{C_p \cdot t^x \cdot S_z^y\, D \cdot z}{S \cdot 100}, \text{ Nm} \quad (10)$$

where, Sz - feed, mm per 1 tooth of the reamer;
z is the number of reamer teeth;
S= Sm - accepted feed, mm / rev.
Investigations of determining the executive dimensions of special reamers for finishing the holes, the serial bushing is pressed into the cylinder head with a maximum tightness of 0.062 mm (Fig. 5). Before pressing, the

ISSN: 2663-8770, E-ISSN: 2733-2055
ETM
EQUİPMENT, TECHNOLOGİES, MATERİALS

bushing is cooled in liquid nitrogen vapor on the installation for cold treatment of the valve bushings of internal combustion engines (Fig. 6). In order to determine the optimal fit for pressing bushings made of metal powders into the cylinder head and the executive dimensions of special rifle reamers for finishing the bushing holes after pressing in, comparative studies of elastic and permanent deformations of the inner and outer diameters of guide bushings made of antifriction cast iron and powder composition have been carried out. For this, experimental cast iron clips were made (outer diameter - 80, inner - 19.01, height - 80 mm), bushings made of powder material and antifriction cast iron (outer diameter 19.05; 19.10; 19.15; 19.20 and 19, 25, internal - 11.62 mm), hard alloy reamers with size 12.024; 12.026; 12.028; 12.030 and 12.032 mm. The mode of reaming the holes of the pressed-in bushings with a diameter of 12 (+0.027) mm: n = 2590 min-1 ,S = 0.086 mm / rev, V = 97.8 m / min. The outer and inner diameters and the height of the processed sleeves have been measured, after which they have been pressed into the prepared holders and the holes were unrolled, the diameter of which has been also measured.

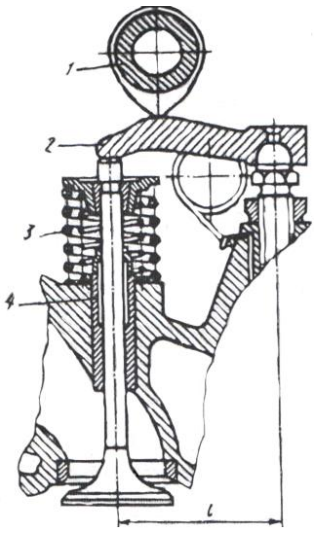

Figure 5. Cam mechanism; 1 - cam; 2 - pusher (lever); 3 - valve springs; 4 – bushing

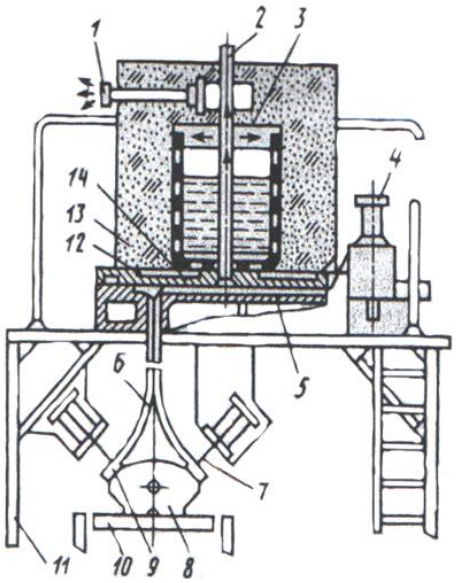

Figure 6. Bushing cooling unit

An installation for cold treatment of valve bushings of internal combustion engines is shown in Fig. 6. In this unit, the bushing are cooled without direct contact with liquid nitrogen. Only in the upper part of the cooling pipe the sleeves come into contact with nitrogen vapors, which are discharged from the reservoir to the

atmosphere through the pipe 1. The valve bushings are cooled in liquid nitrogen vapor (pre-cooling) and by direct contact with a refrigeration tube immersed in liquid nitrogen. After cooling, the bushings are pressed into the block of the V-shaped engine on the assembly line. The refrigeration unit is mounted on a trestle 11. The reservoir 3 with liquid nitrogen is placed in the container 12. There is thermal insulation between the walls of the reservoir and the container 13. The refrigeration pipe 2 passes through the reservoir with liquid nitrogen. The valve bushings are loaded into the upper part of the refrigerating pipe, and unloaded through the hole in its lower part and through the horizontal chute 14 by the pusher 5 are fed alternately into the distribution chutes 6. From there, the bushings are fed to the fixing devices 9. The pusher 5 is driven by the pneumatic cylinder 4.
When the conveyor 10 feeds the next block of the engine 8 to the fixing devices, the pneumatic cylinder 4 is automatically triggered and the pusher 5 delivers the cooled bushings along the distribution trays 6 to the fixing devices. Each bushing is pressed into the engine block by rods of 7 pneumatic cylinders located on the sides of the engine. The area of variation of the sliding friction coefficient in a cam pair of internal combustion engines during normal operation f = 0.01 ... 0.08 (0.1)
After such a complex of works, the bushings were pressed out of the clips and again subjected to a complete measurement. After data processing, the averaged values of elastic (δd2)elas. ,(δd0)elas. and residual (δd2)res., (δd0)res. of deformations of the outer and inner diameters of the bushings, respectively, were obtained (Fig. 7).

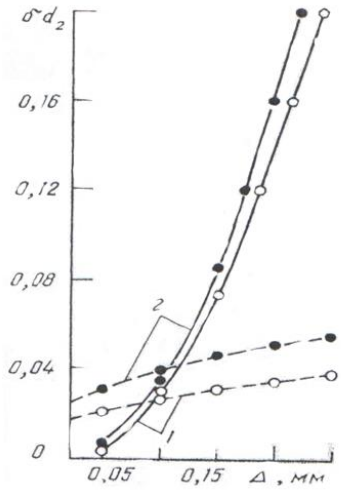

Figure 7. Dependences of elastic (dotted line) and residual (solid line) deformations of the bushing holes from the interference fit: 1 - ЖГр1.5 D 2.5; 2 - Cast iron СЧ15

To calculate the values of (δd2)elas. and (δd2)res., the following relations were used:

$$(\delta d2)\ elas = d2' - Do \quad и \quad (\delta d2)res. = d2 - d2', \tag{11}$$

where, Do - inner diameter of the holder, mm;
d2′ is the outer diameter of the bushing after pressing, mm.
The values (δdo)elas. and (δdo)res. were determined from the dependences:

$$(\delta do)\ elas = d1'' - d1', \quad и \ (\delta d0)res. = d1'' - (d0+\Delta d1), \tag{12}$$

where, d1 - bushing hole diameter after pressing, mm;
d1′- diameter of the hole of the pressed-in bushing after reaming, mm;
d1′′ is the diameter of the bore of the expanded bushing after pressing out;
Δd1 - allowance for the reaming operation, mm.
The interference fit consists of the following values: Δ=(δd2)elas. +(δd2)res.,

CONCLUSION

1. It has been determined that one of the important problems of mechanical engineering, is processing by cutting a hole by reaming in a sintered antifriction powder material in optimal conditions with the achievement of maximum performance.
2. The study was carried out for cylindrical bushings of small diameter and the processing of bushings was carried out for high speed and hard alloy tooling should not exceed the permissible upper limits.

ISSN: 2663-8770, E-ISSN: 2733-2055
ETM
EQUİPMENT, TECHNOLOGİES, MATERİALS

3. Reamer is shown to be a tool for finishing pre-drilled or countersunk holes. The allowance for the rough cut is 0.1-0.15 mm, and for the finishing pass 0.014-0.05 mm.
4. It was determined that the durability of the reamer and the cutting speed increase when processing oil-impregnated antifriction parts due to the fact that the impregnation reduces the surface roughness by about one class, 1.3-1.5 times the cutting force and most significantly affects the processing of powder materials without graphite.
5. It was investigated that, when machining by cutting iron-graphite materials, materials with a ferritic structure are better machined. Then, in order of deterioration of machinability, materials with a ferrite-pearlite, pearlite and pearlite structure with cementite cut-off are arranged. An increase in the porosity of the material from 15 to 30% increases the roughness of the surfaces of the parts by about one class, but the cutting force decreases 1.6-1.7 times.
6. We recommend reaming feed rates up to 50 mm reamer diameter and a general correction factor for cutting speed, taking into account the actual cutting conditions and porosity of the materials.
7. The tools in this case are high-speed steel reamers and reamers equipped with plates of tungsten hard alloys (BK8, BK6M). Preference should be given to reamers with hard alloy plates.
8. It was investigated that, when processing porous materials, the greatest wear is observed at the point of transition of the cutting part to the gauging part, as well as when processing compact materials. As a criterion for determining the amount of wear, the wear on the back surface is taken, which should not exceed 0.2-0.3 mm.
9. The reaming mode for materials on an iron base is determined at 18% and the following is recommended: cutting speed 15-60 m / min, cutting allowance no more than 0.1-0.2 mm, feed no more than 0.2-0.3 mm / rev. Geometric parameters of the sweeps: φ=10o, γ = 0o, α = 6o.
10. Investigations of determining the executive dimensions of special reamers for finishing the holes. The serial bushing is pressed into the cylinder head with a maximum tension of 0.062 mm.
11. It has been determined that the temperature of the instrumentation should not exceed the permissible upper limits. To press the bushings, it is necessary to use small interference fits in the cold state.
12. Comparative elastic and residual deformations of the inner and outer diameters of the guide bushings made of antifriction cast iron and powder composition were carried out. To calculate the values of (δd2)elas. and (δd2)res., we used the following relations: (δd2)elas. = d2′ - Do и (δd2)res. = d2 - d2′
13. It was determined that the range of variation of the sliding friction coefficient in a cam pair of internal combustion engines during normal operation f = 0.01 ... 0.08 (0.1)

REFERENCES

1. Makarov A.D. Optimization of cutting processes. 2nd ed. –M .: Mechanical engineering, 1976, -278 p.;
2. Karimov J.A. Mechanical engineering technology. –Baku: Chashyoglu, 2010, -508 pages;
3. Putilova U.S. Strength, reliability and service life of the cutting tool: a textbook. Nekrasov R.Yu., Putilova U.S. –Tyumen: from "Vector Buk", 20078, -160 p .;
4. E.V. Artamonov etc. Efficiency of tools and physical and mechanical characteristics of instrumental hard alloys and processed materials. Tyumen: Publishing house "Vector BCC", 2008, -160 p .;
5. Astakhov V.P. experimental investigation of the effect cutting depth, tool rake and work piece material type on the main cutting force during a turning process, 2006 UKL;
6. Eldarzade H.H., Guliyev A.A. Perforation processing of particles made of abrasive materials. ADNSU, News of Azerbaijan Higher Technical Schools, No. 2, 2015, p. 41-46;
7. Guliyev A.A., Eldarzade H.H., Huseynov S.S. Mechanical processing of parts made of abrasive materials. Problems of metallurgy and materials science. Materials of the I International Scientific Conference, Baku, AzTU, 2013, p. 33-37;
8. Eldarzade E.G., Guliev A.A. Features of grinding parts made of iron-based powder materials. Actual problems, no. 12, 2016, p. 154-158;
9. Karimov JA, Suleymanov GA, Badalova TA Interchangeability and thermal measurement of machinery and equipment. –Baku: Chashyoglu, 2003, -580 pages;
10. Handbook of a technologist - mechanical engineer. In 2 t. Vol.1 / Ed. WHITE. Kosilova and R.K. Meshcheryakov. –M .: Mechanical engineering, 1985, -656 p.

ISSN: 2663-8770, E-ISSN: 2733-2055
ETM
EQUİPMENT, TECHNOLOGİES, MATERİALS

EQUİPMENT, TECHNOLOGİES, MATERİALS

VOLUME 05 ISSUE 01 2021

STUDY OF DESIGN FEATURES AND MAIN CAUSES OF VALVE FAILURES IN RECIPROCATING COMPRESSORS

Natig Seyidakhmedov

Azerbaijan State Scientific Research Institute. Labor Protection and Safety Engineering.

E-mail: n.natiq.az@mail.ru

ABSTRACT

At present, the compressor industry of the oil sector of Azerbaijan is one of its leading links. If by the end of the 20th century the number of wells using the gas-lift method of production was about 42-46%, then by the end of 2019 it exceeded the 50% level. Compressors are an integral part of this technological process and require a strict improvement in the technical level of their safe operation. Therefore, improving the technical and economic performance of the compressor unit is an important task.

This work is devoted to the study of design features and the main causes of valve failures in reciprocating compressors, as well as an assessment of their safe operation.

Keywords: reciprocating compressor, reliability, valve, safety, gas-lift extraction method.

Relevance of the topic. As the long-term practice of operating reciprocating compressors in the system of gas-lift operation of oil wells shows, the efficiency, safety, reliability and tightness of the valves are sharply reduced due to dynamic processes, i.e. frequent changes in pressure and physical and chemical properties of associated petroleum gas in the general system of "collection, treatment and transportation of gas". Under these conditions, the high-frequency components of the pressure change, as well as the resulting vibrational mechanical vibrations of the plate, accompanied by a breach of tightness or breakage of the plate, is the main cause of valve failures.

The versatility of the design of compressor machines determines the use of a variety of self-acting valves. Despite the extensive experience in the use of reciprocating compressors, the initial practical work on the creation, improvement and use of self-acting valves continues to this day.

The purpose of the work. The purpose of the work is to study the design features and the main causes of valve failures in reciprocating compressors

Study of design features of valves. Figure 1 shows the main types of self-acting reciprocating compressor valves. The self-acting valves of reciprocating compressors can be divided into two main types according to the shape of the closing body - poppet and plate. Poppet valves have mushroom or bowl-shaped closing organs. Lamellar - closing organs in the form of plates of various shapes and, depending on the shape of the plates, they are divided into annular, disc, tape, strip and reed direct-flow. This classification is basically adhered to by all existing standards for self-acting valves of reciprocating compressors.

More than 250 units of different modifications of reciprocating compressors are operated in the SOCAR system, however, two of them are the main ones: - ring and direct-flow.

The types of self-acting valves, depending on the shape of the closing bodies and the main landing dimensions of the valves, are regulated by GOST 13529-77.

Ring valves are mainly used on high-pressure stages and gas piston compressors (up to 5.0 ÷ 10.0 MPa).

With the transition to more progressive opposed compressor cylinders with increased rotational speed, ring valves began to meet the requirements imposed on them to a lesser extent. Ring valves, possessing whole bore sections and large lifting masses, increase the power consumption of the compressor and have a short service life. Therefore, ring valves are gradually being replaced by disc and straight-flow valves with large bore sizes without a spring.

ISSN: 2663-8770, E-ISSN: 2733-2055
ETM
EQUİPMENT, TECHNOLOGİES, MATERİALS


Ring valve


Disc valves


Strip (band) valve


PIK straight-through valve

Figure 1. Self-acting valves for reciprocating compressors

More than 250 units of different modifications of reciprocating compressors are operated in the SOCAR system, however, two of them are the main ones: - ring and direct-flow.
The types of self-acting valves, depending on the shape of the closing bodies and the main landing dimensions of the valves, are regulated by GOST 13529-77.
Ring valves are mainly used on high-pressure stages and gas piston compressors (up to 5.0 ÷ 10.0 MPa).
With the transition to more progressive opposed compressor cylinders with increased rotational speed, ring valves began to meet the requirements imposed on them to a lesser extent. Ring valves, possessing whole bore sections and large lifting masses, increase the power consumption of the compressor and have a short service life. Therefore, ring valves are gradually being replaced by disc and straight-flow valves with large bore sizes without a spring.
Disc valves are characterized by the fact that the protective element is made in the form of flat discs with slots for gas passage located along concentric circles. The disc diameter is usually 50-150 mm, thickness 1-3 mm. Depending on the disc diameter, the number of rows of concentric slots can be up to eight.
The advantage of the newest designs of disc valves is a high lift of the plate compared to ring valves, which is achieved by the presence of damper plates and the use of springs of variable stiffness.
Strip valves are made with self-springing plates, which are rectangular strips 0.4–1 mm thick [1].
The rise in the center of the plate is much greater than at its ends. This deformation of the plate causes it to return to its original state due to its own elastic forces. The use of such valves is limited to low pressure compressors only. At high pressures of 5.0 ÷ 10.0 MPa, the elastic force quickly disappears and the plates break.
Tongue valves are made with plates, one end of which is rigidly clamped. The shape of the plates is varied and is determined by the design of the seat. Reed valves are used on low pressure or vacuum compressors only.
The most progressive type of plate valves are direct-flow valves, which are mainly used on general-purpose air compressors, reciprocating compressors of main gas pipelines, gas-lift and booster compressor stations [2,3]. In all these cases, they have practically replaced the self-acting valves of other designs.
The use of direct-flow valves allows you to reduce the specific consumption of power consumption, increase the reliability of the compressor, maintain performance by reducing the tightness of the compressor valve plates, according to technical data sheets, and reduce the noise level it produces.
Figure 2 shows the design of the once-through valve and its assembly diagram. As can be seen from Fig. 2, the valves are assembled in a package of the same type of elements, consisting of a saddle and an adjacent spring plate (Fig.2, b). The package of elements is fastened with rings, fixed by locking strips. The reverse side of the seat serves as a lift limiter for the adjacent member plate. Valve seats are made of aluminum alloy or steel. The plates are installed in the valve parallel to the gas flow, which enters the seat cells, pushes them to the lift stop and enters the cylinder (if the valve is suction) or leaves it (if the valve is discharge).

ISSN: 2663-8770, E-ISSN: 2733-2055
ETM
EQUİPMENT, TECHNOLOGİES, MATERİALS
EQUİPMENT, TECHNOLOGİES, MATERİALS
VOLUME 05 ISSUE 01 2021

In the design of the PIK-AM valve proposed by prof. M.I. Frenkel retained the relative position of the plates and channels for the gas passage.

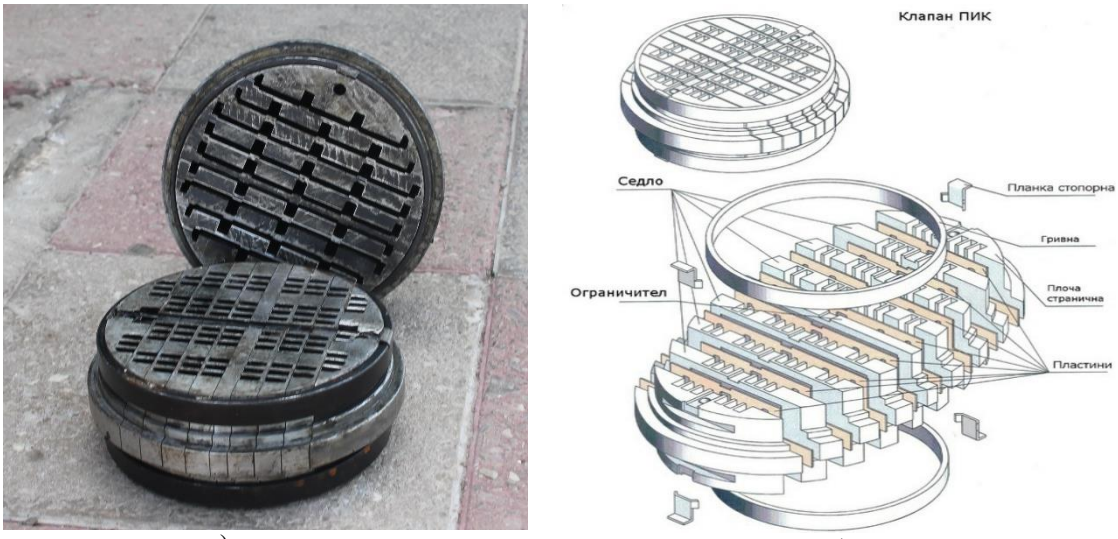

а) в)

Figure 2. Direct-flow PIK valve (a) and assembly diagram (b).

However, the valve plate consists of several closing elements connected by a common bridge along the clamped edge. Each movable element covers several channels in the saddle (usually no more than three or four). This shape of the plates makes it possible to significantly increase the perimeter of the slot, its useful area of passage and, as a consequence, reduce the gas velocity in the valve. In addition, the use of narrower closing elements in the PIK-AM valves makes it possible to increase the tightness of the valves and maintain the performance of the reciprocating compressor.

The operating experience of PIK direct-flow valves with rectangular plates without slots shows that the tightness and durability of valves depends on a number of factors: the pressure drop across the valve, the presence of gas pressure pulsations, the presence of moisture, oil and oil vapors in the gas, mechanical impurities, the travel of the plate and its shape, etc.

Research results and their discussion. We have analyzed the failures of some parts and assemblies of the MMC and their fittings (see Table 1) installed at the GKS NGDU named after N. Narimanov. Moreover, out of the installed 10 units of MMC on one GCS, the table contains failures of parts and assemblies of 4 MMC. It should be noted that in Table 1 indicates those elements, the failures of which lead to large downtime of the compressors. It was found that within six months each mining and metallurgical plant was on average 3665 in operation, 550 in idle time, 795 in repair (or in reserve).

Table 1

Analysis of failures of some parts and assemblies of MMC

Name of parts and assemblies	Number of failures and within six months for GKS No. 4 NGDU named after N. Narimanov			
	GMK-1	GMK-2	GMK-3	GMK-4
Compressor cylinder valves	75	71	79	82
GMK spark plug	51	64	70	72
Tristor ignition system	17	18	16	17
MMC flow line check valves	3	2	4	1
Gas outlet valve GMK	5	6	4	7
Safety valves on flow lines	1	0	0	2
Other failures associated with the shutdown of the MMC	10	7	4	5

ISSN: 2663-8770, E-ISSN: 2733-2055
ETM
EQUİPMENT, TECHNOLOGİES, MATERİALS

The data presented indicate the need to improve the trouble-free operation of the mining and metallurgical complex, where the main cause of failures is malfunctions with valves (direct-flow type).
The analysis of the state of the failed parts operating in different conditions (reception, injection) is carried out. The analysis of the results of observations of the operation of the intake and discharge valves of the compressor cylinders installed at the I stages of the MMC showed that in 67 cases the failures refer to the suction valves and 148 to the discharge valves of the 1st stage, and 95 to the discharge and 43 to the suction valves of the II stage.
Thus, the largest number of failures is accounted for by the valves installed on the compressor cylinders of the first stage, where the temperature and compression ratio of the discharged gas are much higher than others. Consequently, the temperature has a significant effect on the number of failures of direct-flow valves, which, and mainly, occur as a result of the destruction of their plates.
The main factor determining the insufficient MTBF of self-acting valves is cyclic dynamic loads as a result of frequent changes in the pressure of associated petroleum gas at the intake and injection of a reciprocating compressor associated with frequent changes in the pressure of compressed gas in the gas lift, which is accompanied by the vibrational nature of the plates valve. In this case, the number of cycles of movement of the plates increases significantly, self-oscillations arise, which sharply reduce the efficiency of the plates. In addition, associated petroleum gas with solid mechanical impurities, vapors of heavy hydrocarbon components and moisture passes through the valve. In this case, the valve plates, having received additional stresses from local bends during closing, adhere to the seat and collapse, and nicks, risks and other damage appear on the seats . In most cases, the plates break along the line of their pinching in the valve or at the edge of the seat. In this case, due to the leakage of the valve plate, the temperature of the booster gas rises sharply and the performance of the compressor decreases and an emergency situation is created.
After breakage of one or several petals of the plates, the valve begins to heat up, and the suction and discharge pipes are heated. In this operating mode, the temperature of the valve and cylinder in the valve installation zone reaches 205 ÷ 210 ° C in a short time of operation. At such a temperature, the valve seats warp, their depressurization, a further increase in temperature, failure of other parts of the compressor cylinder, especially the 1st stage, where the compression ratio reaches 4 ÷ 5. In connection with this, the task of increasing the reliability, tightness and safety of the operation of direct-flow valves for the conditions of gas-lift operation of oil wells
Positive experience in operating single-flow valves in general-purpose air compressors, their high performance in terms of efficiency and durability dictates the need for both experimental research and the development of technical solutions that would provide an expansion of the field of effective application of single-flow valves, in particular, on compressors used for gas-lift operation of oil wells.
In the harsh conditions of gas-lift operation of oil wells, PIK-type valves practically had an operating time to failure of no more than 1500 ÷ 1700 hours. However, by improving the shape of the plates (making several slots in it) of the PIK-A valves, their tightness was achieved. At the same time, the time of their operation to failure reached 2500 ÷ 3000 hours.
Thus, as a result of the study of the main characteristics and causes of failures of individual units, including the valves of reciprocating compressors, it was shown that
- the efficiency of gas-lift operation is largely determined by the reliability of the compressor equipment;
-the main reasons for the failure of reciprocating compressors are the assembly of the intake and discharge valves of the compressor cylinders (46-54%), spark plugs (30-50%), a violation associated with the ignition system (10-11%), etc.;
- the largest number of failures are associated with direct-flow valves installed on the compressor cylinders of the 1st stage;

REFERENCES

1. Куликов С.П. Разработка и исследование двухмерной математической модели клапанов пластинчатых полосовых поршневых. Автореферат дисс. Канд.техн наук. 2009. Тюмень
2. http://allcompressors.ru/page/KlapanCPK.php Цельнолитые прямоточные клапаны (Клапаны ЦПК)
3. Калекин В.В. Разработка и исследование поршневых пневмодвигателных агрегатов самодействующими клапанами. М.: РГБ, 2005. 234с.

ISSN: 2663-8770, E-ISSN: 2733-2055
ETM
EQUİPMENT, TECHNOLOGİES, MATERİALS

EQUİPMENT, TECHNOLOGİES, MATERİALS

VOLUME 05 ISSUE 01 2021

THE STUDY OF PHYSICAL AND MECHANICAL PROPERTIES OF PACKERS' CUFFS

[1]Zenfira Huseynli, [2]Elkhan Nazarov

[1]Azerbaijan State of Oil and Industry University, PhD in Technical Sciences. (Azerbaijan).

[2]Azerbaijan State Oil and Industry University, Master. (Azerbaijan).

E-mail: huseynli_z@rambler.ru

ABSTRACT

In the drilling of wells, cementing of protective pipelines, development of productive horizons, as well as in operation, wells need to be divided into permanent or temporary areas. More advanced than these processes is the use of packing devices in the technological separation of layers and the insulation of protective belts. For example, delivery of the buffer mixture to the absorption zone by packer-mounted drill pipes saves 40-60% of time and reduces material consumption by 1.5-2 times compared to previous non-packer technologies.
Keywords: packer, cuff, protective pipeline, sliding, sealing

In the early stages of the oil industry, packers were mainly used to insulate surface water leaking from holes in the protective belt. In the study of wells in engineering-geological and hydrometeorological processes, packers began to be used for the practical injection of liquids. These packers worked at low pressure drops in shallow wells, distinguished by the simplicity of their design and the technological scheme of sealing. In recent years, significant progress has been made in the field of theoretical research in drilling exploration and production wells, as well as in the technology of using packers and improving the performance of packer cuffs.
Relevance of the case: The packer cuff is one of the important nodes of reliable sealing of packer equipment. One of the most pressing issues is the study of the inability of the packer's sealing sleeve to provide sealing without friction during contact with rocks when operating in aggressive environments. To study the causes of wear of cuffs without friction, the physical and mechanical characteristics of its use in various packers have been studied [1].
The purpose of the work: To investigate the causes of wear of packer cuffs, which is one of the main equipment during the operation of oil and gas wells, and to eliminate these causes and ensure the reliable operation of packer cuffs.
As the depth of the wells increased, and the goals and issues of layering and piping separation expanded, so did the loads on the packers' sealing sleeves, and their operating conditions and use became more complex. This has led to the development of many different packer constructions and constructive executions. Such a wide variety of packers of the required type size is very difficult to collect, analyze, group, and apply in practice. When systematizing packer constructions, packers are divided into four groups [2]:
1. Packers with elastic elements covering the well by swelling and deformation of the grains located in the inner strip of the sealing sleeve under the influence of pressure. Such packers are not used in modern times.
2. Packers with anchors or skirts. In this group, the sealing sleeves are attached to the well wall by means of an axial force, such as the weight of the pump-compressor pipes after the packer has been installed in the well.
3. Wall packers. This group includes packer devices where deformation of the sealing sleeves occurs after the friction plates are fixed to the well wall. Wall packers, in turn, are divided into two subgroups: first, the packers 'plates are working under the influence of friction springs, and second, the packers' friction plates stick to the walls of the well after the load falls on the surface of special drill pipes.
4. Hydraulic packers. Sealing of the well with these packers is carried out by deformation of the sealing sleeve and compression of the well wall under the influence of the working pressure of the liquid injected from the surface.
By analyzing the constructions and technological schemes of packers used in the operation of oil wells with hydraulic piston pumps, injection of water into injection wells and hydraulic fracturing of the formation, a classification of a large number of packers with different impact principles was prepared. The main features of this classification are: types of packer installation in the well; types of deformation of the sealing cuff; the cost of lowering the packer into the well and the pressure drop it can accept.
Packers are divided according to the type of installation in the well: packers installed on the well with support, without support or "hanging". Packers are divided into hydraulic and mechanical packers according to the type of deformation of the sealing element and the sealing of the protective belt. Mechanical packers include all packers

ISSN: 2663-8770, E-ISSN: 2733-2055
ETM
EQUİPMENT, TECHNOLOGİES, MATERİALS

whose sealing sleeve is deformed due to the weight of the pipeline. Hydraulic packers - packers that seal the pipe by deforming the rubber sleeve as a result of a pressure drop from below or above the installed packer. According to the type of discharge into the well: they are divided into packers, which are released into the well by pipes and thrown.

Slip-backed packers have a device that seals the well after it is anchored in the wall of the well, it is a special knot, open or closed type spring, combined with special slip pulls and placed under the sealing sleeve. The main difference between inverted packers and slip packers is that the support knot is located under the "sealing cuff".

Self-sealing packers are characterized by the fact that their sealing sleeves are bell-shaped, the outer diameter of which exceeds the diameter of the well, which is covered in a free state. Therefore, its compression in the well wall is carried out due to the elasticity of the rubber of the cuff material, sealing occurs automatically, as the degree of compression of the cuff on the walls of the well increases under the influence of pressure drop.

Combined packers are a combination of self-adhesive packers and well-wall packers. In modern times, they are widely used in test tool kits used to test productive horizons of oil and gas wells and aquifers of hydrogeological wells. The advantage of slip-backed packers in the well wall is that the sand plugs do not affect their performance, and they do not require a tail support to perform their work, as the flowers of the well walls are below the place where they are installed. Despite some construction complexity, these packers are considered to be more promising than compression-type packers, which makes them widely used in hydraulic fracturing, injection of water into the reservoir, and insulation of the absorption zone with detergent. Packers installed without a support at the bottom or wall of the well do not have the above advantages, so the method of creating a support is used in all types of packers.

Properties of rubber cuffs. Many researchers have studied the mechanical properties of rubber used in packers. Physical and technical characteristics of rubber cuffs are given in Table 1. The following features of rubber cuffs are taken into account:

- working deformation of the cuff σ 50% longitudinally; 25% in diameter;
- the rate of deformation of the cuff at work is several centimeters;
-packer can stay in work for 30 minutes to several hours in case of deformation;
-sealing cuff is designed for multiple use;
-packer works in high temperature and pressure conditions.

Resistance methods of materials allow to calculate the strength condition in one stress type for another stress state type according to the strength condition [3]. However, such calculations do not take into account the effects of stresses, loads, temperatures, environments and other similar factors occurring in the process.

Deformation properties of rubber cuffs. The elastic deformation ability of rubber is one of the main reasons why it is widely used in all industries, including in the manufacture of packing cuffs for packers. Table 1 shows the physical and technical characteristics of the rubber cuff.

Table 1.

Physical and mechanical characteristics of cuffs

Name	Symbol	Numerical unit
The crowd	ρ	q/sm2
Temperature limit in brittleness	∂_{xp}	0C
cuffs elastic module	EБ	MPa
frost-resistance coefficient,	КБ	-
wear durability	σ_p	MPa
cuffs relative elongation	ε	%
tension to relaxation	РБ	%
Mass tensions	Qk	%
volume change	QH	%
Stretch Time	τ	min
Slip speed	υ	min
Relative residual deformation in compression	G	%

The description of rubber as a structural material can be compared with its high elastic deformation, which is due to the ability of long-chain molecules of rubber polymer to change their configuration under the influence of external forces. This change in the configuration of the polymer is not accompanied by any significant change in the distance between the molecules. In undeformed rubber, individual areas or points of the molecular chain are

ISSN: 2663-8770, E-ISSN: 2733-2055
ETM
EQUİPMENT, TECHNOLOGİES, MATERİALS
EQUİPMENT, TECHNOLOGİES, MATERİALS
VOLUME 05 ISSUE 01 2021

randomly located in space. If the temperature is high, the molecular bonds have a sufficiently large mobility, and the nature of their mutual arrangement and heat transfer is the same as in low molecular weight liquids. The application of an external force causes the dams to focus on the force acting in parts.
The free recovery of a highly elastic body after the application of an external force is the result of thermal action and its disorientation effect on the location of the dams. The processes of orientation and disorientation of dams occur when the balance between the force and the deformation caused by it is not instantaneous, it takes a certain amount of time, and the process of sliding takes place. Crawling is the process of restoring the balance between stress and strain. It occurs in a constant voltage mode. Here, slip is a continuous process of increasing the initial deformation to the equilibrium value of the deformation from the time of application of a constant load force. The slippage of the rubber leads to significant changes in the tightening joints of the constrictive dimensions and the elastic cuff of the packer.
Suppose a packer works under the following conditions: maximum pressure drop:
$\Delta P = 50$ MPa, the diameter of the sealing sleeve before compression d=250 mm, outer diameter of the protective belt $d_{q.k.} = 210{,}6$ mm, $\rho_{st} = 6840$ kq/m^3,

$$E_{st} = 2 \cdot 10^{12} \text{MPa},$$

Poisson's ratio of rubber cuff $\mu = 0{,}573$,
elasticity of rubber $E_r = 188 \cdot 10^5$MPa,
packer durability coefficient k=1,25.
First, calculate the annular cross-sectional area of the sealing sleeve (Figure 1).

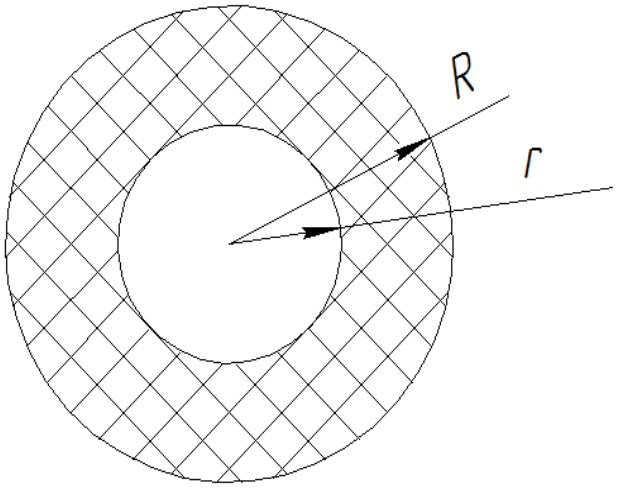

Figure 1. Ring section of Packer's sealing sleeve

$$F = \pi R^2$$

where: R is the outer diameter of the packing sleeve of the packer and r is the inner radius.

$$F = \pi R^2 - \pi r^2 = 3{,}14 \cdot 0{,}1025^2 - 3{,}14 \cdot 0{,}045^2 = 26{,}6 \text{ mm}^2 \quad (1)$$

To check whether the packer is airtight in the well, we calculate the contact pressure between the protective belt and the sealing sleeve:

$$P_k = P_{s.k.t} + P_{t.d.} \quad (2)$$

Where $P_{s.k.t}$ - contact pressure due to pre-compression of the seal ;
$P_{t.d.}$ pressure drop accordingly [4].
The hardness of the rubber is in itself a design indicator. However, there is a limited connection between rubber stiffness and tension. Resistance methods of materials allow to calculate the strength condition in one stress type for another stress state type according to the strength condition. However, such calculations do not take into account the effects of stresses, loads, temperatures, environments and other similar factors on the process. The thermodynamics of the state of a rubber assumes that there is a relationship between elongation, moving force, temperature, and energy.
The deformation mechanism of rubber has a superior kinetic origin, and the mechanical stress in the deformed material depends on the amount of entropy.

ISSN: 2663-8770, E-ISSN: 2733-2055
ETM
EQUİPMENT, TECHNOLOGİES, MATERİALS

Given the equality of loading and deformation, it is assumed that the stiffness of the packing sleeve of the packer is always lower at reloading than at the first loading. The modulus of elasticity in the reloading of the cuff is 44% lower than in the initial loading [5]. The residual deformation measured as the load is taken depends on the value of the transverse deformation of the element. For 25% transverse deformation (maximum deformation in the well), the residual deformation averages 4.5%; has a value of 1.2% to 9.5% in inclinations on individual samples. Residual deformation at reloads is more stable and is only 1.15%, ie several times lower than the deformation of the element under initial loading. It follows that the cuffs must be manufactured at the factory with a transverse compression of 25-30%. In this case, elements with a residual deformation of more than 5% must be considered defective.

The cuffs used in inflated packers are made on the basis of nitrile rubber, in which the movement of molecular chains significantly affects the strength and deformation behavior of the cuff, causing a large number of conformations at the ends of macromolecules. The friction force of the cuff in contact with rocks depends on many factors, the most important of which are: the composition and properties of the environment, the nature and area of the contact surfaces; normal pressure; deformation rate and. Researchers note that the greatest dry friction occurs when the cuff comes in contact with solid rocks (sand, lime, gypsum, salt, etc.). In this case, the frictional resistance is quite large, and the energy required for the deformation of the rubber is used to break down the material during the viscous-plastic process.

CONCLUSION

The reasons for the low performance of the packers' cuffs have been studied.

1. Residual deformation at reloads is more stable and is only 1.15%, ie several times lower than the deformation of the element under initial loading.
2. It follows that at the manufacturing plant, the cuffs must be made with a transverse compression of 25-30%.

REFERENCES

1. Kasumova S.A., Huseynli Z.S., Mamedov G.V. Investigation of the load of the packer packer during planting and in the process of sealing it with the use of a boom depth pump. AGNA, Izvestia of the highest technical educational institutions of Azerbaijan, 2012, magazine, № 2 (78) 2012, pp.19-21.
2. Dzhanakhmedov A.Kh. Tribotechnical problems in oil and gas equipment. Baku: Elm-1998.p.216
3. Mammadov VT Basics of calculation and design of elastic elements of hermetic knots of oilfield equipment. - Baku: Elm, 1997, p.46
4. Mammadov V.T. Calculation of hermetic knots of oilfield equipment. Baku: Elm, 1998, 198 p.
5. Hajiyeva L.S. Study of the effect of deformation characteristics of an elastic element on its sealing effect. Scientific works of AzTU, XII volume, №3, 2003, -p.70-72

ISSN: 2663-8770, E-ISSN: 2733-2055
ETM
EQUİPMENT, TECHNOLOGİES, MATERİALS

EQUİPMENT, TECHNOLOGİES, MATERİALS

VOLUME 05 ISSUE 01 2021

THE STUDY OF THE WEAR RESISTANCE OF THE PLATE NODES IN FRICTION DURING THE PACKER ASSEMBLY

[1]Zenfira Huseynli, [2]Miralam Karimov

[1]Azerbaijan State of Oil and Industry University, PhD in Technical Sciences. Associate professor. (Azerbaijan)

[2]Azerbaijan State Oil and Industry University, Master. (Azerbaijan)

E-mail: huseynli_z@rambler.ru

ABSTRACT

The article provides information on the research carried out to eliminate this problem due to the friction of the plates with integral sealing nodes during the mounting of packers used in the drilling, operation and technological processes of oil and gas wells. The problem of the packers losing their ability to work without friction during the installation of the packer is that the packer is removed from the well prematurely and replaced with new ones, which leads to both loss of time and material and technical losses.
Keywords: plate, worn out, mounting, cohesion, packer.

Experience with the use of packers in the testing of layers shows that in many cases the packing elements lose their ability due to the collapse of the lower part of the rubber element. In practice, it is very important to ensure reliable fixation of the packer at the wellhead in the separation of the space between the pipes by placing the packers in different ways. This is due to the different anchors, plate knots and packers of different constructions. An analysis of the design of the packers' anchor nodes used showed that a more reliable design of the fixation is a plate-type structure that separates in a radial direction when in contact with the spacing cones. Relevance of the work: The plates are one of the important knots in the sealing of the packing device. When the packer is installed in the wellbore, the teeth on the surfaces of the plates are attached to the metal holes on the outside of the protective pipe wall. The problem of friction wear of the anchor knot plates during the interaction with the pipe is relevant and requires further research, taking into account the factors of friction wear and tear of the plates with the pipe.
The purpose of the work: To investigate the causes of friction wear of the knot during the implementation of various technological processes in the packers during the implementation of various technological processes and to conduct research to eliminate this problem.
Over time, the improvement of packing facilities is due to the expansion of the use of hydraulic fracturing in wells. The implementation of such a technological process in oil and gas wells has placed the following requirements on packer systems.
- packers should be sealed at a pressure of up to 50 MPa for 30-40 minutes;
- The strength properties of the sealant (in aggressive environments) must be resistant to temperatures of 1200C.
"A", "NII-B" brand constructions of auto-controlled packer structures have such qualities. A characteristic feature of this type of packer is that its sealant can create a self-sealing effect. Such a constructive approach can be found in the packers PS-500 and PQ-500.
Petroleum equipment (NMA) is classified into 4 groups, which are structurally complex, functionally multifaceted: drilling, operation, ancillary and control equipment. The structures of this equipment include various types of joints, mechanisms that move them, transmissions, motors, nodes that perform power and displacement functions, parts that are subject to friction and deformation, and so on. include. At the same time, the design of the NMA, as well as the uniqueness of the technological processes used in their manufacture, the dynamics, aggressiveness and complexity of the operating conditions of the equipment further complicate the requirements.
Operational equipment is broadly divided into two groups: wellhead and wellbore equipment. The installation, maintenance and repair of the second group of equipment is very different from the first. Thus, the method and technology used to place this type of equipment inside the well is very difficult and complicated.
One of the most widely used methods of placing operating equipment inside a well is to anchor them with special holders. Anchors are typically used when underground equipment is required to be placed in a well to prevent it from slipping.
In general, when anchoring wells, the principles of anchor installation are used in 2 variants:
1. Supporting equipment performs the function of anchors independently.

ISSN: 2663-8770, E-ISSN: 2733-2055
ETM
EQUİPMENT, TECHNOLOGİES, MATERİALS

2. The anchoring mechanism is intended as a separate knot on the equipment (packers). Independent plate anchors are designed for mounting and centering equipment inside the well. They are produced in 4 groups (ЯЭЦ, ЯК , ЯГМ, ЯТ and ЯГ).
ЯЭЦ -type anchors are used in inclined wells. Here, anchoring is provided by eccentricity between the wellbore axis and the equipment axis. The constructive solution of the problem was solved with the help of the centering element and spring in the structure of the equipment.
ЯК -type anchors are commonly used to drill a second well in a wellbore. The advantage of the equipment is that the operation of supporting the bottom of the well is eliminated when fixing the wellbore.
ЯГМ -type hydromechanical anchors can prevent PVC-designed packers from sliding up and down when placing the wellbore inside.
ЯТ-type anchors prevent the NKB from sliding downwards, referring to the production belt.

At present, the reliable separation of the inter-pipe space with a packer is very important, especially in the use of high-pressure working solution during the hydraulic fracturing. Analysis of various studies in this area has shown that the force of interaction of the pipe plates with the pipes has a significant effect on the height of the plates and their conductivity [5].
In the following formula, the maximum carrying capacity of the tubes of the pipeworker depends on the live cross section of the pipe, its radius, the height of the plates and the angle of their interaction:

$$\sigma_{RƏ} = \frac{\sigma_T F_{e.k.s.} Q_{p.ə}}{R_2^2 CK} \quad (1)$$

where:
σa - flow limit of the pipe material;
Fen k.s - cross-sectional area of the worn pipe;
Q - inner radius of the pipe;
h - is the height of the plate;
ε - capacity coefficient of the pipe perimeter;
R2 - radius from the outside of the pipe;
C - coefficient characterizing the voltage concentration in the dangerous section;
K - is the coefficient of retention of the plates from the surface of the pipe and the coefficient of inclination of the conical surface of the plates to the body of the device;
σRƏ - is determined for the interconnection of the pipeline (6 units) and the suspension of the pipeline.
A similar problem can be solved by ensuring that the packer is fixed with plates when exposed to excess pressure from below during hydraulic fracturing:
(1) it is clear from the formula that as the height of the plates increases, so does the packer's storage capacity. If we assume that the height of the plates is close to zero, then the G-force that the packer receives and transmits to the plates is a force directed to infinity. This time

$$\sigma_q = \frac{PD}{2\delta^2} \quad (2)$$

where:
p - fluid pressure;
D - inner diameter of the protective belt;
δ - wall thickness of the protective belt.

It can be seen from the obtained formula that the contact voltages that can be released at the boundary of the "sealing-protective pipe pipe wall" can be determined from the known force received by the packer and transmitted to the plate.
It is known from practice that the contact voltages at the boundary of the packer's seat belt can be 10-15% higher than the working pressure [3]. From formula (2) it is possible to determine the permissible value of pressure P:

$$P = \frac{\sigma_{b.} 2\delta}{D}$$

The analysis of the obtained result shows that the threat of contact voltages at the boundary of the "sealing-protective pipeline pipe" is close, which should be taken into account, especially in the coverage of the space between the pipes in these worn protective pipelines. The use of the traditional method of radial deformation of the sealant due to axial loading requires a sufficiently large load. In this case, the sealing mechanism of the

ISSN: 2663-8770, E-ISSN: 2733-2055
ETM
EQUİPMENT, TECHNOLOGİES, MATERİALS
EQUİPMENT, TECHNOLOGİES, MATERİALS
VOLUME 05 ISSUE 01 2021

sealant must be changed, if a detachable plate cone is used for radial deformation of the sealant, then the tension is evenly distributed along the length of the sealant. Experience with this method has shown that the axial force required to deform the sealant is significantly reduced when the detachable cone of the plate is used.

During hydraulic fracturing, the sealant may lose its tightness due to the high pressure received by the packer from below (the force that pushes the anchor plates with a blow) and the packer may move from where it is installed. This leads to the cessation of the fixation process. The protection of the tightness of the interstitial space depends directly on the plates of the anchor knot. Therefore, it is necessary to develop new structures and anchoring devices for the installation of the packer. Some packers' cut plates are equipped with cut spring rings that are fixed to the protective belt body at the calculated depth. Fig. Figure 2 shows a single-pass hydraulic packer. Anchor from anchor body, 9 or 12 round plates; It consists of springs (9 or 12 pieces) that hold the plates in a compressed position during operation, cover shafts and fastening screws that restrict the radial movement of the plates.

A rubber ring is placed on the lower surface of the round plates. These plates are placed in the appropriate slots opened on the body (according to the rules of chess) and a bow is placed under each round plate. After the plates are installed in three or four rows by 4 on the perimeter of the body, the cover shafts (there are four of them, of course) are fastened with screws. The lower plate knot consists of a cone, three or five plates (in packers for 8 service belts) and a plate holder. On the outer surface of the cone are placed plates in three wedges opened at an angle of cone to α = 12o ... 15o (side protrusions of the conical surface of the plates), but the lower "T" -shaped ends of the plates are placed in the corresponding "T" -shaped wedges of the plate . After the packer is released into the well and brought to the required depth, water is pumped into the packer barrel (via the NKB). In this case, the fluid pressure in the packer's hydraulic cylinder, to which the valve is closed, rises, and the piston moves, tightening the rubber sleeves through the support washer and sealing them to the inner surface of the service belt. The cone is also pushed under the plates and thus the packer is seated. To direct the lower layer into the packer, the pressure is increased by an additional 3.5MPa (23 …25MPa from the seating pressure) and the cutting screws are cut, releasing the ball from the packer together with the saddle. Packer's channel opens. In this case, due to the pressure of the well product (oil or gas), the circular plates on the anchor are pressed into the belt, which prevents the packer from being pulled up. Under the influence of the pushing force, the packer leaves the place of installation. It is necessary to increase the number of holes in the body of the packer by increasing the depth. Also, the anchor should be provided with teeth in the body at a given depth, covering the entire body of the plates. Such a constructive design is implemented in the structures of the anchor with two protrusions along the height of the plates, which increases the adhesion of the anchor plates to the protective belt. It has been experimentally determined that the friction of the anchor plates with the pipes during the installation of the packer at the bottom of the well is due to the friction of the material surface of the two bodies, their pressure on each other, the relative speed of corrosion. Friction also depends on the quality and nature of the treatment of friction surfaces. In addition, the coefficient of friction depends on the speed. Friction forces are forces created by tangential interactions in the relative displacement of objects in contact with each other.

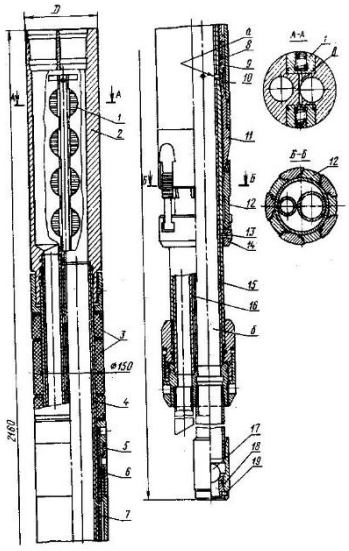

Figure 1. Single-acting hydraulic packer

1 - anchor plate; 2- the body of the anchor; 3 - cuffs; 4 - barrel; 5,13,19- cut screws; 6 - slips; 7- piston;

ISSN: 2663-8770, E-ISSN: 2733-2055
ETM
EQUİPMENT, TECHNOLOGİES, MATERİALS

8 - cylinder; 9 - slide; 10-handle; 11 - cone; 12-plate; 14 - plate holder; 15,16-guide tube; 17-ball; 18- saddle.

CONCLUSION

1. It is recommended to take the conical angle of the cone-plate pair in the packer plate node. In this case, the compressive force transmitted to the plates ensures a smooth fit of the plates.
2. As a result of the analysis of the work on the plate knot, increasing the height of the plate to reduce friction and increasing the number of teeth along the length of the body of the plate increases the adhesion strength, which reduces friction by increasing its efficiency.

REFERENCES

1. Janahmedov A.X., Mammadov V.T., Mammadov H.V. Hajiyeva L.S. Sealing knots. ADNA, Baku: Elm, 2011, 306 p.
2. Abubakirov V.F. Drilling equipment: Handbook in 2 volumes - Drilling tool / V.F. Abubakirov, Yu.G. Буримов, A.H. Gnoev and others. / M: OAO Nedra Publishing House - 2003 - p. 434-475.
3. Vahidov M.A., Karimov O. M., Eyvazova Z.E. Oil and gas production equipment. Textbook. Baku “Azerneshr” publishing house, 2008, 440 pages.
4. Huseynli Z.S. "Improving the sealing efficiency of packer structures used in the repair of production wells ." - Guidelines. DNA printing house, 2015, 26 pages
5. Mammadov H.V. Study of tribological parameters in sealing nodes of Packer structures. ADNA, the 51st STC of students, is dedicated to the "National Revival" Day of the Republic of Azerbaijan. Baku, 2002, p. 71-72

ISSN: 2663-8770, E-ISSN: 2733-2055
ETM
EQUİPMENT, TECHNOLOGİES, MATERİALS

EQUİPMENT, TECHNOLOGİES, MATERİALS

VOLUME 05 ISSUE 01 2021

PERSPECTIVES OF CYCLOID TRANSMISSION

[1]Alesker Aliyev, [2]Aydan Qasimova

[1]Azerbaijan State of Oil and Industry University, Doctor of technical Sciences. Professor. (Azerbaijan).

[2]Azerbaijan State Oil and Industry University, Master. (Azerbaijan).

E-mail: [1]alesker.meherrem@gmail.com; [2]gasimovaaidan@gmail.com

ABSTRACT

In modern mechanical engineering, transmissions with the use of an involute tooth profile are widespread. However, one of the main disadvantages of these transmissions is that they exposure to wear. In this study, research on the cycloid profile is conducted as an alternative option. Cycloid profiles are one of the profiles applied to the teeth in order to transmit motion.

Although cycloid profiles are mainly used in instrumentation, satellites are made of cycloid profile in planetary gears. Cycloid profile teeth are less exposed to wear during operation. Practically, the shape of cycloidal teeth does not allow them to break, so there is no bending deformation in the teeth. In planetary gear transmission, the satellites are usually made of a cycloid profile. Cycloid profile teeth are exposed to less wear. Currently, planetary gear reducers are widely used mainly in the oil industry, drilling equipments, in the lifting mechanisms, gearboxes, on chain conveyors, rotary tables, in robotics, manufacturing, mechanical and chemical engineering fields and so on.

The increased load capacity of the cycloid pinion gears is due to the multi-pair contact surface and it has a superior adhesion profile than the involute profile. The loading schemes of cycloidal and evolvent profile teeth shows that the normal force in contact Fn and its dangerous section on the tooth of the cycloidal profile is much less than in the case when the tooth has an involute profile. This is due to the fact that with cycloid profile transmission the number of teeth simultaneously transmitting the load is significantly greater than when implementing the same transmission with involute teeth. Cycloid profile gear reducers can be considered as a modern solution to current requirements such as high efficiency, smooth and quiet work, ability to accept short-term maximum loads, small overall size, minimum technical requirements etc.

The simulation of the real load conditions and interference generated during the rotation of the shaft was developed in Solidworks in order to determine the contact stresses and the contact areas resulting from these stresses of the teeth of the gear and satellites of cycloid profile planetary gear reducers. This simulation determines the values of the teeth involved in the contact, the interference of those teeth, the contact areas and the contact stresses generated in these areas, depending on the angle of rotation of the shaft. The profile of the proposed teeth allows to achieve the minimum size with the maximum transmission ratio.

Keywords: cycloid profile, cycloid transmission, planetary reducer, interference, simulation, contact area.

The actuality of the subject. At present, industrial transmissions are required not only for high efficiency, but also for high longevity and reliability. Although the use of evolvent profile transmissions is widespread, it has many disadvantages. In this study, research on the cycloid profile is conducted as an alternative option. Cycloid profile gear reducers can be considered as a modern solution to current requirements such as high efficiency, smooth and quiet work, ability to accept short-term maximum loads, small overall size, minimum technical requirements etc.

The purpose of this work is to determine the interference, contact stresses and the contact areas resulting from these stresses through a simulation of the real load conditions of the cycloid profile teeth of the gears and satellites of the planetary reducer, developed in Solidworks. This work allows to achieve the minimum size with the maximum transmission ratio.

Problem statement. Cycloid profiles are one of the profiles applied to the teeth in order to transmit motion. The transmission of motion through a cycloid profile is called a cycloidal transmission. A cycloid curve is a curve represented by a straight line or circular trajectory in which a point at a constant distance from the center of the circle is rotated without slipping. The cycloid curve is based on the circumference of the base. If a rotating circle rotates along the outer surface of the base circle, its trajectory is called an epicycloid curve. If the rotating circle rotates along the inner surface of the base circle, this curve is called a hypocycloid curve.

Let's suppose that, point A is located inside a rotating circle which its radius is r. (fig. 1) This circle rolls around the base which its radius is R and it’s located at a distance of OA = e from the center. In this case, the curve is

ISSN: 2663-8770, E-ISSN: 2733-2055
ETM
EQUİPMENT, TECHNOLOGİES, MATERİALS

called shortened epicycloid curve. The ratio $\frac{e}{r}=\lambda$ is called the epicycloid shortening factor. The shortened epicycloid equations are as follows:

$$x_e(\tau) = (R + r)\cos\tau - \lambda r\cos(\frac{R + r}{r}\tau)$$

$$y_e(\tau) = (R + r)\sin\tau - \lambda r\sin(\frac{R + r}{r}\tau)$$

where τ – independent coefficient, $\tau = 0\ldots2\pi$.

The number of teeth of a cycloidal profile gear is equal to the ratio of the radii:

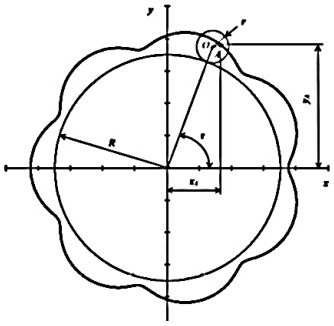

$$z_1 = \frac{R}{r}$$

Figure 1. Schema of a shortened epicycloid transmission.

The design and working principle of a cycloid gearbox is as follows:
The figure 2 is shown a planetary gear transmission consist of a gear (1) over cylindrical pins (2) and a satellite

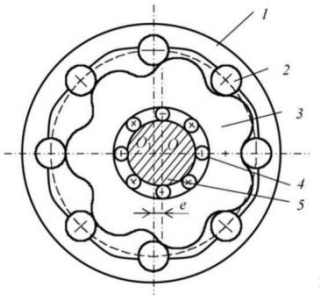

(3) with cycloid profile teeth. The satellite (3) is mounted on the ball bearing (4) of the eccentric shaft (5) in this position. The rotation of the eccentric shaft around the point O1 forces the satellite to roll on the pins and slowly rotate around the axis of rotation of the satellite, indicated by the point O.

Figure 2. Construction of a cycloid gear reducer

The increased load capacity of the cycloid pinion gears is due to the multi-pair contact surface and it has a superior adhesion profile than the involute profile. If the difference between the teeth of the gear (1) and the teeth of the satellite (3) is equal to the unit, then, in theory, about half of the cylindrical pins are involved in contact.
Solution of problem. Let us determine the interference values of the load condition and the teeth under load at different values of eccentricity. (fig. 3) Partial elastic deformation will occur between the teeth of the gear and the satellites by rotating the shaft to determine the contact stresses of the teeth participated in contact and the contact areas resulting from these stresses. Displays the appearance of the interference - simulation of one tooth overlapping another developed in Solidworks. This interference allows to determine the contact stresses and the contact areas resulting from these stresses. (figure 4-6, table 1-3, diagram 1-3)
Table 1.

ISSN: 2663-8770, E-ISSN: 2733-2055
ETM
EQUİPMENT, TECHNOLOGİES, MATERİALS
EQUİPMENT, TECHNOLOGİES, MATERİALS
VOLUME 05 ISSUE 01 2021

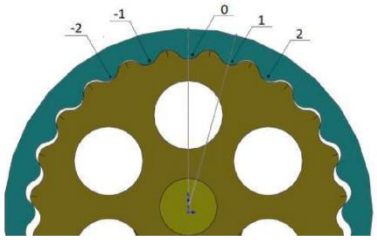

Figure 3. Pairs of gear teeth

Eccentricity = 4.86

№	Angle of gear rotation, φ_1, deg	Angle of satellite rotation, φ_2, deg	Interference, mm3			
			«0»	«1»	«2»	∑
0	0	0	0	0	0	0
1	0,01	0	0	0	0	0
2	0,02	0	0	0	0	0
3	0,03	0	0	0	0	0
4	0,04	0	0	0	0	0
5	0,05	0	0	0	0	0
6	0,06	0	0	0	0	0
7	0,07	0	0	0	0	0
8	0,08	0	0	0	0	0
9	0,09	0	0	0	0	0
10	0,1	0	0	0	0	0
11	0,2	0	0	0	0	0
12	0,21	0	0	0	0	0
13	0,22	0	0	0,11	0	0,11
14	0,23	0	0	0,39	0	0,39
15	0,24	0	0	0,8	0	0,8
16	0,25	0	0	1,3	0,16	1,46
17	0,26	0	0	1,88	0,46	2,34
18	0,27	0	0	2,54	0,84	3,38
19	0,28	0	0	3,26	1,3	4,56
20	0,29	0	0,00074	4,04	1,82	5,86074
21	0,3	0	0,21	4,88	2,39	7,48

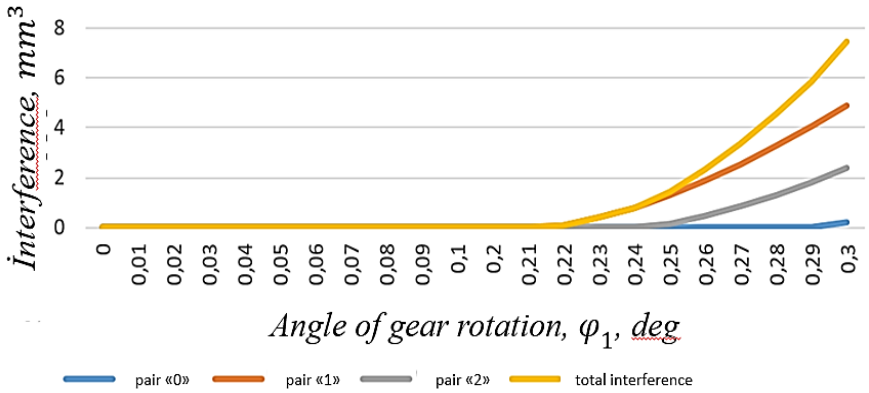

Diagram 1. Load diagram of teeth when eccentricity = 4,86

ISSN: 2663-8770, E-ISSN: 2733-2055
ETM
EQUİPMENT, TECHNOLOGİES, MATERİALS

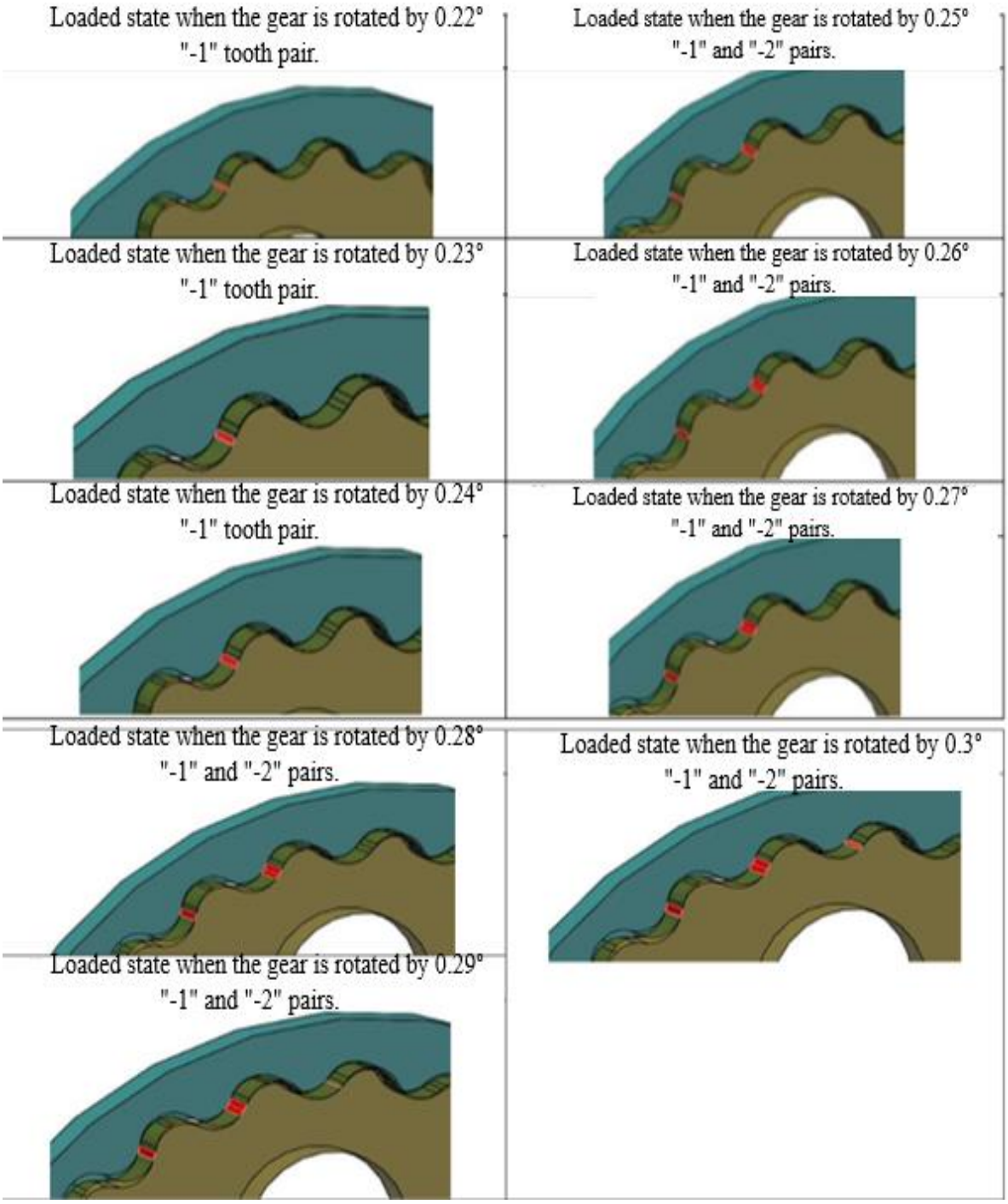

Figure 4. Load states
Eccentricity = 4.6

ISSN: 2663-8770, E-ISSN: 2733-2055
ETM
EQUİPMENT, TECHNOLOGİES, MATERİALS
EQUİPMENT, TECHNOLOGİES, MATERİALS
VOLUME 05 ISSUE 01 2021

Table 2.

№	Angle of gear rotation, φ_1, deg	Angle of satellite rotation, φ_2, deg	Interference, mm^3			
			«0»	«1»	«2»	∑
0	0	0	0	0	0	0
1	0,01	0	0	0	0	0
2	0,02	0	0	0	0	0
3	0,03	0	0	0	0	0
4	0,04	0	0	0	0	0
5	0,05	0	0	0	0	0
6	0,06	0	0	0	0	0
7	0,07	0	0	0	0	0
8	0,08	0	0	0	0	0
9	0,09	0	0	0	0	0
10	0,1	0	0	0	0	0
11	0,2	0	0	0	0	0
12	0,21	0	0	0	0	0
13	0,22	0	0	0	0	0
14	0,23	0	0	0	0	0
15	0,24	0	0	0,01	0	0,01
16	0,25	0	0	0,2	0	0,2
17	0,26	0	0	0,52	0,07	0,59
18	0,27	0	0	0,94	0,32	1,26
19	0,28	0	0	1,45	0,67	2,12
20	0,29	0	0	2,03	1,1	3,13
21	0,3	0	0	2,67	1,59	4,26

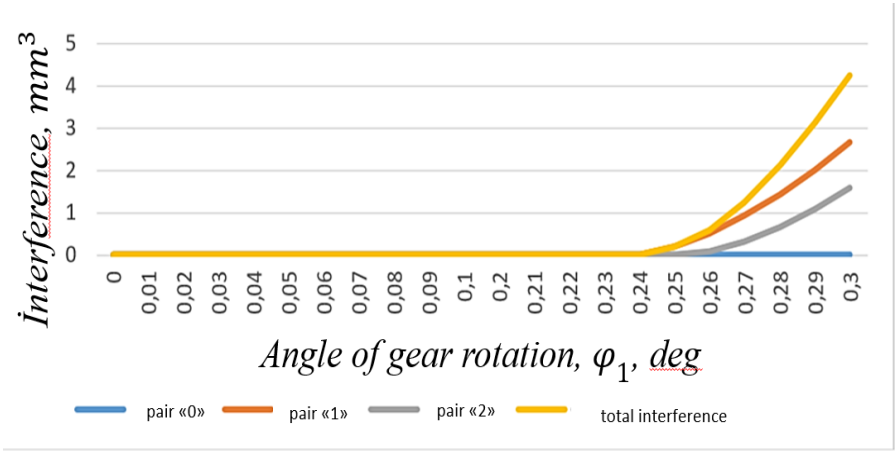

Diagram 2. Load diagram when eccentricity = 4.6

ISSN: 2663-8770, E-ISSN: 2733-2055
ETM
EQUİPMENT, TECHNOLOGİES, MATERİALS

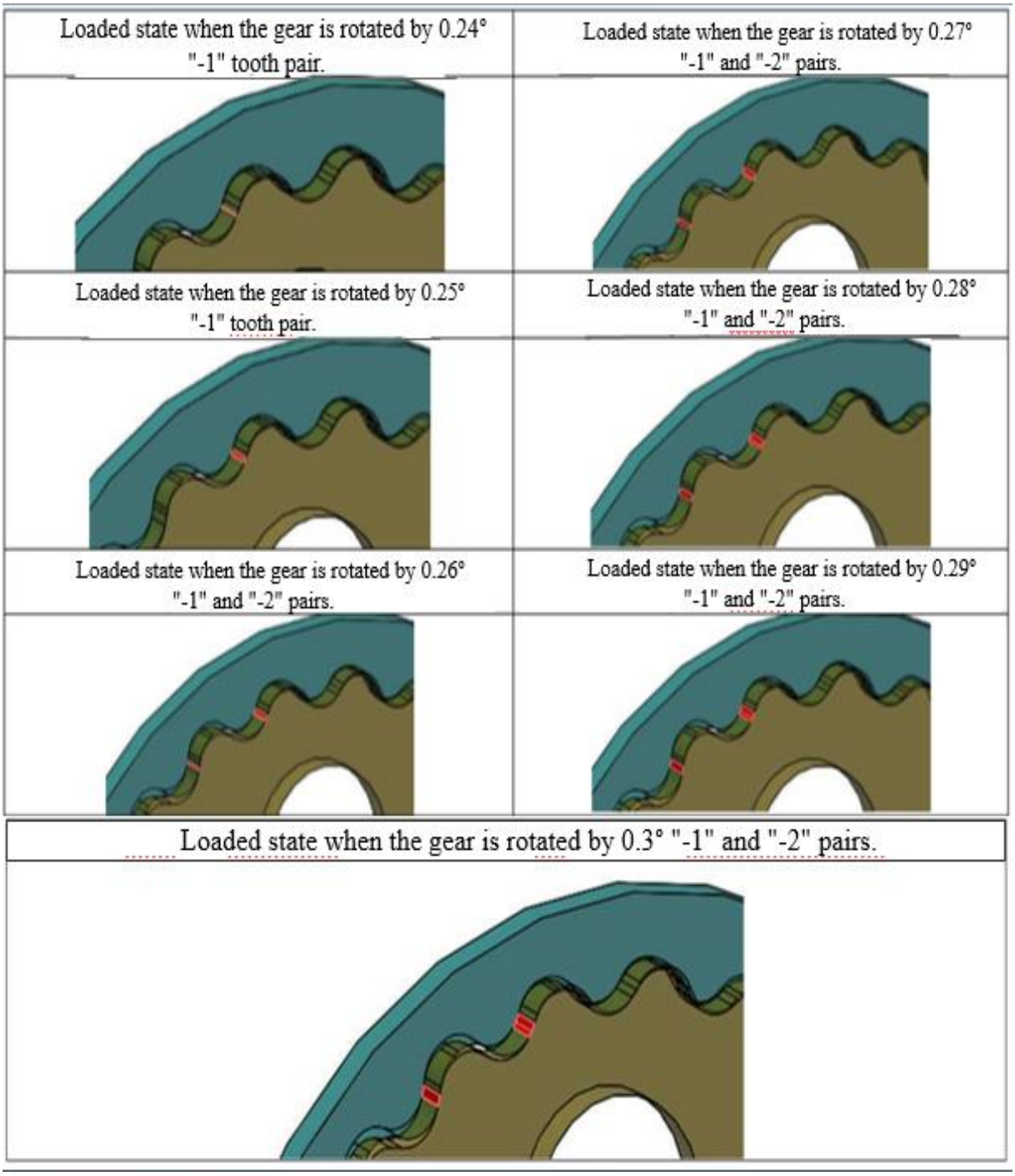

Figure 5. Loaded states

Eccenctricity = 4.5

ISSN: 2663-8770, E-ISSN: 2733-2055
ETM
EQUİPMENT, TECHNOLOGİES, MATERİALS
EQUİPMENT, TECHNOLOGİES, MATERİALS
VOLUME 05 ISSUE 01 2021

Table 3.

№	Angle of gear rotation, φ_1, deg	Angle of satellite rotation, φ_2, deg	Interference, mm^3			
			«0»	«1»	«2»	∑
0	0	0	0	0	0	0
1	0,01	0	0	0	0	0
2	0,02	0	0	0	0	0
3	0,03	0	0	0	0	0
4	0,04	0	0	0	0	0
5	0,05	0	0	0	0	0
6	0,06	0	0	0	0	0
7	0,07	0	0	0	0	0
8	0,08	0	0	0	0	0
9	0,09	0	0	0	0	0
10	0,1	0	0	0	0	0
11	0,2	0	0	0	0	0
12	0,21	0	0	0	0	0
13	0,22	0	0	0	0	0
14	0,23	0	0	0	0	0
15	0,24	0	0	0	0	0
16	0,25	0	0	0	0	0
17	0,26	0	0	0	0	0
18	0,27	0	0	0	0	0
19	0,28	0	0	0,14	0,12	0,26
20	0,29	0	0	0,43	0,4	0,83
21	0,3	0	0	0,81	0,77	1,58

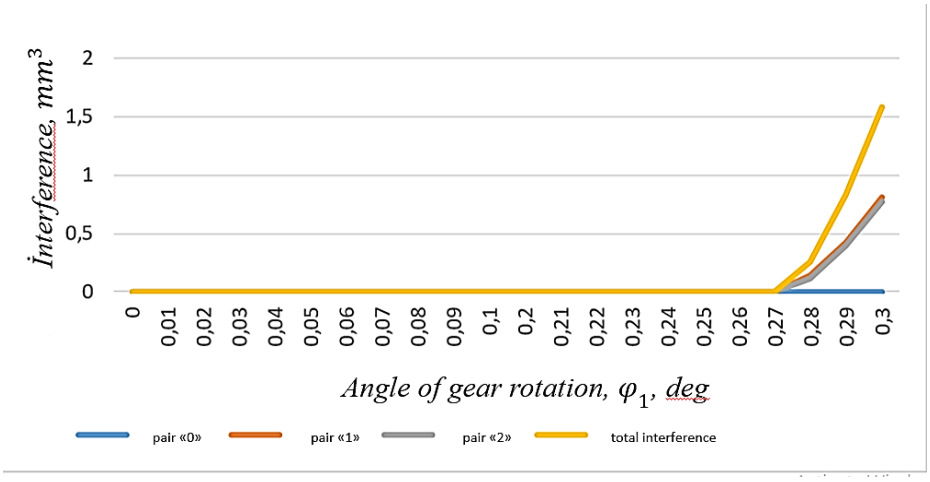

Diagram 3.

Load diagram when eccentricity = 4.5

ISSN: 2663-8770, E-ISSN: 2733-2055
ETM
EQUİPMENT, TECHNOLOGİES, MATERİALS

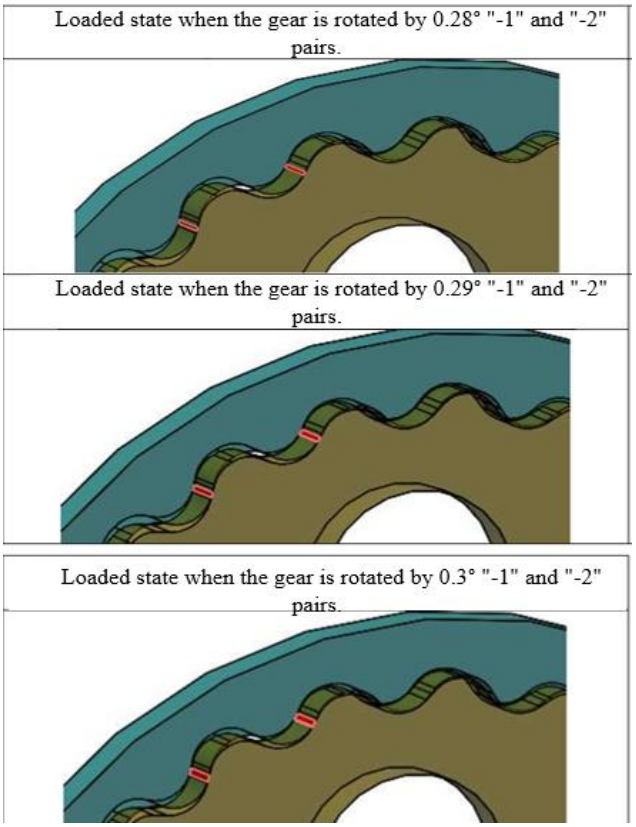

Figure 6. Loaded states

Material selection and calculation of strength.The material of the gear, satellite and eccentric shaft is determined by the manufacturer. Exp: 20XH3A. Young's modulus for this material E=132 GPa.
Firstly, we find the relative deformation in order to determine the compression stress: the volume of interference should be divided by the volume of the tooth.

$$\varepsilon = \frac{V_{int}}{V_{tooth}}$$

The yield strength of 20XH3A steel is □ys = 690 MPa
According to Hooke's law

$$\sigma = E \cdot \varepsilon$$

The result obtained σ is compared with the maximum allowable stress (table 4)

Table 4.

Comparative analysis of cycloid and evolvent profile tooth loading.

Angle of gear rotation, φ_1,deg.	Volume of interference, mm3	Volume of tooth, mm3	Strain	Compression stress, MPa
0.22	0.11	2340	0.00004701	6.21
0.23	0.39		0.00016667	22.01
0.24	0.8		0.00034188	45.13
0.25	1.3		0.00055556	73.33
0.26	1.88		0.00080342	106.05
0.27	2.54		0.001088547	143.68
0.28	3.26		0.00139316	183.89
0.29	4.04		0.0017265	227.89
0.3	4.88		0.00208547	257.28

ISSN: 2663-8770, E-ISSN: 2733-2055
ETM
EQUİPMENT, TECHNOLOGİES, MATERİALS
EQUİPMENT, TECHNOLOGİES, MATERİALS
VOLUME 05 ISSUE 01 2021

The figure 7 shows that the normal force in contact Fn and its dangerous section on the tooth of the cycloidal profile is much less than in the case when the tooth has an involute profile. This is due to the fact that with cycloid profile transmission the number of teeth simultaneously transmitting the load is significantly greater than when implementing the same transmission with involute teeth. Although transmissions with involute profile teeth are common in modern engineering, these transmissions do not show high wear resistance. Practically, the shape of cycloidal teeth does not allow them to break, so there is no bending deformation in the teeth.

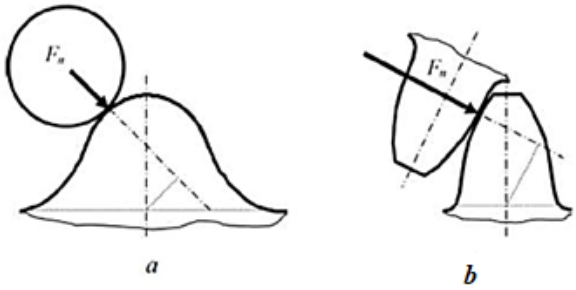

Figure 7. Gear tooth loading schemes
a) cycloid profile; b) involute profile

Results of research: 1. As a result of the research, it can be concluded that the reducer rotates evenly in the unloaded state. However, when the torque is simulated, we see that there are no teeth when in contact up to a certain value of the load. Only when the gear is rotated more than 0.27°, then the teeth begin to come into contact. For this reason, it is very important to calculate the correct eccentricity for cycloidal gears during design.
2. In planetary gear transmission, the satellites are usually made of a cycloid profile. Cycloid profile teeth are exposed to less wear. Currently, planetary gear reducers are widely used mainly in the oil industry, drilling equipments, in the lifting mechanisms, gearboxes, on chain conveyors, rotary tables, in robotics, manufacturing, mechanical and chemical engineering fields and so on.
3. The shape of the proposed teeth allows to achieve the minimum size with the maximum transmission ratio. Several teeth coming into contact makes the high-load reducer more compact.

REFERENCES

1. Казакявичюс С.М. Работоспособность эксцентриковоцик...дального зацепления при изменении межосевого расстояния колес. Модификация вершин и впадин зубьев // Вестник машиностроения. – 2011. - №3, стр. 7-9
2. Леонтьев, М.Ю. Обзор достоинств и недостатков эксцентриковоциклоидального зацепления [Текст] / М.Ю. Леонтьев, В.А. Раевский, А.Е. Смоловик // Актуальные проблемы гуманитарных и естественных наук. – 2016. – № 7-5. С. 54 – 57.
3. Краснощеков Н. Н., Федякин Р. В., Чесноков В. А. Теория зацепления. М.: Наука, 1976 – 175 с.
4. Становской, В.В. Двухступенчатый редуктор на основе эксцентриково-циклоидального зацепления / В.В. Становской, С.М. Казакявичюс, Т.А. Ремнева, В.М. Кузнецов, А.М. Бубенчиков, Н.Р. Щербаков, Й. Шмидт // Вестник машиностроения. – 2011. - № 12. – С. 4144.

ISSN: 2663-8770, E-ISSN: 2733-2055
ETM
EQUİPMENT, TECHNOLOGİES, MATERİALS

RESEARCH OF THE WAVE FACTOR INFLUENCING HYDRAULIC STRUCTURES

[1]Sevda Aliyeva, [2]Mahmud Ismayilov

[1]Azerbaijan State of Oil and Industry University, PhD of Technical Sciences. Associate professor. (Azerbaijan).

[2]Azerbaijan State Oil and Industry University, Master. (Azerbaijan).

E-mail: [1]sevda.aliyeva.66@bk.ru; [2]max.company@bk.ru

ABSTRACT

It is known that a large block of deep-sea foundations consists of a truss sheathed with wood, a metal beam system, floating structures and four pyramidal metal blocks with a truss structure. The design characteristics of the foundations of oil platforms depend on the conditions under which the vertical interaction, along with the calculation of permanent and temporary loads, is accompanied by the specific gravity of drilling equipment and rigs or horizontal wind pressure, as well as the influence of horizontal wave loads on the foundation blocks. Horizontal waves and wind loads can be constant and variable in different conditions, therefore the effect of each of these loads on the device must be considered separately. To determine the wave pressure acting on the support blocks of stationary offshore installations, SN-92-60 was used under the editorship of the team of authors under the leadership of Doctor of Technical Sciences, Professor N.N.Tsunkov.
Keywords: hydraulic structures, wave factor, wave pressure, wave profile, pressure diagrams, 3D model.

The actuality of the subject. The development of the operating oil and gas fields of the Caspian Sea is of great importance in the economy of Azerbaijan. One of the key issues for the development of these fields is the design of offshore platforms. When designing these hydraulic structures, it is important to correctly assess the forces acting on them during the calculation [1-5].
Objective. This paper discusses a methodology for calculating large block deep-water structures for wells with a depth of 4000 m and a sea depth of 60 m using our algorithm in Excel.
Formulation of the problem. To study the wave factor on offshore platform foundations, you first need to build a wave profile and then consider applying this wave to the foundations.
The influence of the wave profile on the foundations of a hydraulic device can be studied by plotting the effect of the wave load on the supports. To define a wave profile, the wave elements are first calculated, then the wave profile is calculated and the profile is built in accordance with the results obtained.
To establish the effect of the wave on the platform supports, it is necessary to determine the loads generated by the wave.
In the case under consideration, the sea wave profile was calculated from the storm wave formed in the Caspian Sea. The dimensions of the platform supports are conventionally taken in accordance with the designs of existing offshore platforms.

Discussion of the solution.
1. Determination of wave elements.
When calculating the foundations for wave loads, the Oil Rocks fields with a more severe hydrometeorological regime were selected. At the suggestion of the State Oceanographic Institute for the region under study, the average wave height:

$$\hbar_{\mathrm{d}} = 4{,}5 \text{ m}$$

The average annual sea depth H = 60 m, we determine the dimensionless parameter, taking it and writing [1]:

$$\frac{\hbar_{\mathrm{d}}}{\mathrm{H}} = \frac{4{,}5}{60} = 0{,}075$$

We set the report wave height at 1%:

$$\mathrm{K_h} = \frac{\mathrm{h_i}}{\hbar_{\mathrm{d}}} = 2{,}4$$

ISSN: 2663-8770, E-ISSN: 2733-2055
ETM
EQUİPMENT, TECHNOLOGİES, MATERİALS
EQUİPMENT, TECHNOLOGİES, MATERİALS
VOLUME 05 ISSUE 01 2021

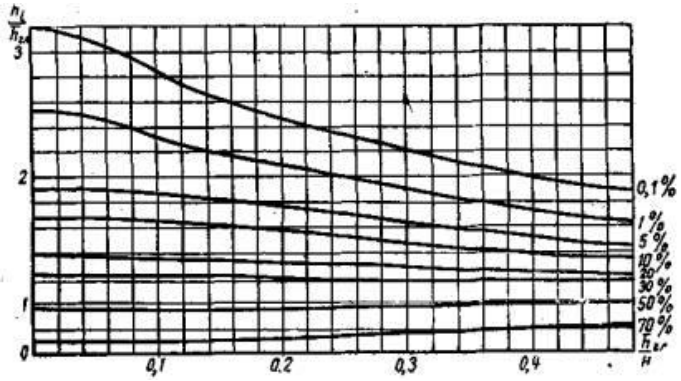

Figure 1. Graph for determining the change in the spectrum of wave heights during transformation. [1]

From the approximation, we obtain the following empirical formulas:

$$K_h = -26{,}305(\hbar_d/H)^4 - 2{,}7808(\hbar_d/H)^3 + 13{,}495(\hbar_d/H)^2 - 6{,}0483(\hbar_d/H) + 2{,}8 \quad (1)$$

From Figure 1 Formula (1) we determine the height of the calculated wave:

$$h_i = K_h \cdot \hbar_d = 2{,}42 \cdot 4{,}5 = 10{,}89\ m$$

Knowing the height of the wave, we set a calculated dimensionless parameter.

$$\frac{h_i}{H} = \frac{10{,}89}{60} = 0{,}18$$

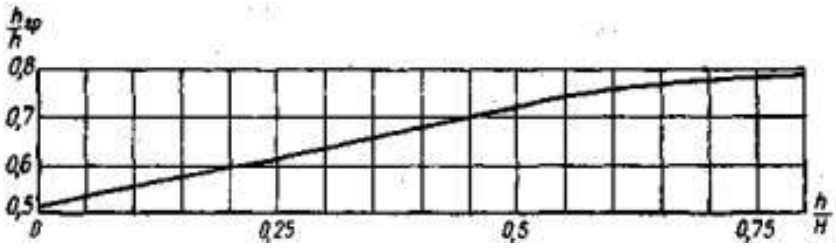

Figure 2. Graph for determining the calculated elevation of the wave crest.

From the approximation, we obtain the following empirical formulas:

$$\hbar_d/h = 2{,}4471(h/H)4 - 3{,}8062(h/H)3 + 1{,}4382(h/H)2 + 0{,}345(h/H) + 0{,}5 \quad (2)$$

From Figure 2 or Formula (2) we find the corresponding values of the calculated non-dimensional parameters [1]:

$$\frac{h_{qr}}{h_i} = 0{,}599$$

Based on this, we determine the height of the calculated wave peak above the reporting level:

$$h_{qr} = 0{,}59 \cdot h_i = 0{,}599 \cdot 10{,}89 = 6{,}52\ m$$

We determine the values of the rising peak peaks in terms of the coefficient of increase of the static level obtained by 0.5 m. Taking into account the bearing capacity of the drilling rig, we take 0.75 m, by adjusting the static average annual level of the sea to the maximum possible ratio of peaks, performed by the guide to the depth of 60 m. In this way:

$$h_{qr.max} = h_{qr} + 0{,}75 = 6{,}52 + 0{,}75 = 7{,}27\ m$$

The calculated average height of the wave:

ISSN: 2663-8770, E-ISSN: 2733-2055
ETM
EQUİPMENT, TECHNOLOGİES, MATERİALS

$$h_0 = h_i - h_{qr.max} = 10,89 - 7,27 = 3,62 \text{ m}$$

The maximum calculated height of the wave top relative to the seabed:

$$z_{max} = H + h_{qr.max} = 60 + 7,27 = 67,27 \text{ m}$$

The calculated wavelength can be set as follows:

$$\lambda = 10 \cdot h_i = 10 \cdot 10,89 = 108,9 \text{ m}$$

2. Determination of wave profile.
Thus, in order to obtain a reportable wave profile, we determine their coordinates. We determine the calculated dimensionless quantities:

$$\frac{h_i}{H} = \frac{10,89}{60} = 0,18 < 0,25$$

Thus, we are sure that you need to use the upper curved graphics. Setting arbitrary abscissa to X and calculating their immeasurable values $x' = \frac{x}{\lambda}$ respectively, find the coefficient for determining the profile φ-wave according to the graph (empirical formula for program 3).
The following empirical formula for determining the wave profile is obtained:

$$\phi = -53,022\ddot{x}^4 + 62,173\ddot{x}^3 - 19,583\ddot{x}^2 - 1,1825\ddot{x} + 1 \quad (3)$$

The ordinates of the wave profile, ie the distance measured from the base of the wave, are calculated according to the following formula:

$$\eta = \varphi \cdot h_i$$

The ordinates calculated from the seabed are determined according to the following formula:

$$z = \eta + H_C$$

All reports are executed in a program compiled in Excel. The results of the calculations are shown in Table 1.
The obtained ordinates allow you to build a wave profile with a 1% supply.

Table 1

Wave parameters calculated by the developed program

№	x, m	$\ddot{x} = \frac{x}{\lambda}$	$\varphi, \frac{h}{H} < 0,25$	$\eta = \varphi \cdot h_i, m$	$z = \eta + H_0, m$
1	0	0	1,02	11,09	67,37
2	4	0,04	0,95	10,36	66,64
3	8	0,07	0,85	9,24	65,53
4	12	0,11	0,73	7,90	64,18
5	16	0,15	0,59	6,47	62,75
6	20	0,18	0,47	5,07	61,35
7	30	0,28	0,20	2,19	58,47
8	40	0,37	0,06	0,63	56,91
9	50	0,46	0,01	0,09	56,37
10	54,46	0,5	0	0	56,28

In the blue cells - the given, in the white cells - the calculated parameters are shown.
After calculating the parameters of the wave, the profile of the wave is established according to Table 1 (Figure 3):

ISSN: 2663-8770, E-ISSN: 2733-2055
ETM
EQUİPMENT, TECHNOLOGİES, MATERİALS
EQUİPMENT, TECHNOLOGİES, MATERİALS
VOLUME 05 ISSUE 01 2021

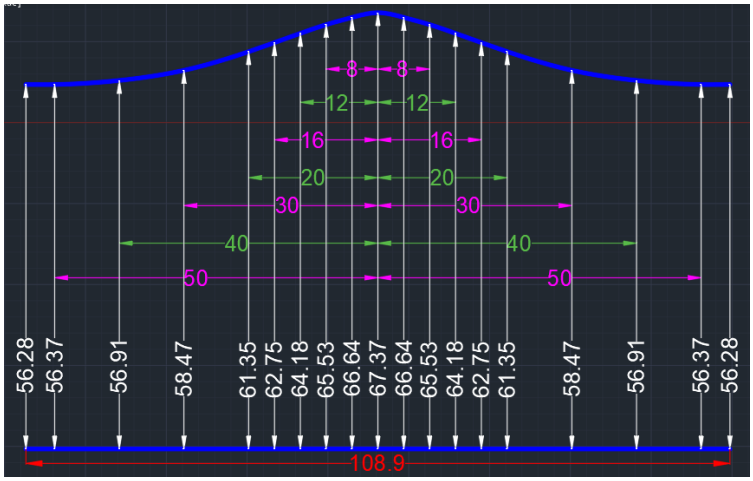

Figure 3. The profile of the wave.

Once the wave profile was constructed, a model of the impact of the wave on the conventional support blocks was constructed using the profile in Figure 1 (Figure 4):

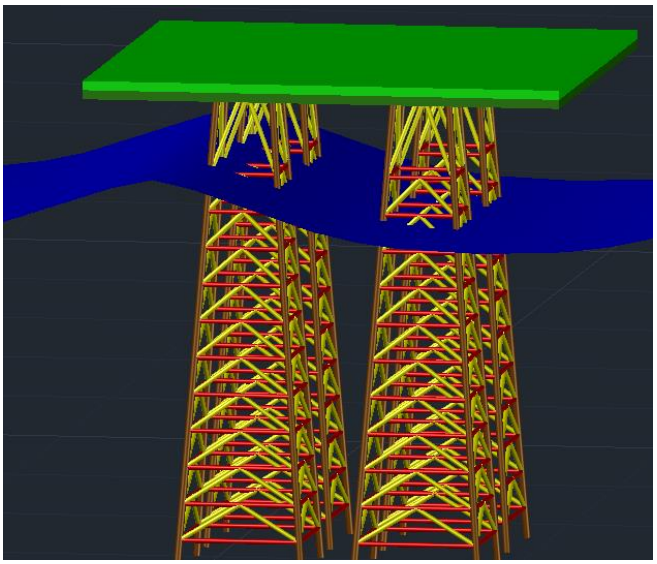

Figure 4. 3D model of the wave.

The drawing of the model was made using AutoCAD program, based on the parameters in Table 1.

3. Determination of wave loads.

In order to determine the wave loads, the vertical axis of one of the blocks is connected to the apex of the wave. In this case (Fig. 5), the axis of the second block is located at 28.5 m from the top of the wave, but greater forces will be formed on the elements of the foundations. The wave loads acting on the structural elements are perceived due to their longitudinal division along the axis. The calculation of the wave pressure will be the same as the calculation of the vertical elements. Bend the smooth cylindrical support at $4^{\circ}22''$.

ISSN: 2663-8770, E-ISSN: 2733-2055
ETM
EQUİPMENT, TECHNOLOGİES, MATERİALS

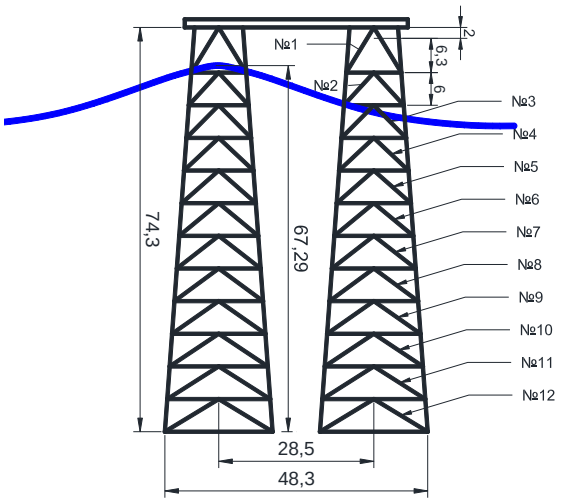

Figure 5. Influence of waves on support blocks.

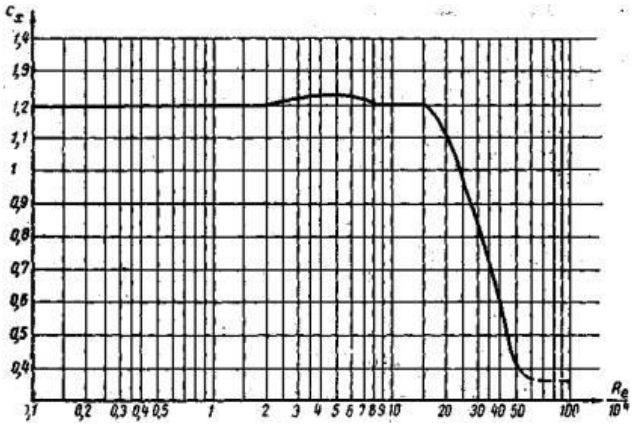

Figure 6. Graph for determining the drag coefficient.

From Figure 6 the following empirical formula for determining the coefficient of resistance is obtained:

$$Cx=4E\text{-}11(Re)6\text{-}1E\text{-}08(Re)5+1E\text{-}06(Re)4\text{-}7E\text{-}05(Re)3+0{,}0013(Re)2\text{-}0{,}0227(Re)+1{,}42 \quad (4)$$

We define the interaction of waves as follows:

$$\frac{h_i}{H} = 0{,}18 \prec 0{,}25$$

where h_i is the height of the wave; H is the depth of the sea.
The inner diameter of the wash support for this area is calculated as follows:

$$d \leq \frac{1}{50}\lambda = \frac{108{,}9}{50} = 2{,}19\ \text{m}$$

The wave pressure generated by the horizontal flow velocity in the support blocks is calculated using the following formula:

$$P_{x,v} = C_x \cdot \frac{\gamma}{2g} \cdot v \cdot x^2 \cdot d$$

where γ is the volume weight of water, assumed to be 1,0 t/m^2. g is the acceleration of gravity equal to 9,81 m/san^2. C_x is the coefficient of resistance [1].
Depending on the Reynolds number, the report is as follows:

$$R_e = \frac{v_x \cdot d}{\nu}$$

ISSN: 2663-8770, E-ISSN: 2733-2055
ETM
EQUİPMENT, TECHNOLOGİES, MATERİALS
EQUİPMENT, TECHNOLOGİES, MATERİALS
VOLUME 05 ISSUE 01 2021

where: ν- is the kinematic viscosity coefficient, given for water $0{,}015 \cdot \frac{10^{-4}m^2}{san}$. v_x – is the calculated horizontal velocity of water particles at the points under consideration, determined by the following formula

$$v_x = v_{x.orb} + u$$

where: $v_{x.orb}$ is the calculated horizontal orbital velocity and is calculated as follows:

$$v_{x.orb} = \frac{\pi^2}{\lambda} C \frac{ch\frac{4\pi}{\lambda}(H - z_0)}{sh\frac{2\pi H}{\lambda}} \cdot \cos\frac{2\pi}{\lambda}x$$

$$C = \sqrt{\frac{g\lambda}{2\pi} th\frac{2\pi h}{\lambda}}$$

u – is the velocity of the calculated flow and is determined by the following formula:

$$u = \frac{\pi^2}{2\lambda^2} h^2 C \frac{ch\frac{4\pi}{\lambda}(H - z_0)}{sh^2\left(\frac{2\pi H}{\lambda}\right)}$$

z_0 – is the calculated distance below the static level at the point in question; x is the distance from the support to the wave top; $P_{x,v}$ – to construct the velocity pressure curve, we construct the v_x -approximate curve, calculate the ordinate values for the points according to the height of the support, clarify the R_e – value for these points if necessary, and assign the values C_x and $P_{x.v.}$

At the intersection of the static sea level with the symmetrical axis of the block, the horizontal abscissa axis to the right, and the vertical ordinate axis downwards. By summing, we determine the numerical values of the velocities of the horizontal particle at the points under consideration. Given that the support block is a pipe with a diameter d = 478mm, we calculate the values of velocity pressure at selected points. When calculating the parameters specified in the program we compiled in Excel, we get the values of the wave loads (Table 2):

Table 2.

Determination of wave loads.

№	Z0	H-Z0	vx.orb	u	vx	Re	Cx	Px.v.	P'x.v.
1	-7,37	67,37	4,80	4,70	9,50	302,89 *10^4	0,4	0,792	0,792
2	-1	61	3,33	2,25	5,58	177,85*10^4	0,4	0,273	0,382
3	5	55	2,36	1,13	3,48	111,01*10^4	0,4	0,106	0,149
4	11	49	1,67	0,56	2,23	71,18*10^4	0,4	0,044	0,061
5	17	43	1,18	0,28	1,47	46,76*10^4	0,4	0,019	0,026
6	23	37	0,84	0,14	0,99	31,40*10^4	0,78	0,019	0,026
7	29	31	0,61	0,07	0,68	21,54*10^4	1,09	0,012	0,017
8	35	25	0,44	0,04	0,48	15,15*10^4	1,16	0,006	0,009
9	41	19	0,33	0,02	0,35	11,01*10^4	1,14	0,003	0,005
10	47	13	0,25	0,01	0,26	8,42*10^4	1,09	0,002	0,003
11	53	7	0,21	0,01	0,22	6,96*10^4	1,2	0,001	0,002
12	59	1	0,20	0,00	0,20	6,41*10^4	1,2	0,001	0,002

4. Construction of wave pressure loops in support blocks.

To construct plots of wave pressure on the support blocks, consider several n joints of the block on the support and the area where the plots of wave pressure affect the node (Figure 7). We take these areas as trapezoids and

ISSN: 2663-8770, E-ISSN: 2733-2055
ETM
EQUİPMENT, TECHNOLOGİES, MATERİALS

formulate expressions for the nodes in question to calculate the loads on the nodes. For nodes other than n = 1 and n = 2, (n> 2) the following expression is executed:

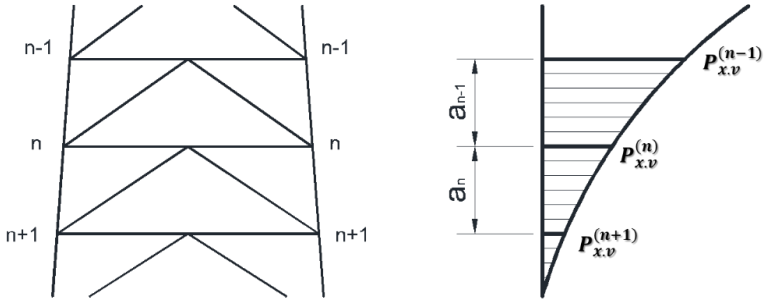

Figure 7. Wave pressure diagram for node n block.

From Figure 7:

$$P_n^d = \frac{1}{3}\cdot\frac{P_{x.v}^{(n-1)}\cdot a_{n-1}}{2} + \frac{2}{3}\cdot\frac{P_{x.v}^{(n)}\cdot a_{n-1}}{2} + \frac{2}{3}\cdot\frac{P_{x.v}^{(n)}\cdot a_n}{2} + \frac{1}{3}\cdot\frac{P_{x.v}^{(n+1)}\cdot a_n}{2}\cdot k_1\cdot k_2 \quad (5)$$

The wave pressure diagram for the upper part of the support block (n = 1 and n=2) (Figure 5):

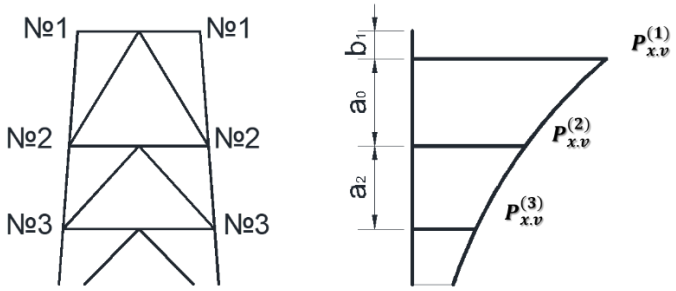

Figure 8. Wave pressure plot at n = 1 and n = 2 nodes.

From Figure 8:

$$P_1^d = \frac{\frac{P_{x.v}^{(1)}\cdot a_0}{2}\cdot\frac{2}{3}\cdot a_0}{a_0+b_1} + \frac{\frac{P_{x.v}^{(1)}\cdot a_0}{2}\cdot\frac{1}{3}\cdot a_0}{a_0+b_1}\cdot k_1\cdot k_2 \quad (6)$$

$$P_2^d = \frac{\frac{P_{x.v}^{(1)}}{2}\cdot\left(b_1+\frac{1}{3}\cdot a_0\right)}{a_0+b_1} + \frac{\frac{P_{x.v}^{(2)}\cdot a_0}{2}\cdot\left(b_1+\frac{2}{3}\cdot a_0\right)}{a_0+b_1} + \frac{2}{3}\cdot\frac{P_{x.v}^{(2)}\cdot a_2}{2} + \frac{1}{3}\cdot\frac{P_{x.v}^{(3)}\cdot a_2}{2}\cdot k_1\cdot k_2 \quad (7)$$

By assigning the values $P_{x,v}$ and $P'_{x,v}$ in the resulting expressions, it is possible to determine the values of all node loads acting on the block. We accept the following data for the calculation:
b_1=2 m - distance from the top of the wave to the top of the 1st knot; a_0=6,3 m- distance from the top to the top of the 2nd wave; a_2=a_3=⋯=a_n=6 m- distance from the vertices of the previous node to the vertices of the considered node; k_1=1,25 – coefficient taking into account the static load; k_2 = 1,2 – coefficient, taking into account the dynamic load. After calculating the load, we determine the load of the nodes with the help of the developed software algorithm (Table 3).

Table 3.

Knot loads

ISSN: 2663-8770, E-ISSN: 2733-2055
ETM
EQUİPMENT, TECHNOLOGİES, MATERİALS
EQUİPMENT, TECHNOLOGİES, MATERİALS
VOLUME 05 ISSUE 01 2021

Node loads , t		
Node No.	*With coverage*	*Excluding coverage*
1	2,221	2,352
2	3,793	4,570
3	1,114	1,560
4	0,451	0,631
5	0,207	0,289
6	0,158	0,221
7	0,110	0,155
8	0,062	0,086
9	0,032	0,045
10	0,018	0,025
11	0,013	0,018
12	0,009	0,013

CONCLUSION

1) On the basis of SN-92-60 was developed a program in Excel, which significantly simplified the report on wave loads to account for changes in the parameters;
2) built mathematical models of data graphs to determine the parameters of the wave and defined their functions;
3) Established a storm wave profile, which is one of the main factors for the Caspian Sea;
4) Created a physical (3D) model of the application of the wave installed on the support of the structure;
5) The influence of wave pressure on the supports of the type of marine oil and gas hydraulic farms and the construction of pressure logs created on the supports are studied.

REFERENCES

1. Технические условия определения волновых воздействий на морские и речные сооружения и берега. СН 92-60 Государственное издательство литературы по строительству, архитектуре и строительным материалам. Москва – 1960
2. Расчёт основания напорного гидротехнического сооружения: учебно-методическое пособие / Д.Ю. Чунюк, Е.С. Гусева; Министерство науки и высшего образования Российской Федерации-Москва Издательство МИ СИ - МГСУ, 2020.-61с.
3. Проектирование и расчеты гидротехнических сооружений: учебное пособие / П.М. Богославчик, Г.Г. Круглов. – Минск: Вышэйшая школа, 2018. - 366 с.
4. А.М. Ибрагимов. Нефтегазопромысловые гидротехнические сооружения «Недра», М., 1996
5. Гаджиев Ф.М. Иследование динамического взаимодействия деформируемого тела и волнового потока, основанное на данных натуральных испытаний. Сб. научных трудов. Н.ИПИ «Гипроморьнефть», выпуск XIV, Баку, 1997

ISSN: 2663-8770, E-ISSN: 2733-2055
ETM
EQUİPMENT, TECHNOLOGİES, MATERİALS

GROUP OF REVIEWERS

Azerbaijan

Ali Hikmat Akhmedov
The head of the faculty “Oil-Mechanics” Candidate of Technical Sciences.
Alesgar Aliyev
Azerbaijan State Oil and Industry University, Head of Department “Mechanics”. Doctor of Technical Sciences.
Alesgar Gulgazli
Azerbaijan State Oil and Industry University, Department “Mechanics” Doctor of Technical Sciences
Camaladdin Aslanov
Azerbaijan State Oil and Industry University, Department “Oil and gas equipment” PhD in Technical Sciences, Associate Professor.
Gasim Mammadov
Azerbaijan State Oil and Industry University, Vice-Rector for Academic Affairs. Candidate of Technical Sciences.
Ibrahim Habibov
Azerbaijan State Oil and Industry University, Head of Department “Engineer and Computer Graphics”. Doctor of Technical Sciences.
Jahid Kerimov
Azerbaijan State Oil and Industry University, Department “Mechanical Engineering and Materials Science”. Doctor of Technical Sciences.
Maleyka Mammadova
Azerbaijan State Oil and Industry University, Department “Engineer and Computer Graphics” Doctor of Technical Sciences.
Rasim Ismayilov
Azerbaijan State Oil and Industry University, Head of Department “Oil and gas equipment” Doctor of Technical Sciences.
Tahir Cabbarov
Azerbaijan State Oil and Industry University, Head of Department “Mechanical Engineering and Materials Science” PhD in Technical Sciences.
Zuleykha Eyvazova
Azerbaijan State Oil and Industry University, Associate Professor “Oil and gas equipment” Associate professor. PhD in Technical Sciences.

German

Xudaverdi Karimov
Director of “IXUN Lasertechnik Gmb”, Associate professor. PhD in Technical Sciences.

Turkey

Shevket Levent Ergun
Hacettepe University, Professor, Faculty of Mining Engineering.

Russia

Iskander Kuzeev
Ufa State Petroleum Technical University. Professor, Department of “Machines and devices of chemical production”.

RƏYÇILƏR QRUPU

JOURNAL INDEXING

© THE BALTIC SCIENTIFIC JOURNALS
ISSN: 2663-8770, E-ISSN: 2733-2055, DOI: 10.36962/ETM

©Publisher: Azerbaijan State Oil and Industry University. İ/C 1400196861 (Azerbaijan)
Rector: Mustafa Babanli. Doctor of Technical Sciences. Professor.
Editors-in-chief: Ibrahim Habibov
Technical and reviewer team manager: Zuleykha Eyvazova.
Registered address: 20, Azadlig pr., Baku, Azerbaijan, AZ1010.
©Editorial office: 20, Azadlig pr., Baku, Azerbaijan, AZ1010.
©Typography: Azerbaijan State Oil and Industry University İ/C 1400196861 (Azerbaijan).
Registered address: 20, Azadlig pr., Baku, Azerbaijan, AZ 1010.

Publisher: International Research, Education & Training Center. MTÜ (Estonia, Tallinn), R/C 80550594
Director and Founder: Seyfulla İsayev. (Azerbaijan)
Deputy and Founder: Namig Isazade. PhD in Business Administration. (Azerbaijan)
©Editorial office / Redaksiya: Harju maakond, Tallinn, Kesklinna linnaosa, Narva mnt 5, 10117
Telephones / Telefonlar: +994 55 241 70 12; +994 51 864 88 94
Website/Veb səhifə: http://sc-media.org/
E-mail: sc.mediagroup2020@gmail.com, sc.mediagroup2017@gmail.com

ISSN: : 2663-8770, E-ISSN: 2733-2055, DOI: 10.36962/ETM

EQUİPMENT TECHNOLOGİES MATERİALS

AVADANLIQLAR, TEXNOLOGİYALAR, MATERİALLAR

ОБОРУДОВАНИЕ, ТЕХНОЛОГИИ, МАТЕРИАЛЫ

VOLUME 05 ISSUE 01 2021

CİLD 05 BURAXILIŞ 01 2021

http://emtasoiu.com/index.php/en/

http://sc-media.org/etm/